



UNIVERSITY OF
BIRMINGHAM

**Air Pollution Climatology of Particulate
Matter in Dammam, Saudi Arabia:
Composition, Sources & Toxicity**

By

Manna M. Alwadei

A thesis submitted to the University of Birmingham
for the degree of Doctor of Philosophy

School of Geography, Earth and Environmental Sciences

University of Birmingham

September 2021

UNIVERSITY OF
BIRMINGHAM

University of Birmingham Research Archive

e-theses repository

This unpublished thesis/dissertation is copyright of the author and/or third parties. The intellectual property rights of the author or third parties in respect of this work are as defined by The Copyright Designs and Patents Act 1988 or as modified by any successor legislation.

Any use made of information contained in this thesis/dissertation must be in accordance with that legislation and must be properly acknowledged. Further distribution or reproduction in any format is prohibited without the permission of the copyright holder.

Abstract

Air pollution in many countries is the largest environmental health stressor on their populations. Investigating key air pollutant sources, their properties and processes of formation in different environments is key to understanding how to implement mitigation strategies appropriately in those countries. The world is rapidly urbanising, leading to larger emissions, burning of fossil fuels and thus increasing air pollution. At present one of the main pollutants of concern in urban centres is particles less than $2.5\mu\text{m}$ in diameter ($\text{PM}_{2.5}$). This thesis investigates the air quality in Dammam, Saudi Arabia, including assessment of the air pollution climatology in Dammam using monitoring data from two stations for the period 2016-2019, and primary measurement of particulate matter ($\text{PM}_{2.5}$) composition, sources and toxicity. $\text{PM}_{2.5}$ was collected on Teflon and quartz filters in the winter and summer from two locations in Dammam.

$\text{PM}_{2.5}$ mass concentration and composition were mainly influenced by crustal elements derived primarily from desert and dust storms. Average $\text{PM}_{2.5}$ mass concentrations doubled in the summer compared to the winter and were (on average) three times higher during dust storms than non-dust storm periods. In general, the mean concentrations of most of chemical components of PM were higher in the summer than in the winter. The impact of dust storms on $\text{PM}_{2.5}$ composition was studied. This analysis showed that dust storms increased the concentration of crustal species in $\text{PM}_{2.5}$ by five times, compared to non-dust samples. The mean concentration of organic carbon (OC) was significantly higher during dust storms. The influence of dust storms on most anthropogenic

species in PM was limited. Secondary aerosols and OC were the most abundant components of PM_{2.5} in Dammam, under non-dust periods.

PM sources were identified using positive matrix factorisation, based upon detailed chemical composition data. Six factors were estimated to be the sources of PM_{2.5}. These factors were identified as crustal elements, a nitrate-rich factor, a sulfate-rich factor, sea salt, traffic and biomass burning factors. In addition, the sources of PM_{2.5} in Dammam excluded the data affected by dust storms data, demonstrating the high contribution of anthropogenic sources, compared with natural sources.

The toxicity of PM_{2.5} in Dammam was measured in vitro using the dithiothreitol (DTT) assay. The results illustrated a negative correlation between crustal elements abundance and DTT activity per unit PM mass (DTT_m). DTT_m values were lower for dust storm periods than non-dust storms, and DTT_m had an inverse correlation with total PM mass. A strong correlation was observed between DTT activity per unit air volume (DTT_v) and PM mass concentration. These results provide insight into the toxicity of the constituents of the particles. Thus, linking the predicted health impacts of aerosols to oxidative potential (OP) may be more relevant than considering PM mass concentrations only. In addition, the contribution of sources of PM to DTT values was investigated using PMF. The traffic emission source showed the highest contribution to DTT_m, although the traffic factor was the smallest contributor to the PM_{2.5} mass concentration. Crustal sources, which contributed to 40% of PM_{2.5} in Dammam, have the lowest contribution (6%) to DTT_m. Anthropogenic sources account for 86% of DTT_m and 60% of DTT_v (and hence the health impacts of PM).

Acknowledgements

First and foremost, I am very thankful to Allah for reaching this point of my life.

In this part I would like to thank many people for helping me and standing with me during this journey. Many thanks to my father and mother for their support, trust and patient as they are the most to whom I dedicate this work. Thank you to brother and sisters for their support. Special thanks to wife Ghadeer alwadei for standing with me all these years. Thanks for her love, time and patient, and thanks for helping me specially during the time of COVID-19 where I did most of my work from home. Thanks to the candles of my life my daughters Mohrah and Lubna. In some cases, words are not enough to thank people; however, they are the least that can describe the appreciation. Special thanks to my supervisors Bill Bloss and Zongbo Shi for all their help and support during this work. Bill and Zongbo have been great supervisors providing me with all the knowledges, supports and advises.

Also, I would like to thank many people who helped me for the lab work. Thanks to Louisa Kramer, Leigh Crilley, Salim Alam, Nick Davidson and Eimear Orgill. Thanks to my colleague Steven Thompson with whom we spent more than a year in the lab developing the DTT assay. Thanks to Deepchandra Srivastava for helping me running the PMF model. I am sorry if I forget anyone, but all the help and efforts are really appreciated.

Finally, I would like to thank Imam Abdulrahman Bin Faisal University in Saudi Arabia for funding and supporting me from the first day of my PhD.

List of abbreviations

AA	Ascorbic acid assay
CMB	Chemical mass balance
CRM	Certified reference material
CV	Coefficient of variation
DIW	deionised water
DTNB	5,5'-Dithiobis (2-nitrobenzoic acid)
DTT	dithiothreitol assay
EC	Elemental Carbon
EEA	European Environmental Agency
EDTA	Ethylene Diamine Tetraacetic Acid
EF	Enrichment factor
EPA	Environmental protection agency of America
ESR	Electron spin resonance
GSH	glutathione assay
IAU	Imam Abdulrahman Bin Faisal University
IC	Ion chromatography
MDL	Method detection limit
MEWA	Ministry of Environment, Water and Agriculture

NCEC	National centre for environmental compliance
OC	Organic carbon
OP	Oxidative Potential
PM	Particulate matter
PME	Presidency of Meteorological and Environmental
PMF	Positive matrix factorisation
PQN	Phenanthrenequinone
RH	Relative humidity
RTLFL	Respiratory tract lining fluid
ROS	Reactive oxygen species
SA	Saudi Arabia
SOA	Secondary organic aerosol
SPM	Suspended particulate matter
TCA	Trichloroacetic acid
TSP	Total suspended particles
UK	United Kingdom
VOC	volatile organic compound
WHO	World Health Organization
WSI	Water Soluble Ion
WSOC	Water soluble organic carbon

Table of contents

Contents

Chapter 1 . Introduction and Literature Review	1
1.1 Introduction:	1
1.1.1 Particulate Matter Characteristics: Size	4
1.1.2 Particulate Matter Characteristics: Form in the Atmosphere	6
1.1.3 Particulate Matter Characteristics: Sources	7
1.1.4 Particulate Matter Characteristics: Composition.....	9
1.2 Studies of Airborne Particulate Matter in Saudi Arabia.....	11
1.2.1 Particulate Matter Mass Concentration in Saudi Arabia:	14
1.2.2 Particulate Matter Composition in Saudi Arabia:	18
1.2.3 Sources of Particulate Matter in SA:	20
1.2.4 Dammam, Saudi Arabia:	24
1.3 Oxidative Potential (OP).....	28
1.3.1 Methods of measuring oxidative potential.....	29
1.3.2 Correlation between Oxidative Potential and health end point:	30
1.3.3 Effect of PM Component on Oxidative Potential:.....	32
1.4 Objectives of the Thesis	34
Chapter 2 . Materials and Methods.....	36
2.1 Location.....	36
2.1.1 Meteorological Conditions:.....	37
2.1.2 Sampling Locations:	39
2.1.3 PM Sampling campaigns:	41
2.2 Filter preparation	43
2.3 Samplers.....	44
2.4 Lab analysis	44
2– 10 cm ²	45
2.4.1 Organic Carbon and Elemental Carbon (OC/EC):.....	45
2.4.2 Water soluble Ions (WSI):	48
2.4.3 Metal Analyses	51
2.5 Toxicity	56
2.5.1 OP Assay development:	57
2.5.2 Final Method:.....	61
Chapter 3 . Analysis of the air pollution climate in Dammam (2016-2019)	67
3.1 Introduction	67

3.2	Data Analysis.....	70
3.3	Results and Discussion	72
3.3.1	Seasonal Pattern:	72
3.3.2	Weekly patterns.....	75
3.3.3	Diurnal pattern:.....	78
3.3.4	The effect of wind speed and direction on pollutants in Dammam:	81
3.4	Conclusions	85
Chapter 4 . Chemical characteristics and source apportionment of particulate matter (PM _{2.5}) in Dammam, Saudi Arabia.....		
4.1	Introduction	87
4.2	Materials and Methods.....	91
4.2.1	Sampling:.....	91
4.2.2	Laboratory Analyses:.....	92
4.2.3	Data Approaches:.....	94
4.3	Results and Discussion	96
4.3.1	PM _{2.5} Mass Concentration:	96
4.3.2	Organic Carbon and Elemental Carbon (OC and EC):	99
4.3.3	Water Soluble Ions (WSI):	100
4.3.4	Crustal and Trace Metals:	102
4.3.5	Mass Closure:	104
4.3.5	PM _{2.5} Sources in Dammam:.....	106
4.3.6	Impact of Dust Storms on PM _{2.5} Composition and Sources:.....	115
4.4	Conclusion.....	121
Chapter 5 . Oxidative potential of PM _{2.5} in Dammam, Saudi Arabia: seasonal variation, chemical composition association and source apportionment.....		
5.1	Introduction	123
5.2	Methodology.....	126
5.2.1	Sampling:.....	126
5.2.2	Organic Carbon and Elemental Carbon analysis (OC and EC):.....	126
5.2.3	Water Soluble Ion (WSI) Concentrations:	127
5.2.4	Metal Analysis:	127
5.2.5	Filter Extraction for DTT Assay:	127
5.2.6	DTT assay:	128
5.3	Results and Discussion	129
5.3.1	OP Activity overview:	129
5.3.2	Association between OP and PM Chemical Composition:.....	132

5.3.3	Impact of dust storm on DTT:	136
5.3.4	Source Apportionment of OP:.....	139
5.4	Conclusions	145
Chapter 6	. Conclusions.....	147
6.1	Summary	147
6.2	Conclusion.....	154
6.3	Limitations.....	156
6.4	Suggestions for Future Research	157
Bibliography	159

List of Figures

Chapter 1

Figure 1.1 Production, growth and removal of PM in the atmosphere (Jacob, 1999).	5
Figure 1.2 Particle size and type of particle(Biegalski <i>et al</i> , 2013)	6
Figure 1.3 Map of Saudi Arabia with the location of the country in the right top corner (Munir <i>et al.</i> , 2016)	12
Figure 1.4 Summary of PM _{2.5} composition in SA obtained from literature mentions above where SIA means secondary inorganic aerosol.	20
Figure 1.5 The average of PM _{2.5} sources in SA based on previous literature.	23
Figure 1.6 Map shows administrative provinces and the location of Dammam to SA (Vincent, 2008b).	25
Figure 1.7 Map showing Dammam and its surrounding areas (Google map).	25
Figure 1.8 Wind rose plot showing the percent of wind direction and speed in Dammam from 2008-2018.	26
Figure 1.9 Windrose plot shows the percent of wind direction and speed for each season in Dammam from 2008-2018.....	27

Chapter 2

Figure 2.1 Windrose shows the wind direction and speed during the winter campaign for the period from 15/12/2017 to 20/02/2018.....	37
Figure 2.2 Windrose shows the wind direction and speed during the summer campaign for the period from 15/06/2018 to 20/08/2018	38
Figure 2.3 3D map shows the location of Amanah building.	39
Figure 2.4 MiniVol samplers during winter campaign on the roof of Amanah during normal and dusty days	40
Figure 2.5 3D map shows the location of Imam Abdulrahman Bin Faisal University.	41
Figure 2.6 MiniVol samplers collecting samples at the University location during normal and dusty days.	42
Figure 2.7 Schematic diagram of the DRI Model 2015 Multiwavelength Thermal/Optical Carbon Analyser (DRI, 2015).....	46
Figure 2.8 Scatter graph of the chloride standard prepared for anion analysis.	49
Figure 2.9 scatter graph illustrates the correlation between UV/Vis absorbance and time.	58
Figure 2.10 Scatter graph illustrates DTT consumed per time.	59
Figure 2.11 Scatter graph shows the slope of DTT consumption vs. time.....	60
Figure 2.12 An example of scatter graph for the slope of DTT against time using DIW.....	64
Figure 2.13 An example of scatter graph for the slope of DTT against time using PQN as a positive standard.	64
Figure 2.14 Scatter graph of DTT concentration vs. absorbance.....	65
Figure 2.15 Scatter graph of slope of sample collected from Amanah on 18/07/2018.	66

Chapter 3

Figure 3.1 time series of annual cycle of pollutants from 2016 to 2019 from Corniche station.	72
Figure 3.2 time series of annual cycle of pollutants from 2016 to 2019 from Rakkah station.....	74

Figure 3.3 Weekly pattern for mean hourly concentration from Corniche station.....	75
Figure 3.4 Weekly pattern for mean hourly concentration from Rakkah station.	77
Figure 3.5 Diurnal pattern for mean hourly concentration from Corniche station.....	79
Figure 3.6 Diurnal pattern for mean hourly concentration from Rakkah station.....	81
Figure 3.7 Polar plot of NO ₂ from a) Corniche and b) from Rakkah stations.....	82
Figure 3.8 Map shows the location of Corniche and Rakkah stations and possible sources of pollutants	83
Figure 3.9 Polar plot of NO from a) Corniche and b) Rakkah stations.....	84
Figure 3.10 Polar plot of SO ₂ from Rakkah station.	85

Chapter 4

Figure 4.1 The PM _{2.5} concentration ($\mu\text{g}/\text{m}^3$) timeseries for Amanah (blue line) and University (orange line) sites during the summer and winter sampling 2018 seasons.....	98
Figure 4.2 The OC and EC time series in the PM _{2.5} mass for Amanah (blue and orange lines) and university (grey and yellow lines) sites during the summer and winter sampling 2018.	99
Figure 4.3 Total measured WSI mass and the percentage contribution of such ions to PM _{2.5} mass for Amanah and University sites during summer and winter 2018.	101
Figure 4.4 Mean mass (blue bars) and percentage contribution (orange bars) of total measured metals for Amanah and university sites during summer and winter 2018 sampling seasons.	104
Figure 4.5 Major chemical components of PM _{2.5} in Dammam collected in the winter and summer of 2018 where “Crustal” is the sum of Al ₂ O ₃ , Fe ₂ O ₃ , MnO, TiO ₂ , CaCO ₃ and estimated SiO ₂ , “Other Ions” is the sum of Mg ²⁺ , Na ⁺ , K ⁺ and Cl ⁻ , “Other Metals” is the sum of Co, Cu, Ni, V, As, Sr, Sn, Sb, Ba and Pb.	106
Figure 4.6 Enrichment factor for PM _{2.5} concentration for Amanah and University sites during summer and winter 2018 sampling seasons.....	107
Figure 4.7 Factor profiles for the factors identified with the PMF analysis. Blue bars refer to the concentration ($\mu\text{g}/\text{m}^3$), whereas red squares refer to the percentage contribution of each species.	109
Figure 4.8 Timeseries of the contribution of Factor one.	111
Figure 4.9 Pollution rose graph of the biomass burning factor at the Amanah (left) and the university (right).	113
Figure 4.10 Timeseries of the contribution of Factor Five.....	114
Figure 4.11 Timeseries of the contribution of Factor Six.....	115
Figure 4.12 Crustal metals’ total mass and contribution to PM _{2.5} during dust and non-dust samples.	119
Figure 4.13 Trace metals’ total mass and contribution to PM _{2.5} during dust and non-dust samples.	119
Figure 4.14 Relative contribution of different factors to PM _{2.5} mass during non-dust days (inner circle) compared to all days (outer circle).	120

Chapter 5

Figure 5.1 Average of DTTm values at Amanah and University in the winter and summer. shaded range shows the interquartile range, dark black horizontal line in the middle shows the median, black horizontal lines at the top and bottom of the shaded range show the upper and lower quartile,

the two horizontal lines at the top and bottom show the maximum and minimum and the circular points show the outlier data.....	129
Figure 5.2 Average DTTv values at Amanah and University in the winter and summer. shaded range shows the interquartile range, dark black horizontal line in the middle shows the median, black horizontal lines at the top and bottom of the shaded range show the upper and lower quartile, the two horizontal lines at the top and bottom show the maximum and minimum and the circular points show the outlier data.....	130
Figure 5.3 Relative factor contributions to oxidative potential (DTTm values) and to PM _{2.5} mass concentrations – obtained from all data.	141
Figure 5.4 Relative factor contributions to oxidative potential (DTTv values) and to PM _{2.5} mass concentrations – obtained from all data.	143
Figure 5.5 Relative factor contributions to oxidative potential DTTv values and to DTTm values– obtained from non-dust storm samples only.	145

List of Tables

Chapter 1

Table 1.1 Mean PM mass concentrations and standard deviation (SD) in different cities of SA.	14
Table 1.2 The correlation between different OP assays and health end outcomes.....	30

Chapter 2

Table 2.1 Overview of meteorological parameters for the winter and summer campaigns.	38
Table 2.2 Type and area of filters used for each experiment.	45
Table 2.3 MDL of measured WSI.....	51
Table 2.4 MDL and recovery percent of metals measured by ICP-MS.	53
Table 2.5 concentrations (ppm) of standard metals prepared in the lab for the ICP-MS analysis.....	54

Chapter 3

Table 3.1 Percent of measurements removed.	71
Table 3.2 Mean daily concentration of pollutants at Corniche and Rakkah stations and p value (using paired t.test) comparing these pollutants between the two locations.....	78

Chapter 4

Table 4.1 Mean concentrations and standard deviation of PM _{2.5} , metals, water soluble ions, OC and EC at Amanah and University sites during the winter and summer 2018 campaigns.....	96
Table 4.2 percentage contribution of each species to different factors.	110
Table 4.3 The mean PM _{2.5} concentration and its composition in samples of non-dust storm and dust days.	117

Chapter 5

Table 5.1 comparing mean of DTTm, DTTv and PM _{2.5} mass concentration of this work and earlier studies.....	132
---	-----

Table 5.2 Pearson correlation coefficient (r) and p-values between OP activity and PM _{2.5} mass and composition.	133
Table 5.3 Pearson correlation coefficient (r) between daily PM _{2.5} and each chemical component of all data, dust storm samples, and non-dust storm samples.....	137

Chapter 1. Introduction and Literature Review

The introductory chapter provides definitions of air pollution and an introduction to particulate matter, including size, type, composition and sources. This thesis studies the air quality in Dammam, Saudi Arabia, and thus reviews the current understanding of atmospheric particulate matter in Saudi Arabia from the literature. The use of Oxidative Potential as a candidate proxy metric to assess particulate matter toxicity will also be discussed.

1.1 Introduction:

According to Brimblecombe (1987), human-induced air pollution first became an issue after the invention of fire and it has been ever since. Perhaps the concern about air quality has been noticed by humans from the colour of the air or from difficulty breathing. The World Health Organization (WHO) defines the air pollution as (WHO, 2018a):

“The presence of one or more contaminants in the atmosphere, such as dust, fumes, gas, mist, odour, smoke or vapour, in quantities and duration that can be injurious to human health”.

The definition given by the WHO focuses only on the impact on human health; however, air pollution can produce harm to animals, plants and other environmental components. The European Environmental Agency (EEA) defines air pollution as (EEA, 2021):

“The presence of contaminant or pollutant substances in the air at a concentration that interferes with human health or welfare or produces other harmful environmental effects.”

This definition involves all possible impacts from air pollution. A further definition, which includes the sources of air pollution, was written by Weber (1982) as

“The presence of substances in the ambient atmosphere, resulting from the activity of man or from natural processes, causing adverse effects to man and the environment”

There are many definitions of air pollution, all with a common basis about the existence of substances in the air that can harm human health, animals, plants and other environmental components, such as water and soil. Once a pollutant of a size that can be inhaled is the air, it is inevitable that it will enter the human body - as breathing is not optional.

After the use of coal and the industrial revolution, many air pollution events occurred, leading to experts paying more attention to air quality. More than 60 deaths in 1930 in the Meuse Valley, Belgium occurred because of the very high levels of air pollution from industries. Further, 20 people died and more than 6000 people became sick in 1948 in Donora, Pennsylvania (USA) from industrial air pollution and more than 4000 people died in 1952 as a result of the London smog event (Tiwary and Williams , 2010). These are examples of many historical air pollution events occurred, and many more are recently being observed in megacities, as a result of urbanization. The occurrence of these events has led to many regulations being put in place to mitigate air pollution and protect public health and the environment. Thus, regulations have been improved based on the knowledge and technology available alongside the efforts of scientists who try to explore air pollutant processes in detail.

Understanding the environment in any area is a key factor to protect human health. Air pollutant measurements are necessary to understand the environment of any area. Air quality is one of the most important environmental parameters and is the highest environmental threat to human lives (Sofia *et al.*, 2020). The World Health Organization (WHO) estimated that over than 91% of the 2016 global population was exposed to air pollution levels that exceeded WHO guidelines, and that outdoor ambient air pollution was estimated to cause more than four million premature deaths each year (WHO, 2018b). The emission of air pollutants from different sources is not constant as it increases and decreases based on human activities and the type of sources in the urban area. Knowing and studying air quality patterns and temporal variation is essential for air pollution control, protection of human health and examining the impact on people and the environment.

Air pollutants are typically subdivided by the state of matter, which is either gaseous or particulate. There are specific measurement methods for some gases, such as sulfur dioxide (SO₂), nitrogen dioxide (NO₂), carbon dioxide (CO₂) and ozone (O₃). However, particulate matter (PM) is a complex mixture present in the air with different composition, sizes and shapes. PM consists of a high number of compounds, including organic materials, secondary inorganic elements (e.g. sulfate and nitrate), black carbon, trace metals, sea salt and crustal materials (Guevara, 2016a). In addition, PM can be primary or secondary in nature. The next sections discuss PM size, form in the atmosphere, sources, composition and health impacts.

1.1.1 Particulate Matter Characteristics: Size

The size of PM is important to determine how far the particles can travel in the air, how long the particle can stay in the atmosphere and how far the particle can deposit in the human respiratory system. In general, PM exists in the air as fine and coarse particles. Coarse mode particles have a diameter (d) of more than $2.5 \mu\text{m}$, while fine mode particles have a d less than $2.5 \mu\text{m}$. Fine mode particles are further subdivided into nucleation mode ($d < 0.001 \mu\text{m}$), Aitken mode ($d \approx 0.01 - 0.1 \mu\text{m}$) and accumulation mode ($d \approx 0.1 - 1 \mu\text{m}$) (Hewitt et al, 2009).

Nucleation mode particles, that are emitted as primary particles emit directly from the sources or formed in the atmosphere, are present in high numbers in the air. These particles can coagulate either with other fine particles or with coarse particles in the atmosphere to form accumulation mode particles, as can be seen in Fig1.1. Accumulation mode particles have a longer lifetime in the atmosphere than other modes because they are less impacted by natural removal methods, such as rain or dry deposition processes (Harrison, 2015). Accumulation mode particles usually originate from the condensation of gases and tend to accumulate in the size range $0.01-1 \mu\text{m}$ (Jacob, 1999). Ultrafine particles with a diameter of less than $0.1 \mu\text{m}$ are commonly found near sources, and their concentrations decline rapidly with distance away from the source (Seinfeld, 2016). Most of the nucleation mode particles are formed from gas-to-particle conversion or condensation processes, while Aitken and accumulation modes are formed from condensation or coagulation (Hewitt et al, 2009).

Coarse particles are usually primary particles produced from mechanical processes such as, wind erosion and crushing and grinding (Tiwarly et al, 2018). Plant fragments, pollen, sea salt and wind-blown dust particles usually have a size that is larger than $1\ \mu\text{m}$, while particles, that are formed in the atmosphere via photochemical processes, are typically smaller than $1\ \mu\text{m}$ (Seinfeld, 2016).

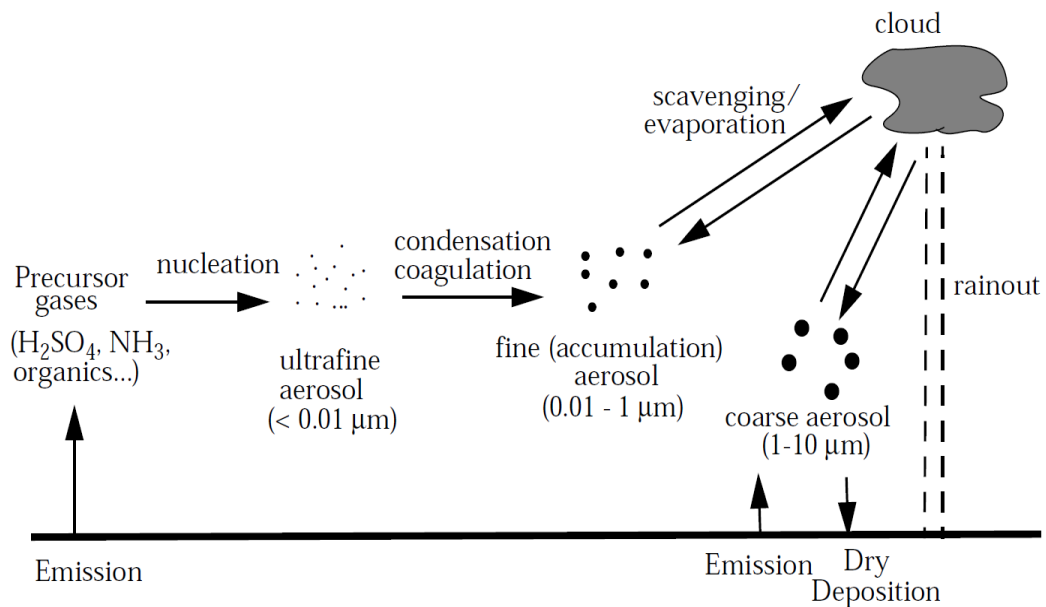


Figure 1.1 Production, growth and removal of PM in the atmosphere (Jacob, 1999).

Regulations and policies of air quality are typically based on the mass of PM_{10} (particle matter with an aerodynamic diameter less than $10\ \mu\text{m}$) and $\text{PM}_{2.5}$ (particle matter with an aerodynamic diameter less than $2.5\ \mu\text{m}$), as these sizes can be inhaled inside the respiratory system and impact human health (Allan *et al.*, 2003; Zereini and Wiseman, 2010). Ultrafine particles (with an aerodynamic diameter of less than $0.1\ \mu\text{m}$) may make up a small proportion of the total mass, however, they probably have greatest health consequences because of their

capability to enter into the bloodstream and their bigger reactive surface area is able to produce greater damage to the body (Zereini et al, 2010).

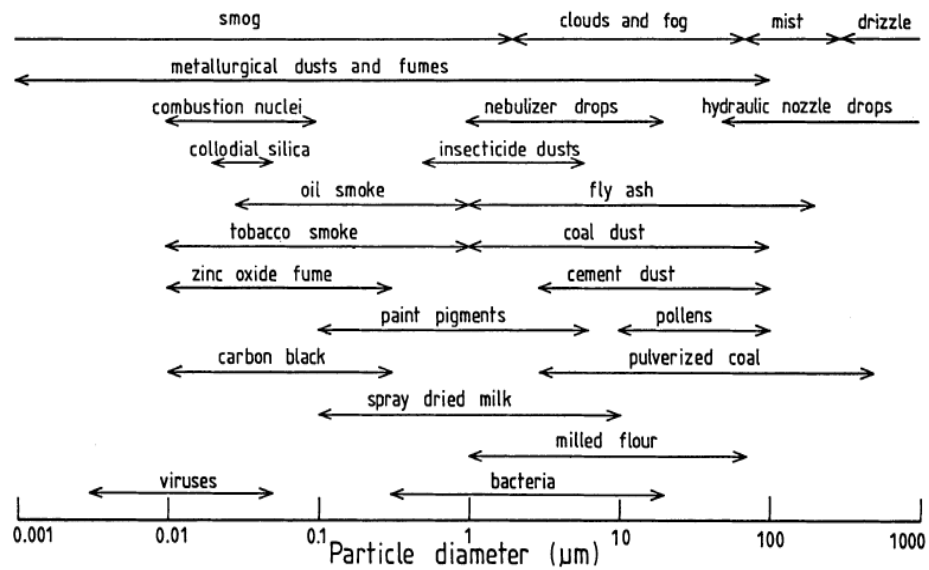


Figure 1.2 Particle size and type (Biegalski *et al*, 2013)

1.1.2 Particulate Matter Characteristics: Form in the Atmosphere

There are many types of PM based on their physical form and their formation method. Some of these types are (Biegalski *et al.*, 2013; Tiwary *et al*, 2018):

- Suspended particulate matter (SPM) or total suspended particles (TSP): these refer to total particles without specific size.
- Particulate matter (PM): particles with specific sizes as described above.
- Aerosols: suspension of solid or liquid particles in the air (in this thesis the term aerosols is used to refer to the particles).
- Dust: solid particles that are formed by mechanical processes from natural soil.
- Smoke: visible particles formed via an oxidation process, such as incomplete combustion.

- Fog and mist: suspended liquid particles formed by the disintegration or evaporation of liquid.
- Smog: this term refers to the combination of smoke and fog. Smog consists of liquid and solid particles made from photochemical reactions.

1.1.3 Particulate Matter Characteristics: Sources

PM can be emitted into the air from natural sources, such as sea spray, volcanic emission and mineral dust from arid areas, and anthropogenic sources, such as oil combustion, industry and traffic emissions (Hewitt and Jackson, 2009; Von Schneidmesser *et al.*, 2015). Natural sources contribute to background PM values and are difficult to control, while anthropogenic sources contribute to the PM values from human activities (Theodore, 2008). Some particles are clearly emitted from natural sources, such as volcanic dust and soil dust (mostly naturally occurring), and other particles are clearly emitted from human-made sources, such as industrial processes. Some particles can be emitted from both natural and anthropogenic sources (e.g. biomass burning) meaning differentiating between natural or anthropogenic sources is difficult (Biegalski *et al.*, 2013).

Particles are found in the atmosphere as either primary aerosols, which are emitted directly from the source to the air, or secondary aerosols, which are formed in the atmosphere as a result of a chemical or physical transformation (Hewitt *et al.*, 2009). Sulfur dioxide emissions from power stations and carbonaceous emissions from diesel engines are an example of primary pollutants. Oxidation of sulfuric acid from sulfur dioxide and forming nitric acid from nitrogen dioxide in the atmosphere are examples of secondary pollutants (Harrison, 2015).

Aerosols in urban areas are a mixture of primary particles from industries, power plants and vehicles, beside the natural sources and secondary particles formed in the air. Most of the PM number in urban areas are the accumulation mode size (0.1-1 μm) and coarse particles while small volume of Aitken and nucleation modes are found in these areas (Seinfeld, 2016). On the other hand, rural aerosols, which are away from air pollution sources, are mainly influenced by natural sources with a moderate impact from human-made sources.

Sea salt particles are formed at the air-sea interface from bursting bubbles (Seinfeld, 2016). When seawater droplets are in the air they evaporate and concentrated saline particles are formed (Biegalski *et al*, 2013). A range of 1-3 x 10⁴ Tg/ year of sea spray particles are estimated to be produced globally (Seinfeld 2016).

Road transport is considered as one of the main contributors to PM as this source is responsible for 40-50% of PM in the urban areas (Guevara, 2016b). PM is emitted from road transport from the combustion of fuel (gasoline or diesel), referred to as exhaust emissions. Alternatively, PM can be emitted from the interaction between vehicular tyres and the road surface, known as non-exhaust emission, and includes grinding, crushing, corrosion and abrasion of brake wear, tyre wear and road surface wear. The quantity of pollution emitted by vehicles is usually impacted by the engine type, fuel property, engine age, technology used in the vehicle to mitigate emissions, environmental conditions, vehicle weight and driving style. For instance, diesel vehicles exhaust emit significantly more PM than gasoline vehicles, and heavy-duty diesel vehicles produce a higher amount of PM compared to other diesel vehicles (Guevara, 2016b).

Fossil-fired power plants, refineries and industrial activities contribute to a considerable amount of PM emission, especially in urban areas. In Europe, these activities are responsible for the second largest sources of air pollution, accounting for 28% and 21% of primary PM₁₀ and PM_{2.5}, respectively (Guevara, 2016b). Many industrial activities emit PM, including manufacturing (fuel combustion, smelting, furnaces and welding) and non-manufacturing (mechanical treatment of raw material, handling, storage, and transport of dusty materials) processes.

1.1.4 Particulate Matter Characteristics: Composition

The composition of PM varies based on the time and location. Secondary aerosols that are produced by photochemical processes, such as sulfate, often have high mass concentrations in the PM during summertime. The contribution of organic particles to PM is usually larger in the wintertime because of burning fuel for heating and the lower boundary layer resulting in less mixing/dilution. Moreover, diurnal variation is observed for some elements where some particles increase at midday, preferring high temperatures, and decrease rapidly after sunset. Particles with mixed of different compositions is called external mixed particles, while particles with mixed of the same composition is called internal mixed particles.

Fine particles' main components are nitrate, sulfate, ammonium, carbonaceous material, lead, certain transition metals and organic and elemental carbon elements. Coarse particles' main components are crustal material, including silicon, magnesium, aluminium, calcium and iron, and biogenic

organic particles, including plant fragments, pollen and spores (Biegalski *et al.*, 2013; Seinfeld, 2016).

Mineral dust aerosols occur mainly from the wind action on loose soil in deserts and arid areas. Dust particles from dust storms with a diameter larger than 100 μm may not travel over long distances as they are only suspended for a short time. On the other hand, smaller particles with diameters of 0.1-5 μm can travel for longer distances up to 5000 km away from the source (Biegalski *et al.*, 2013). PM originated from wind-blown dust have a chemical composition close to the elements from the earth's crust such as iron, aluminium, silicon calcium and titanium.

The composition of PM is mainly influenced by the emitting source. PM emission from metal industries is rich with toxic heavy metals Pb, Cr, Cd, As, Zn and Ni. Significant fractions of P, Si, Al, Fe, Ca, K and Ti are emitted from coal combustion sources, and brake wear associated elements are Mg, Fe and Ba (Liang, 2013).

1.1.5 Particulate Matter Health Impacts

Acute and chronic exposure to fine particles has been linked with several human health impacts, including cardiovascular diseases, respiratory disorders, mortality and morbidity (Rai *et al.*, 2016; Shi *et al.*, 2019; Hama *et al.*, 2020). The World Health Organization (WHO) reported that more than 91% of the population in 2016 was exposed to air quality that exceeded the WHO guidelines (Global Air Quality Guidelines 2005 version). Further, in the same year the outdoor ambient air pollution was estimated to cause more than four million premature deaths globally each year (WHO, 2018b). The adverse health impact

of PM is most significant for vulnerable people, such as children, elderly people, those who are pregnant and people with chronic diseases, where even low concentrations of PM can cause harm.

The size and chemical composition of PM are thought to be the primary factor determining toxicity to humans, as smaller particles have a bigger health burden because they are more inhalable than the same mass of large particles (Crilley *et al.*, 2017). Studying the composition and sources of PM_{2.5} is critical for understanding the capability of these substances while harming people and the environment. Moreover, it has been suggested that low-toxicity outcomes are derived from soil dust and sodium chloride, although they make up the majority of the PM bulk (Borm *et al.*, 2007a; Kundu and Stone, 2014). In contrast, transition metals that make up a small portion of the total PM mass cause high-toxicity outcomes (Sørensen *et al.*, 2003; Borm *et al.*, 2007a; Kundu and Stone, 2014).

1.2 Studies of Airborne Particulate Matter in Saudi Arabia

Saudi Arabia (SA), formally known as Kingdom of Saudi Arabia, is in the southwest of Asia. SA has an area of 2,149,690 km², which is almost 9 times the area of the United Kingdom (Farahat, 2016). More than 90% of SA is desert (El-Mubarak *et al.*, 2014) where the country has three deserts namely Ad-Dahna desert, Nefud desert and Rub Al-Khali (Empty Quarter) desert. Saudi Arabia is home to more than 30 million people (GAS, 2021).

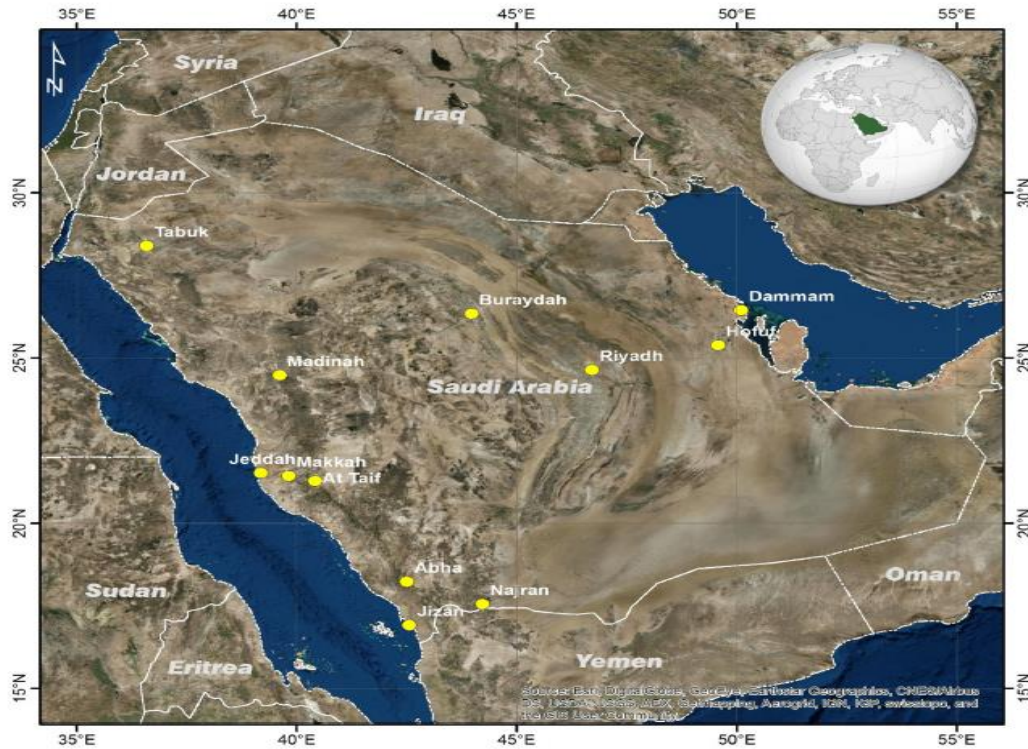


Figure 1.3 Map of Saudi Arabia with the location of the country in the right top corner (Munir *et al.*, 2016)

Dust storms are a frequent phenomenon that can occur any time in the year. They mostly occur in the hot months in the South of the country, and are more frequent in the spring in the North (Prakash *et al.*, 2015; Farahat, 2016). Dust emission is estimated to be 1019 ± 45 Tg every year globally (Miller *et al.*, 2004), which impact the air quality, visibility and radiation budget (Francis *et al.*, 2021). The occurrence of the dust storms is one of the most severe environmental issues in SA. In Riyadh (the capital city of SA), the air quality exceeded the Saudi Arabia's standards of PM by mass on approximately 600 days over a period of 5-years and more than two thirds of these days were due to dust storms (Alharbi *et al.*, 2013). The wide surface area of the desert, aridity and wind speed and direction increases the concentration of wind-transported dust from the desert to inhabited areas. Particles from dust storms can stay for hours or days in the air.

The SA climate is arid to semi-arid apart from the southwest part of the country, which is semi-arid area (Nayebare *et al.*, 2018). The country rarely experiences rain, with a precipitation annual average of 82.4 mm, while the driest location in England (Essex, Cambridgeshire and Suffolk) records 550 mm annually (Milleret al, 2004). However, some areas in SA recorded their total annual precipitation in just few days from heavy intense rainfall (Almazroui *et al.*, 2012). Rainfall usually occurs in the winter whilst the summer is generally dry. Summer in SA is characterised by very hot temperatures reaching 50 °C with a hazy sky (Vincent, 2008). Winter is the season of precipitation and mild temperatures during the day, with temperatures getting colder at night, often falling below 0 °C. Spring and fall are similar as they are transition periods characterised by warm days and mild to cool nights.

According to the Ministry of Environment, Water and Agriculture (MEWA, 2017), the first agency that was responsible for the environment in SA was the Directorate General of Meteorological which was established in 1950. This directorate was restructured in 1981 to become the Department of Meteorological and Environmental Protection. In 2001, the department was reformed to become the General Presidency of Meteorological and Environmental protection (PME), which was under the Ministry of Defence. The main role of PME was to give environmental permits for industries and workshops and represented SA internationally. PME became an independent agency in 2017 when its name changed to the General Authority for Meteorological and Environmental protection. This independence offered more freedom and power to this organisation that reflected on the environmental law and implications in SA. In 2019, the responsibilities and roles of PME were

relocated to four new centres: (i) the National centre for environmental compliance (NCEC), (ii) the National Centre for Wildlife, (iii) the National Centre for Meteorology, and (iv) the National Centre for Vegetation Cover and Combating Desertification. These four centres are part of the Ministry of Environment, Water and Agriculture (MEWA). NCEC works to enhance the environmental standards and regulations to protect the environment and public health, and assesses pollution in the country; having the authority to take actions against uncommitted and unpermitted activity.

1.2.1 Particulate Matter Mass Concentration in Saudi Arabia:

Much literature has indicated a high level of PM in SA mainly due to vehicular emission, rapid urbanisation, industrial activities and the influence of the arid climate (Nayebare *et al.*, 2016). Table 1.1 provides the mean PM mass concentrations in different cities of SA found in the literature.

Table 1.1 Mean PM mass concentrations and standard deviation (SD) in different cities of SA.

Reference	City	time	PM size and concentration ($\mu\text{g}/\text{m}^3$) \pm SD
(Nayebare <i>et al.</i> , 2018)	Makkah	Spring 2014	PM _{2.5} = 113 \pm 67
		Summer	PM _{2.5} = 88 \pm 36
		Fall	PM _{2.5} = 67 \pm 24
		Winter	PM _{2.5} = 67 \pm 36
(Nayebare <i>et al.</i> , 2016)	Rabigh	May- June 2013	PM _{2.5} = 37 \pm 16

(Harrison <i>et al.</i> , 2017)	Jeddah	June 2011- June 2012	PM _{2.5} = 20.7 PM ₁₀ = 108
(Khodeir <i>et al.</i> , 2012)	Jeddah	June – September 2011	PM _{2.5} = 28.4 ± 25.4 PM ₁₀ = 87.3 ± 47.3
(Lim <i>et al.</i> , 2017)	Jeddah	June 2011- May 2012	PM _{2.5} = 21.9 ± 11.6 PM ₁₀ = 107.8 ± 72.6
(Shaltout <i>et al.</i> , 2015)	Taif	October 2011 to June 2012	Industrial site PM _{2.5} = 57 Residential site PM _{2.5} = 37 High traffic site PM _{2.5} = 50
(Alharbi, Shareef and Husain, 2015)	Riyadh	September 2011- September 2012	PM ₁₀ = 289 ± 228
(El-sharkawy and Zaki, 2015)	Dammam	January 2012- December 2012	PM _{2.5} = 32.9 ± 31.5 PM ₁₀ = 81.7 ± 92.2

In Makkah, which accommodates for an influx of more than 4 million people in the Islamic months of Ramadan and Dhu Al-Hajjah (Islamic calendar), the average mass concentration of PM_{2.5} was lower in the fall (67 µg/m³) and winter (67 µg/m³), compared to the summer (88 µg/m³) and spring (113 µg/m³). This is due to the little rainfall in these two seasons (Table 1.1). The highest level of PM_{2.5} (260 µg/m³) was recorded in the month of Ramadan as the result of very

high traffic during this time. Harrison *et al.* (2017) found that the average mass concentration of PM₁₀ (108 µg/m³) was relatively larger than the average mass concentration of PM_{2.5} (20.7 µg/m³) in Jeddah. Also, in Jeddah, Khodeir *et al.* (2012) found the ratio of PM_{2.5}/PM₁₀ to be 0.33, significantly lower than many other places in Europe where PM_{2.5}/PM₁₀ is 0.60-0.70. The lower PM_{2.5}/PM₁₀ ratio in Jeddah could be because of the impact of desert dust that influences PM₁₀ more than PM_{2.5}. Lim *et al.* (2017) collected PM_{2.5} and PM₁₀ samples three times per week for one year (June 2011 – May 2012) from Jeddah and found that the average mass concentration of PM_{2.5} and PM₁₀ were 21.9 µg/m³ and 107.8 µg/m³, respectively. The highest seasonal average concentration of PM_{2.5} (23.4 µg/m³) and PM₁₀ (114 µg/m³) was observed in spring, while the lowest seasonal average concentration of PM_{2.5} (20.3 µg/m³) and PM₁₀ (83.1 µg/m³) was observed in fall. Further, for the weekly variation in Jeddah, PM_{2.5} was reduced by 15% and PM₁₀ was reduced by 25% in the weekends, compared to weekdays.

Taif is a mountain city in SA. The average PM_{2.5} mass concentration for samples collected from October 2011- June 2012 was 37 µg/m³ in a residential site, 50 µg/m³ in high traffic site and 57 µg/m³ in an industrial site located inside the city of Taif (Shaltout *et al.*, 2015). It has been found that the average concentration of PM_{2.5} in the summer was higher than that recorded in other seasons. In the capital and largest city of SA (Riyadh), the annual average mass concentration of PM₁₀ (289 µg/m³) was three times higher than the annual standard of PM₁₀ (80 µg/m³) in SA (Alharbi *et al.*, 2015). The authors in Riyadh divided their results into hot months (April – September) and cold months (October – March), and the average concentration of PM₁₀ was 84% higher in the hot months, compared to the cold months. The high concentration of PM in hot months compared to cold months in

Riyadh was attributed to the dust storms that are common in hot months and the little precipitation experienced. El-sharkawy and Zaki. (2015) studied the concentration of PM_{2.5} and PM₁₀ in Dammam using satellite reading “Horiba APDA-371 continuous particle Monitor” from January to December 2012. The average mass concentration of PM_{2.5} was 32.9 $\mu\text{g}/\text{m}^3$ and it was 81.7 $\mu\text{g}/\text{m}^3$ for PM₁₀. The highest average concentration of PM₁₀ in Dammam was recorded in fall (116 $\mu\text{g}/\text{m}^3$) followed by summer (91.9 $\mu\text{g}/\text{m}^3$), then spring (76.4 $\mu\text{g}/\text{m}^3$) and the lowest average concentration was in the winter (45 $\mu\text{g}/\text{m}^3$). The maximum average concentration for PM_{2.5} in Dammam was recorded in the summer (40 $\mu\text{g}/\text{m}^3$), then winter (29.5 $\mu\text{g}/\text{m}^3$), fall (29.5 $\mu\text{g}/\text{m}^3$) and the lowest was in spring (27.9 $\mu\text{g}/\text{m}^3$).

Munir *et al.* (2016) studied the PM_{2.5} concentration in twelve cities from different parts of SA for ten years from 2001 to 2010 using satellite images provided by the Moderate Resolution Imaging Spectroradiometer (MODIS). The authors concluded that the average PM_{2.5} concentrations have increased in ten cities over the ten years and only two cities showed a lower average PM_{2.5} concentration. Dammam had the highest increase among other cities, where the mean PM_{2.5} concentration was 24.1 $\mu\text{g}/\text{m}^3$ in 2001 and 42.9 $\mu\text{g}/\text{m}^3$ in 2009. Tabuk, located in the northwest of SA, had the lowest average PM_{2.5} concentration with an average of 9 $\mu\text{g}/\text{m}^3$. On average, the highest PM_{2.5} concentration in SA was in 2008 and 2009 while the lowest concentration was in 2001 and 2002.

PM mass concentration in SA is directly impacted by air temperature and precipitation as hot and dry months showed higher PM level than cold and wet months. Thus, this variation is mainly attributed to dust storms and resuspension

of soil. In addition, human activities during weekdays increases the PM level, compared to weekends which usually characterised by low anthropogenic influence. The difference between PM₁₀ and PM_{2.5} mass concentration was high in SA compared to European countries because of the natural impact of desert particles that contribute to PM₁₀ more than PM_{2.5}.

1.2.2 Particulate Matter Composition in Saudi Arabia:

In the holy city of Makkah, Nayebare *et al.* (2018) studied the metal composition of PM_{2.5} between February 2014 to January 2015. PM_{2.5} was dominated by crustal elements (Si, Ca, Fe, Al, K, Mg and Na) followed by high concentrations of sulfur (S) as the highest anthropogenic elements were detected in this place, indicating the influence of industrial emissions from Jeddah and Rabigh cities which were supplemented by air mass trajectories. Many other anthropogenic elements were also detected in Makkah, including Pb, Br, V, Ti, Zn, Ni, Sr, Ce, Lu, Er and Cr which are emitted primarily from vehicle and fuel combustion. More than 50% of PM_{2.5} mass in Rabigh was due to crustal elements, 31.8% from secondary ions (sulfate, nitrate, oxalate and ammonium), 4.5% from sea spray and 3.4% from black carbon, while anthropogenic trace elements explain only 0.64% (Nayebare *et al.*, 2016). The average concentration of crustal elements (Si, Fe, Ca, K, Sr and Ti) were high in Taif in March, compared to other months, and were impacted by natural sources, such as windblown dust. Trace elements (S, Cu, C, Zn and Pb) were not impacted by windblown dust as they showed constant levels, which indicate these elements were mainly from human activity sources (Shaltout *et al.*, 2015). Measured metals and black carbon were responsible for 24%, 34% and 36% of PM_{2.5} in Taif for industrial, residential and traffic sites, respectively. The average

contribution of metals and ions to PM₁₀ mass in Riyadh was 21.5% and 16.2%, respectively (Alharbi et al, 2015). Metals mass measured in Alharbi's work were dominated by more than 90% crustal elements (Al, Ca, Fe and Mg), and ions mass measured in this work were dominated by 70% SO₄²⁻, NH₄⁺ and Cl⁻. Crustal elements (Fe, Ti, Mn, Ca⁺² and Mg⁺²) were several folds higher in the summer than in the winter, while Na⁺, Cl⁻ and NO₃⁻ were higher in the winter than in the summer. Other ions (SO₄²⁻, K⁺ and NH₄⁺) had the same level in both seasons. In Jeddah, PM_{2.5} was dominated by S (45%), Si (13.7%), Pb (9.9%), Ca (7%), Fe (5.5%) and Al (5.1%) while PM₁₀ was dominated by Si (28%), Ca (18.4%), Fe (11.2%), S (10.2%), Al (8.7%) and Cl (6.9%).

The average concentration of OC and EC of PM_{2.5} collected on quartz filters from Riyadh in the period from April to September 2012 was $4.8 \pm 4.4 \mu\text{g}/\text{m}^3$ and $2.1 \pm 2.5 \mu\text{g}/\text{m}^3$, respectively (Bian *et al.*, 2017).

For the average of measured species in both PM₁₀ and PM_{2.5}, crustal elements (Ti, Al, Si, Fe and Ca) have been found to be 90% in PM₁₀ and 10% in PM_{2.5} for samples collected in Jeddah from June 2012 to June 2013 while anthropogenic elements (Ni, As, Pb and V) were 40-60% in PM_{2.5} (Harrison *et al.*, 2017). Similarly, Khodeir *et al.* (2012) found anthropogenic element S to be the main contributor to PM_{2.5} in Jeddah while Si was the main contributor to PM₁₀.

A summary of previous literature finding is presented in Fig 1.4. The pie chart was made from the average of the contribution of each source in literature then averaging similar sources. The composition of PM in SA is dominated by crustal (31%) and secondary inorganic aerosol (SIA, 29%). Anthropogenic

metals account for 15% of the PM composition which is attributed to large sulfur mass concentrations found in Jeddah and Riyadh. Ions also account for 15% and organic and elemental carbon (OC and EC) account for 6%. This summary shows the high contribution of crustal element to PM in SA as an arid area.

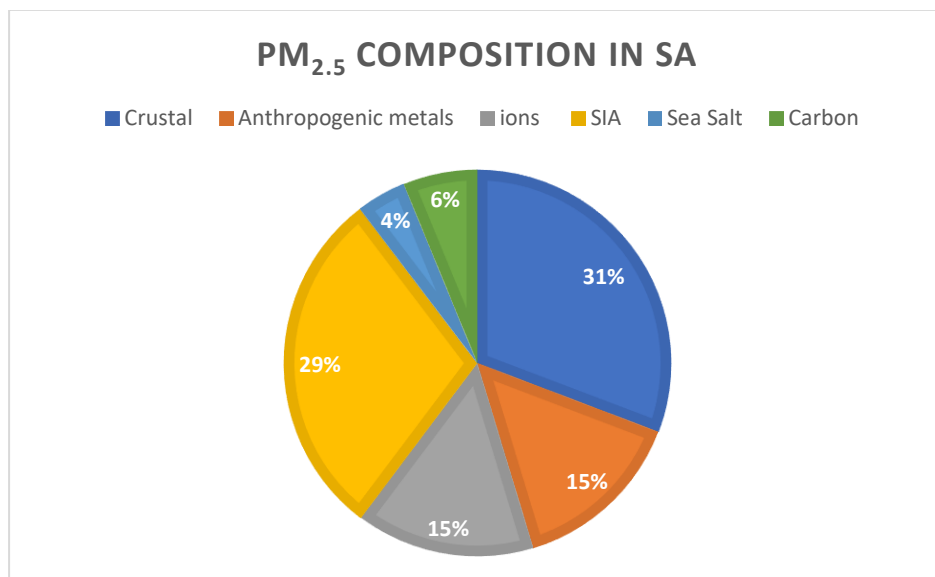


Figure 1.4 Summary of PM_{2.5} composition in SA obtained from literature mentions above where SIA means secondary inorganic aerosol.

1.2.3 Sources of Particulate Matter in SA:

Alongside dust storms as a natural source of PM in SA, many other anthropogenic sources, such as traffic emission, oil combustion, industrial activities, and commercial activities, negatively impact the PM level. Four factors of PM_{2.5} were identified in Makkah using positive matrix factorisation (PMF) including vehicular/automobile emission (30.1% of PM_{2.5}), industrial mixed dust (28.9% of PM_{2.5}), soil/earth-crust (24.7% of PM_{2.5}) and fossil-fuel/oil combustion (16.3% of PM_{2.5}) (Nayebare *et al.*, 2018). In Rabigh, an industrial city on the west coast of SA, five sources were suggested by PMF. The first was the Soil/Earth crust (39.9% of PM_{2.5}) dominated by Si, Al, Ti, Mn and Fe. The second source was fossil-fuel combustion (19.9% of PM_{2.5}) dominated by V, Ni,

Pb, NH_4^+ and SO_4^{2-} . The third source was industrial dust (14.7% of $\text{PM}_{2.5}$) dominated by Ca, Al, Fe Si and Cr. The fourth factor was vehicular emission (13.4% of $\text{PM}_{2.5}$) dominated by NO_3^- , $\text{C}_2\text{O}_4^{2-}$, V, Ni and BC and the fifth source was sea sprays (12.1% of $\text{PM}_{2.5}$) dominated by Cl^- and Na (Nayebare *et al.*, 2016).

Two studies have assessed sources of PM in Jeddah, the second largest city in SA. Khodeir *et al.* (2012) collected $\text{PM}_{2.5}$ and PM_{10} from 7 sites in Jeddah between June to September 2011 and identified the sources of $\text{PM}_{2.5}$ and PM_{10} using Varimax rotation. The authors reported five factors responsible for $\text{PM}_{2.5}$, including re-suspended soil (8.3% of $\text{PM}_{2.5}$) dominated by Si, Al and Fe. The second factor was emission of oil combustion (69% of $\text{PM}_{2.5}$) dominated by V, Ni and S. The third factor was traffic sources (3.7% of $\text{PM}_{2.5}$) dominated by Pb, Se and Br. The fourth factor was industry mix 1 (8.2% of $\text{PM}_{2.5}$) dominated by Cu and Zn. The fifth factor was industry mix 2 (0.4% of $\text{PM}_{2.5}$) dominated by Na and Cl. For PM_{10} , four factors contributed with the first including re-suspended soil (64% of PM_{10}) dominated by Si, Al and Fe. the second factor was mixed industrial (10% of PM_{10}) dominated by Zn, Cu, Br, S and Ca. The third factor was oil combustion (18% of PM_{10}) dominated by V, S and Ni. The fourth factor was coarse sea salt (9% of PM_{10}) dominated by Na and Cl. As mentioned earlier, PM_{10} in SA is influenced to great extent by crustal elements from soil than $\text{PM}_{2.5}$. Also, in Jeddah, Lim *et al.* (2017) collected $\text{PM}_{2.5}$ and PM_{10} for the period from June 2011 to May 2012 and investigated the sources of PM using applications of absolute principal component analysis (APCA). Four factors were identified to be responsible for $\text{PM}_{2.5}$ in Jeddah, including windblown soil/road dust (26.9% of $\text{PM}_{2.5}$) dominated by crustal elements (Al, Ca, Ti, Ni, Mn and Mg), residual oil

burning (63% of $PM_{2.5}$) loading on Ni, S and V, solid waste incineration (4.6% of $PM_{2.5}$) loading on Cu and Zn, and traffic emission (5.6% of $PM_{2.5}$) dominated by Pb. Three factors contributed to PM_{10} in Jeddah, including soil/road dust (77.3% of PM_{10}) loading on crustal elements (Si, Al, Mn, Mg, Ti, Fe, K and Ca), traffic emission (8.8% of PM_{10}) dominated by Pb and S and solid waste incineration (13.9% of PM_{10}) dominated by Cu and Zn. These two studies from Jeddah share some similarities and have some differences. The first study collected samples only in summertime while the second studied the PM for a whole year. In the study Khodeir *et al.* (2012) reported resuspended soil to be responsible for 8.3% of $PM_{2.5}$ while Lim *et al.* (2017) found soil to be 26.9% of $PM_{2.5}$ in Jeddah, suggesting that Jeddah was not impacted by dust soil in summer. This suggestion agrees with the $PM_{2.5}$ mass concentration reported in Makkah, located 60 km to the east of Jeddah, which had its highest concentration in the spring (Table.1.1). Moreover, as mentioned earlier, the northern part of SA is impacted by dust storms mostly in spring. Both studies agreed on the high contribution of oil combustion on $PM_{2.5}$ in Jeddah, and low contribution of traffic factors. A factor that was dominated by Zn and Cu was recognised in both studies, however, Khodeir *et al.* (2012) named it as industrial mix 1 while Lim *et al.* (2017) reported this factor as a waste incinerator source.

A summary of $PM_{2.5}$ sources in SA is provided in Fig 1.5. On average, oil combustion was the dominant source (37%) to $PM_{2.5}$ in SA. This high contribution of oil combustion was influenced by the two studies in Jeddah while this factor was responsible by 16.3% and 19.9% in Makkah and Rabigh, respectively. The second highest source of $PM_{2.5}$ mass in SA was crustal elements which was large in all studies. Industrial dust accounts for 15% of

PM_{2.5}, while sea salt and traffic sources account for 11% each and small contribution from waste incineration (4%). Waste incineration was only reported in one study (Lim *et al.*, 2017).

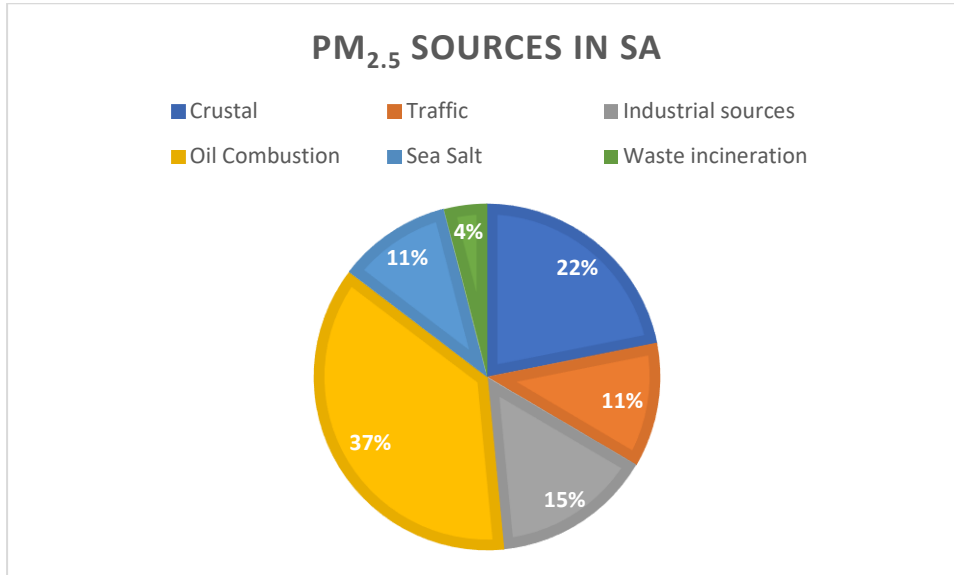


Figure 1.5 The average of PM_{2.5} sources in SA based on previous literature.

All the sources of PM studies in SA were done in the same region. Makkah, Jeddah and Rabigh are located to the western part of the country, and they are all in the same province (Makkah province). Nayebare *et al.* (2016) research in Rabigh was the only study that included sources of ions and OC and EC beside metals, while the other three studies only identified the sources of metal components of PM. No study has been conducted to investigate the sources of PM in Eastern SA. This study will be the first to explore sources of PM in Dammam city, which is the main city in Eastern SA.

In general, Saudi Arabia is divided administratively into thirteen regions. Each region has at least one branch of NCEC, air quality monitor stations and university. Yet, all literature that was found was carried out in three regions of SA. The majority of the literature studied the air quality in the western part of the

country (Jeddah and Makkah), with few studies in Riyadh and much less in the eastern part of SA. No studies have been found that examine the Northern and Southern areas of SA, which may be significantly different to the Western and Eastern parts of SA due to their different environment and potential sources.

1.2.4 Dammam, Saudi Arabia:

In this work, Air Pollution Climatology of Particulate Matter in Dammam, Saudi Arabia: Composition, Sources & Toxicity is reported from Dammam city. Dammam lies on the coast of Arabian Gulf at 26.43°N latitude, and 50.11°E longitude, and is the capital city of the Eastern province of Saudi Arabia. Dammam is home to more than one million people. Dammam is a part of what is called Dammam Metropolitan Area which includes Dammam city, Khobar city and Dhahran city. This wider metropolitan area is home to more than three million people. It is surrounded by the Arabian Gulf with King Abdulaziz seaport to the east, Aljubail industrial city, Ras Tanura (one of the largest oil refineries in SA), the Al Qatif city to the north, the Ad-Dahna desert to the west, and the cities of Dhahran and Al Khobar to the south. As the capital and central city of the eastern province, Dammam holds most of the commercial activities, government departments and manufacturing in the eastern province.



Figure 1.6 Map shows administrative provinces and the location of Dammam to SA (Vincent, 2008b).

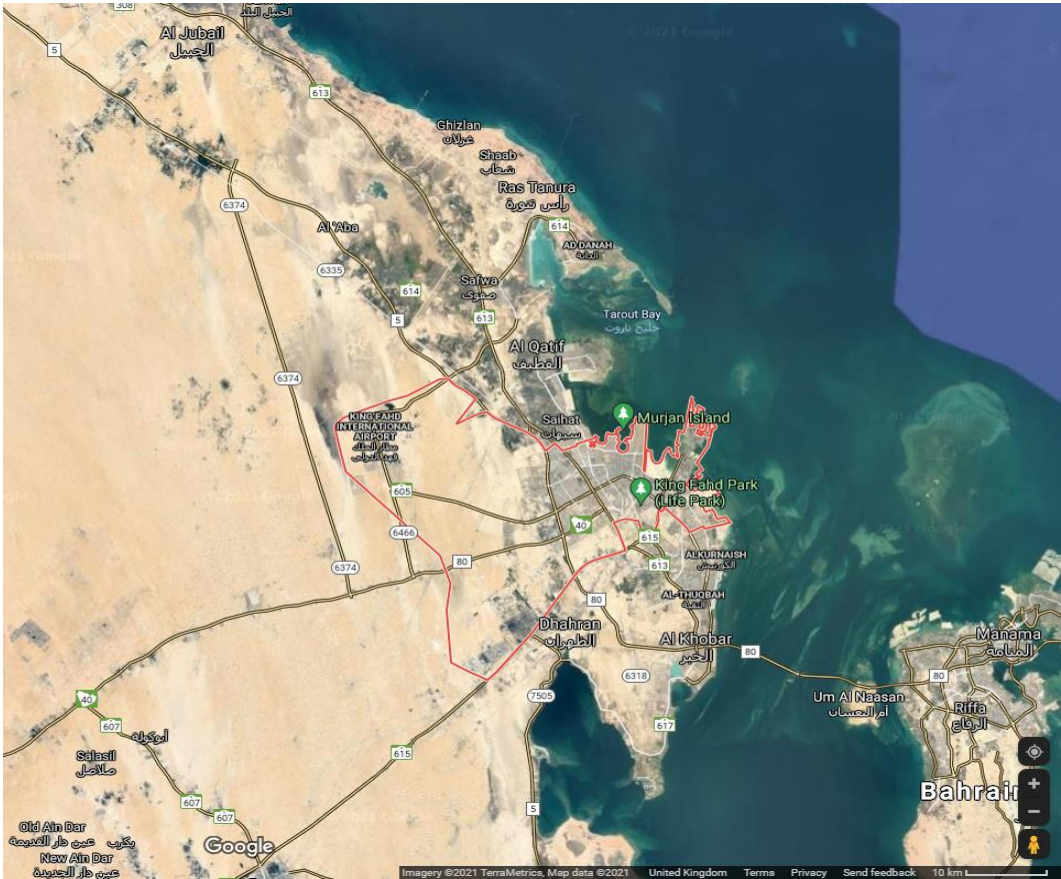


Figure 1.7 Map showing Dammam and its surrounding areas (Google map).

The climate in Dammam is arid and is affected by the Arabian Gulf (Al-garni, Sahin and Al-farayedhi, 1999). The Eastern province is characterised by a hot, humid and very low precipitations climate. According to Barth (2001) the eastern province of SA had in the past been covered by enough vegetation to avert active movement of sand. However, in the last few decades, industrialisation and urbanisation have led to reductions in vegetation cover, hence increased soil movement and sand transport has occurred, including dust mobilisation.

Weather data was collected from King Abdulaziz Air Base in Dhahran between 2008 to 2018 using the "world-met" R package (Carslaw, 2018).

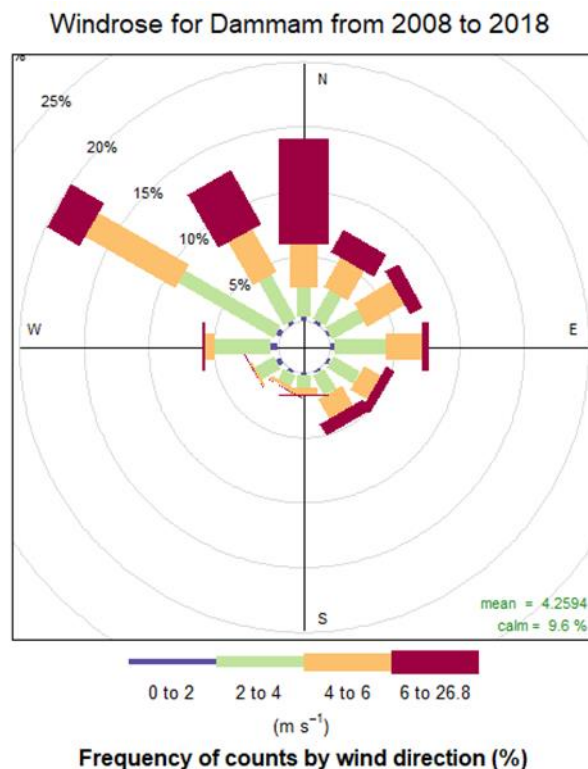


Figure 1.8 Wind rose plot showing the percent of wind direction and speed in Dammam from 2008-2018.

More than 50% of wind in Dammam comes from north and northwest directions as can be seen in fig 1.4. There is a small percentage of wind from the south. This means that Dammam is significantly more frequently impacted by air from the north (Jubail, Qatif and Ras Tanura cities) and west (Ad-Dahna) compared to wind from the south (Dhahran and Al Khobar cities) and the east (the Arabian Gulf). The average wind speed was 4.1 m s^{-1} with minimum of 0 m s^{-1} and the maximum was 26.8 m s^{-1} . The highest wind speeds usually come from the north and northwest.

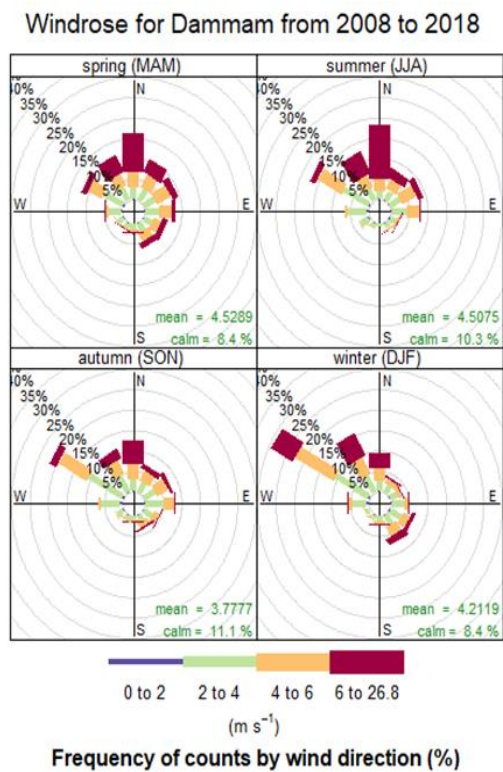


Figure 1.9 Windrose plot shows the percent of wind direction and speed for each season in Dammam from 2008-2018.

In the spring and summer, northerly winds are more frequently experienced, compared to all other directions (Fig 1.4) (Northerly winds represented 18% of the total in the summer and 13% in the spring). Also, wind from north in the summer and spring is characterised by high speeds which lead to increase dust

movement. In the winter and fall the northwest wind is the most frequent where it accounts for 24% in the winter and 20% in the fall. Wind speed tends to be more moderate in the winter and fall, compared to summer and spring.

1.3 Oxidative Potential (OP)

The epidemiological association between PM and adverse health impacts, including cardiovascular and respiratory diseases, is well studied in the existing literature (Charrier *et al.*, 2015; Xiong *et al.*, 2017). Liu *et al.* (2019) studied the association of PM₁₀ and PM_{2.5} with daily cases of cardiovascular and respiratory mortality in 652 cities around the world. The authors concluded that, on average, a 10 $\mu\text{g}/\text{m}^3$ increase in PM₁₀ for two days was associated with a 0.44% increase in daily cardiovascular mortality and a 0.47% increase in daily respiratory mortality. In addition, the same increase for PM_{2.5} was associated with a 0.68% increase in daily cardiovascular mortality and a 0.74% increase in the daily respiratory mortality. Nevertheless, the mechanism behind this impact is not fully understood. Growing evidence suggests that the ability of PM to induce oxidative stress inside the body could be the main mechanism of PM toxicity (M. G. Perrone *et al.*, 2016; Tuet *et al.*, 2017). In the body, oxidative stress occurs when the reactive oxygen species (ROS) concentration is above the body's antioxidant ability (Ntziachristos *et al.*, 2007; Verma *et al.*, 2014; Calas *et al.*, 2019). As a result, ROS induces inflammation in the respiratory and cardiovascular cells (Cho *et al.*, 2005a; Velali *et al.*, 2016; Chirizzi *et al.*, 2017). The capability of PM to induce ROS arises because oxidant species are on or inside particles that are inhaled into human body or the PMs component stimulates cells to produce ROS (Bates *et al.*, 2015; Gao *et al.*, 2017). The ability of PM to produce ROS is called the oxidative potential (OP).

Scientists have developed many mechanisms to measure OP of PM in the laboratory using acellular assays as a candidate proxy metric of PM toxicity. The possibility of measuring OP with acellular assays has led to an increase in measurement of OP for PM globally. Compared to cellular assays, acellular assays are faster, cheaper, have less resource demand and need less environmental control (Wragg *et al.*, 2017; Calas *et al.*, 2019). These advantages have led to extensive measurement of OP worldwide via different methods and provide various results, discussed in the following sections.

1.3.1 Methods of measuring oxidative potential

There are different methods for measuring OP in the lab including the dithiothreitol assay (DTT) (Cho *et al.*, 2005a), ascorbic acid assay (AA), electron spin resonance assay (ESR), glutathione assay (GSH) and respiratory tract lining fluid assay (RTLFL). DTT reduces oxygen to its superoxide anion (O_2^-) that forms ROS where the rate of O_2^- generated from PM sample is measured by the rate of DTT consumption (Saffari *et al.*, 2014). ESR measures the actual ROS generated over time by inducing $\cdot OH$ formation in the presence of H_2O_2 (Gao, J. Godri Pollitt, *et al.*, 2020). RTLFL measures the antioxidant molecule concentration in synthetic human respiratory lining fluid after they are mixed with PM (Visentin *et al.*, 2016; Gao, J. Godri Pollitt, *et al.*, 2020). AA and GSH quantify the antioxidant depletion rate of chemical proxies as proportional to the formation of ROS (Bates *et al.*, 2019). Each technique has its own sensitivity to different PM composition and ROS inducer. In fact, there is no standard method to measure OP in the PM.

Within each assay, different protocols may affect results. Many researchers have commonly used deionised water (DIW) to extract PM for DTT assay (Verma *et al.*, 2012). However, recent studies have found that using methanol as an extraction medium produces DTT activity up to 1.6 times higher than water extraction (Rattanavaraha *et al.*, 2011; Yang *et al.*, 2014; Bates *et al.*, 2019). Water extraction is relevant for measuring the OP activity of water soluble PM, while methanol extraction is more relevant for measuring water soluble and insoluble PM's OP activity. Also, the type of filter used to collect PM has been shown to conclude different results. Yang *et al.* (2014) compared the OP activity using Teflon and quartz filters. They concluded that OP activity per unit air volume was significantly lower for quartz filters, in comparison to Teflon filters, for four different OP activity methods. The OP activity was lower for quartz filters compared to the Teflon filters by 63%, 47% and 21% for AA, ESR and DTT assays, respectively. Different results and responses have been reported by many studies using different methods, and none of these methods have provided a "gold-standard" measure. More studies, methods and criteria are needed to confirm the association between OP assays and health end point and to apply this method as a new candidate proxy metric for PM toxicity.

1.3.2 Correlation between Oxidative Potential and health end point:

The association between OP activity and health end point has been reported in many studies. Some studies have reported a significant positive correlation between some OP assays, others have reported positive non-significant correlation, and in some cases, there was no correlation (Table 1.2).

Table 1.2 The correlation between different OP assays and health end outcomes.

Reference	Assay with positive correlation	Assay with no correlation	Health end point	PM size
(Delfino <i>et al.</i> , 2013)	DTT*		Asthma in Children	PM _{2.5}
	ROS*			
(Janssen <i>et al.</i> , 2015)	DTT*		Respiratory inflammation	PM _{2.5} and PM ₁₀
	AA*			
	ESR*			
(Yang <i>et al.</i> , 2016)	DTT*	ESR	Respiratory health in children	PM _{2.5}
(Strak <i>et al.</i> , 2012)		AA	Respiratory function	PM _{2.5-10} , PM _{0.18-2.5} and PM _{0.18}
		GSH		
(Abrams <i>et al.</i> , 2017)	DTT*		Respiratory diseases	PM _{2.5}
	DTT		Cardiovascular diseases	
(Weichenthal <i>et al.</i> , 2016)	GSH*	AA	Lung cancer mortality	PM _{2.5}
(Atkinson <i>et al.</i> , 2016)		AA and GSH	Mortality	PM _{2.5} and PM ₁₀
(Canova <i>et al.</i> , 2014)		AA and GSH	Pulmonary diseases	PM ₁₀

The correlation between OP activity and adverse health impact is more strongly linked than the correlation of PM mass concentration with adverse health impact in some cases (Borm *et al.*, 2007b; Bates *et al.*, 2019). In their study, Delfino *et al.* (2013) found OP activity using dithiothreitol (DTT) and electron spin resonance (ESR) assays was significantly positively associated with airway inflammation in 45 schoolchildren, but not with PM_{2.5} mass. Also, a significant positive correlation has been found between DTT activity and asthma incidence and the occurrence of asthma symptoms for children in Pima, Netherlands, while the correlation of asthma in children was not significantly associated with ESR or PM_{2.5} mass (Yang *et al.*, 2016). Weichenthal *et al.* (2016) found GSH to be more associated with lung cancer mortality than PM_{2.5} mass concentration where GSH had a 12% risk increase, while PM_{2.5} had 5% risk increase. On the other hand, there was no correlation or positive weak correlation in London between GSH and AA and mortality from cardiovascular and respiratory diseases (Atkinson *et al.*, 2016). All published literature found a positive correlation between DTT and various health end points (Table 1.2). Other OP assays were positive in some reports while in others they were not associated with health end point. In consequence, DTT is a preferred assay, as it provides a better predictor (or measure) of the link between PM and health impact (Rao *et al.*, 2020).

1.3.3 Effect of PM Component on Oxidative Potential:

As DTT showed the best link to human health, and hence is the focus of OP measurement in this thesis, the following section focuses upon DTT-assay derived assessments of the impact of PM composition on OP. The DTT assay was developed by Cho *et al.* (2005), who stated that DTT activity was driven by organic materials and it did not correlate with metals and other inorganic

compounds since they are inactive in the DTT assay. Moreover, Verma *et al.* (2012) did not find a strong positive correlation between DTT activity and any metals for water or methanol extraction of PM_{2.5} collected from Atlanta, United States. However, Charrier and Anastasio (2012) estimated transition metals (especially copper and manganese) were responsible for about 80% of the DTT loss of PM_{2.5} collected from San Joaquin of California. The authors explained the high loss of DTT by metals arose because they did not use Ethylene Diamine Tetraacetic Acid (EDTA), which improves the loss of DTT in the blank, but suppresses the metals' response. Still, in Milan, Italy, a negative correlation was reported between all metals (except nickel) and DTT activity even though researchers did not use EDTA in the DTT assay (M. G. Perrone *et al.*, 2016). Soluble copper and soluble manganese were found to account for about 50% and 20% of volume normalised DTT response in Fresno, California, respectively (Charrier *et al.*, 2015). The various results and correlations between metals and DTT could be related to the method used, including extraction solution, type of filter and addition of some chemicals to the assay, or to the sources of metals in samples. PM mass concentration is usually correlated with DTT volume normalised, so some association between some metals and DTT activity may be due to the same variation of the metals and PM mass concentration rather than those involved in the DTT assay (Bates *et al.*, 2019).

One of the most common parameters that is highly correlated with DTT activity in many studies is organic material, including organic carbon (OC) and water soluble organic carbon (WSOC). Organic aerosols were found to be responsible for approximately 60% of DTT activity in Atlanta, USA (Verma *et al.*, 2015). Chirizzi *et al.* (2017) found DTT activity per air volume to be larger

for samples that have high carbon contents. OC has been reported by many studies to be correlated with DTTv with an r-value range from 0.5 – 0.88 (Verma *et al.*, 2012; Joseph Y. Abrams *et al.*, 2017; Liu *et al.*, 2018).

Water soluble ions (WSI) do not play an important role in the DTT assay. The contribution of WSI including secondary inorganic ions to the DTT assay is very low, however, the positive correlations in some cases is most probably due to their correlation with the redox-active organic compound rather than in the actual DTT assay (Cho *et al.*, 2005a; Verma *et al.*, 2009; Liu *et al.*, 2018).

In general, OP activities have shown a stronger association with health impact than PM mass concentrations alone. Many techniques are available to measure OP, but none of them have been used to be the standard method. The DTT assay has the advantage amongst others with its higher correlation with health end points. The DTT is also the most common method reported in literature. However, more in-depth studies are still needed in order to fully understand OP assays and to know which PM components are driving these assays. Further, a standard method needs to be agreed to be added to PM mass concentration which is the only metric now connecting to health impact in epidemiological studies.

1.4 Objectives of the Thesis

This thesis investigates the air quality in Dammam, SA, by comprehensively characterising the composition, sources and toxicity of PM_{2.5}. The findings of this study will provide insights to mitigate air pollution impacts on the environment and human health. This is addressed through the following objectives:

- Identifying meteorological factors that govern pollutants behaviour and assessing key pollutant diurnal, monthly and yearly trends in Dammam, SA.
- Comprehensively characterising the composition of PM_{2.5} in Dammam, using a range of analytical techniques.
- Understanding the impact of pollution events such as dust storms on PM_{2.5} mass concentration and composition in Dammam.
- Determining the background levels of PM_{2.5} in Dammam particularly during non-dust storms periods.
- Investigating the dominant components of PM_{2.5} during pollution events and assessing the toxicity of the pollutant mix in Dammam.
- Understanding the influence of natural/anthropogenic species and emissions on the oxidative potential of particles.
- Providing an authoritative assessment of the sources and burden characteristics of PM_{2.5} in Dammam.
- Identifying the sources that affect oxidative potential.

Chapter 2 . Materials and Methods

This chapter describes the sampling locations and lab work conducted to analyse the composition and sources of PM_{2.5}. It provides details of sampling locations in Dammam and meteorological conditions during sampling campaigns in the winter and summer. Also, this chapter describes lab analysis for measuring metals, water soluble ions and organic and elemental carbon. The development of DTT assay in the University of Birmingham labs and the assay used to measure OP is also provided in this chapter.

2.1 Location

The location where samples were taken was Dammam city, Saudi Arabia (SA). Dammam lies on the coast of Arabian Gulf at 26.43°N latitude, and 50.11°E longitude, and is the capital city of the Eastern province of Saudi Arabia. Dammam is home to more than one million people. Dammam is a part of what is called Dammam metropolitan area which includes Dammam city, Khobar city and Dhahran city. This wider metropolitan area is home to more than three million people. It is surrounded by the Arabian Gulf and King Abdulaziz seaport to the east, the Aljubail industrial city Ras Tanura (one of the largest oil refineries in SA) and the Al Qatif city to the north, the Ad-Dahna desert to the west, and cities of Dhahran and Al Khobar to the south. As the capital and central city of the eastern province, Dammam holds most of the commercial activities, government departments and manufacturing in the eastern province.

2.1.1 Meteorological Conditions:

During the time of collecting samples for this project in the winter and summer of 2018, meteorological conditions were consistent with the long-term average in the past ten years as shown in fig 2.1 and fig 2.2.

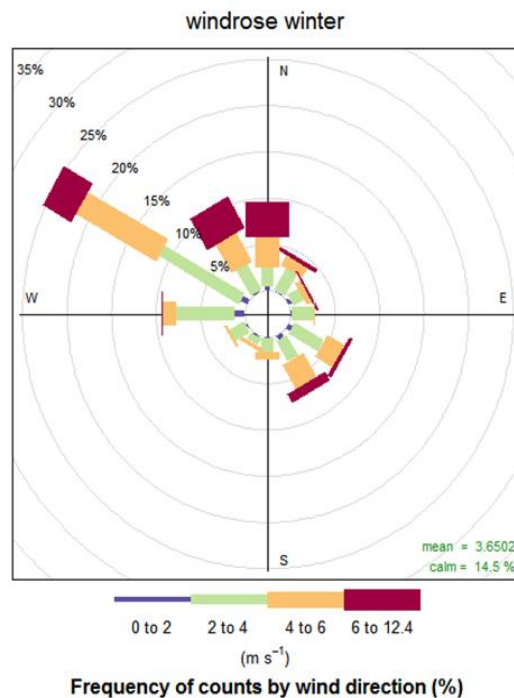


Figure 2.1 Windrose shows the wind direction and speed during the winter campaign for the period from 15/12/2017 to 20/02/2018.

Fig 2.1. shows the wind direction and speed during the winter campaign, where 25% of the wind came from west northwest (WNW), 11% came from north northwest (NNW) and 9% came from north (N) and west (W). The average temperature (T) during the winter campaign was 16.7 °C, with a range of maximum T at 27 °C and minimum T at 7 °C. Relative humidity (RH) was an average of 50.5%, where the maximum RH was 100% and the minimum was 6.2% as seen in table 2.1.

Table 2.1 Overview of meteorological parameters for the winter and summer campaigns.

Meteorological parameters	Winter			Summer		
	Mean	Max	Min	Mean	Max	Min
Temp °C	16.7	27.0	7.0	37.4	48.0	26.0
RH %	50.5	100.0	6.2	25.7	84.0	3.8
Wind speed m s ⁻¹	3.6	11.8	0.0	4.9	13.4	0.0

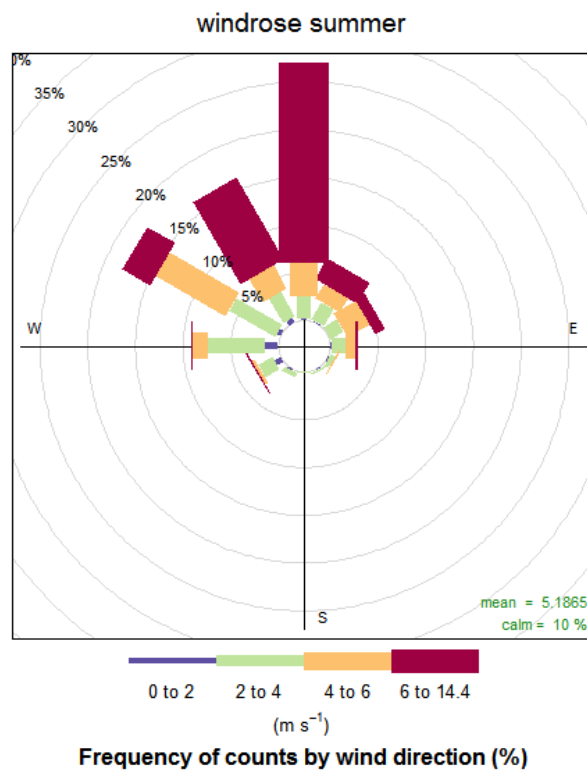


Figure 2.2 Windrose shows the wind direction and speed during the summer campaign for the period from 15/06/2018 to 20/08/2018

In the summer, the prevailing wind was from N, WNW and NNW, with 27%, 17% and 16%, respectively. Compared to the winter period, the summer wind speed was faster and the abundance of fast wind was significant. For the duration of the summer campaign, weather was very hot, with maximum T

reaching up to 48 °C, minimum T was 26 °C and the average was 37.4 °C. RH in the summer was lower than the RH in the winter, where the maximum RH in the summer was 84% and minimum RH was 3.8%, and the average was 25.7%.

2.1.2 Sampling Locations:

Two locations were selected in Dammam. The first location was on the roof of the Municipality of the Eastern Region (Amanah) where the sampler was approximately 15m above the street level. Amanah building is located in the city centre of Dammam where many commercial activities occur, as shown in fig 2.3. Amanah building is located in the middle of Dammam surrounded by many residents building, shops and high traffic roads.

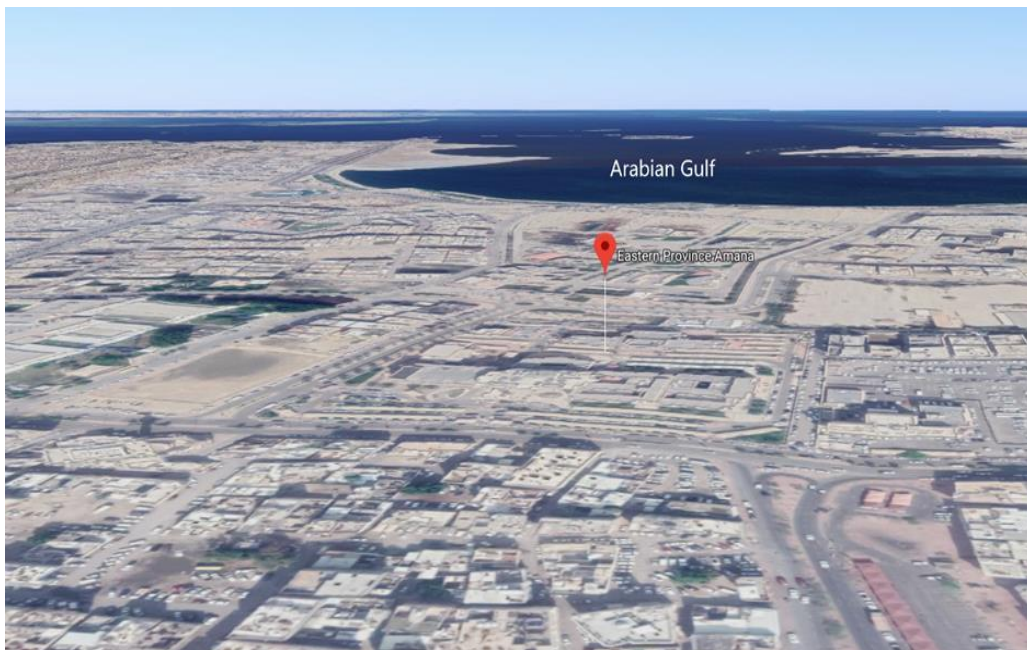


Figure 2.3 3D map shows the location of Amanah building.



Figure 2.4 MiniVol samplers during winter campaign on the roof of Amanah during normal and dusty days

The second location was on the roof of the Public Health College building on the campus of the Imam Abdulrahman Bin Faisal University (IAU) which has a height of about 15 m above the ground.



Figure 2.5 3D map shows the location of Imam Abdulrahman Bin Faisal University.

(University location), as shown in fig 2.5, where the commercial activities and traffic density are lower than the first location, and the campus has limited access to students and staffs only. The university is surrounded by Arabian Gulf to the east and south, an empty land to the north and King Faisal Road and the old campus of the university to the west.

2.1.3 PM Sampling campaigns:

Two sampling campaigns were undertaken. The first was during the winter of 2018. $PM_{2.5}$ was collected from 31/12/2017 until 09/02/2018 at both sites. The second campaign was in the summer of 2018, where $PM_{2.5}$ was collected from 02/07/2018 until 10/08/2018. Two samplers were used at each location, i.e. a total of four samplers. At each location one sampler collected

PM_{2.5} on Zefluor coated PTFE Diameter 47mm, which had a pore size of 2.0um, while the other one collected PM_{2.5} on 100% pure quartz filters with a diameter of 47mm. For Amanah, the filters were changed every day at 12:00pm local time in the winter campaign. For health and safety and to avoid sunstroke the time for changing filters moved to 05:00am local time in the summer campaign. Sampled filters were placed directly in petri dishes, wrapped with foil and then placed in a freezer at -18 °C in the laboratory of the Public Health college.



Figure 2.6 MiniVol samplers collecting samples at the University location during normal and dusty days.

During the winter campaign, the filters at the University location were changed at 12:30pm, whereas during the summer campaign for health and safety reason filters were changed at 05:30am. Sampled filters were placed directly into petri

dishes, wrapped with foil, and then placed in the freezer at $-18\text{ }^{\circ}\text{C}$ in the Public Health college laboratory. Before sampling started, field blank filters were collected for each sampler where a filter was run for one minute (compared with the usual 24 hours). Moreover, one field blank filter for each sampler was collected during the middle and at the end of the campaign. The samplers were cleaned every four days using deionised water and left to dry before re-use to remove dust collected on the sampler tubes. On the last day of the campaign, after the samples and field filters were collected, the samplers were cleaned, and three field blank filters were collected for each sampler. The total number of field blank filters for each sampler was six. When sampling was completed, all filters were kept in a freezer at $-80\text{ }^{\circ}\text{C}$ for 72 hours, then placed with many gel ice packs in an ice box to maintain the temperature below $0\text{ }^{\circ}\text{C}$. This ice box was taken directly to the shipping company (DHL) and shipped to University of Birmingham. Once filters were arrived at the University of Birmingham, they were placed directly in freezer at $-18\text{ }^{\circ}\text{C}$.

2.2 Filter preparation

$\text{PM}_{2.5}$ was collected on Zefluor coated PTFE filters Diameter 47mm, which had a pore size of 2.0um and 100% pure quartz filters with a diameter of 47mm. Thus, Teflon filters were weighed before and after collecting samples to calculate the amount of $\text{PM}_{2.5}$ collected on filters. The Teflon filters were conditioned at temperature $\sim 22\text{ }^{\circ}\text{C}$ and humidity $\sim 39\%$ for 24 hours in controlled room before they were weighed before and after sample collection. Quartz filters were baked in the oven at $550\text{ }^{\circ}\text{C}$ for 5.50 hours before they were used. All filters were kept in plastic petri dishes.

2.3 Samplers

A pair of MiniVol Portable Air Samplers were used to collect PM_{2.5} from Dammam. This sampler has the option to operate with an AC or DC power source. In this project, the DC option was used where batteries were changed every time the filters were replaced. The MiniVol uses impaction to achieve particle size separation. Air is moved through a particle separator and then through a filter medium. The MiniVol can collect PM₁₀ and PM_{2.5} by using an impactor with 10 micron cut-point or 2.5 micron cut-point, respectively. Moreover, the MiniVol has the ability to collect total suspended particles (TSP) by operating the sampler without any impactor. In order to achieve the correct particle size separation, the sampler needs to be operated at 5 litres per minute total flow rate at ambient conditions. For collecting PM_{2.5}, as collected throughout this work, the PM_{2.5} impactor was installed in the pre-separator/filter holder and the PM₁₀ impactor was also installed on the pre-separator tube.

2.4 Lab analysis

Filters were kept in the freezer in the lab until the time of analysis. Before each experiment filters were taken from freezer and returned to the freezer until they were needed for another assay. Filters were analysed for water soluble Ions, Metals, Organic Carbon and Elemental Carbon (OC/EC) and Oxidative Potential (OP) as a candidate proxy metric of toxicity of PM. The quartz filters were used for metal, ions and OC/EC analysis while the Teflon filters were used for OP as shown in the table.

Table 2.2 Type and area of filters used for each experiment.

	Filter Type	Teflon	Quartz
Lab analysis	water soluble ions	X	5 cm ²
	OC/EC	X	0.5 cm ²
	Metals	X	Half of the filter
	OP	2– 10 cm ²	X

2.4.1 Organic Carbon and Elemental Carbon (OC/EC):

The total organic carbon loading, separated into organic (OC) and elemental (EC) carbon fractions, were measured through analysis of samples collected on the quartz filters through measurement of the amount of carbon evolved from the filter samples as a function of temperature (Watson, Chow and Chen, 2005). OC/EC were analysed using the DRI Model 2015 Multiwavelength Thermal/Optical Carbon Analyser, which is a developed version of the DRI Model 2001 system that has been widely-used for measuring OC/EC. Thermal/optical carbon analysis is based on the fact that organic compounds are volatilised at low temperature in a non-oxidizing helium (He) environment, while elemental Carbon is burned at a high temperature with an oxidizer (DRI, 2015). The sample filter was taken out of the freezer and kept at room temperature for at least 40 minutes. A small punch (0.5 cm²) was taken and loaded onto a holder which automatically takes the filter inside the oven, as shown in the fig 2.7.

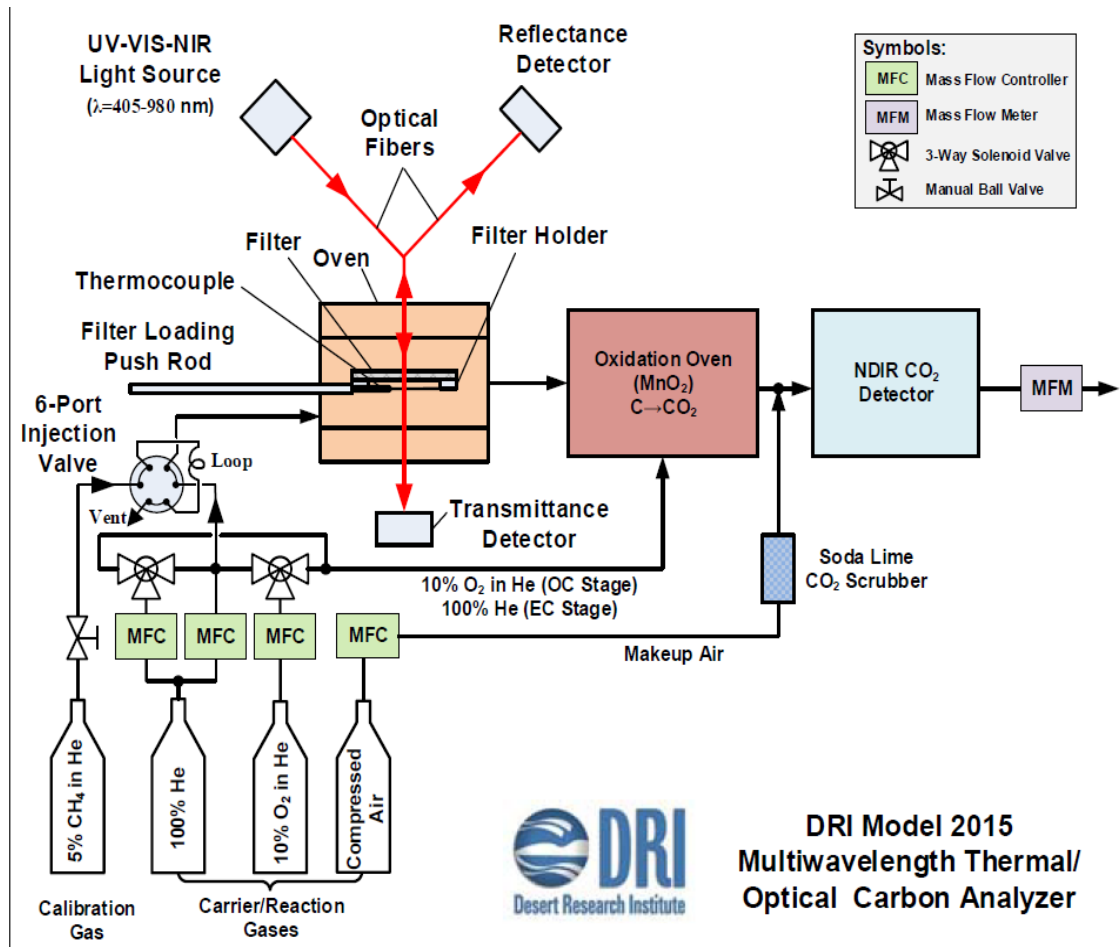


Figure 2.7 Schematic diagram of the DRI Model 2015 Multiwavelength Thermal/Optical Carbon Analyser (DRI, 2015)

Inside the oven, the filter was exposed to different temperatures. In order to analyse OC, the filter was volatilised in four heating stages using 100% helium.

These stages were:

- OC1 : From ambient temperature to 200 °C
- OC2 : from 200 °C to 300 °C
- OC3 : from 300 °C to 450 °C
- OC4 : from 450 °C to 650 °C

EC was analysed by burning the filter in a O₂/He atmosphere, where the mixture consisted of 2% O₂ and 98% He. Another four stages of heating were also applied to get the EC result:

- EC1 : at 500 °C
- EC2 : from 500 °C to 550 °C
- EC3 : from 550 °C to 700 °C
- EC4 : from 700 °C to 850 °C

The volatilised Organic Carbon from the filter is converted to Carbon Dioxide (CO₂) through manganese dioxide (MnO₂), then CO₂ is quantified by a CO₂ detector (nondispersive infrared (NDIR)), while the rest of carbon is pyrolyzed at a very high temperature. This pyrolyzed carbon is considered as organic carbon because it is a byproduct of the heating process. The reflectance and transmittance from the filter were measured by seven diode lasers at wavelengths from 450 to 980 nm. In this study, transmittance at 635 nm was used to correct the OC/EC fraction since this laser wavelength keeps the constancy with DRI and correct the pyrolyzed carbon charring from OC to EC compound (DRI, 2015). Because some of the EC would include some Pyrolyzed OC, part of the measured EC needs to be moved to OC value. Without using this correction, the EC would be overestimated whilst OC would be underestimated. Every day before starting the sample analysis, a blank filter was baked in order to remove any Carbon contamination. This was carried out by using the Bake protocol which uses a temperature of 900 °C for 10 minutes. Moreover, after baking, either a methane calibration using the Autocal protocol or a sucrose standard (1800 ppm) was carried out every day following the DRI manual instruction.

At the end of each run, a thermograph was produced by the software that produced information about the 8 stage temperatures, NDIR signal, time and the reflectance and transmittance signals. The first four stages of the 8 stages give values for OC measurement and the last four stages of the 8 stages give values for EC measurement. OC was calculated as follow: $OC = OC1 + OC2 + OC3 + OC4 + OP365$, while EC was calculated as follow: $EC = (EC1 + EC2 + EC3 + EC4) - OP365$. The method detection method for DRI2015 is $0.41 \mu\text{g}/\text{cm}^2$ for OC and $0.11 \mu\text{g}/\text{cm}^2$ for EC (DRI, 2015). Field blank filters were treated exactly like filter samples where all results were corrected by taking out the field blank OC and EC which was $0.5 \mu\text{g}/\text{cm}^2$ for OC and $0 \mu\text{g}/\text{cm}^2$ for EC.

2.4.2 Water soluble Ions (WSI):

Water soluble ions were analysed via a Dionex ICS 1100 ion chromatograph fitted with the IONPAC AS22 2×250 mm column to measure anions, while DionexTM Integrion HPIC fitted with (DionexTM ionpac cg12a) column for cations. Typically, any IC consists of a liquid eluent delivery, a pressure pump, a sampler injector, a separator column, a suppression, a detector and data collection system. IC separates ions based on their charge and affinity to ion exchange.

2.4.2.1 Filter extraction:

Four punches of Quartz filter (two punches 1×1.5 cm and two punches 1×1 cm) were used for the Ion extraction. Punches were placed in 15ml centrifuge tubes. 5 ml of $18.2\text{M}\Omega\text{-cm}$ deionised water (DIW) was added to each tube for subsequent anion and cation analysis using a calibrated automatic pipette. Tubes were sonicated for 60 minutes using an ultrasonic bath where the temperature of the water was kept below 27°C by adding ice packs as required, which follows

EPA standards (Procedure and Analysis, 2009). The sample mixture was shaken overnight using a mechanical shaker. The extraction liquid was then filtered using 0.45 μm syringe filters into a new 15 ml centrifuge tube. Extractions were kept in the refrigerator at 4 °C until the time of analysis.

2.4.2.2 Anion Standard:

1000 ppm (mg/L) Anions stock solution was prepared by dissolving a salt form of sodium chloride (NaCl), sodium nitrite (NaNO₂), sodium fluoride (NaF), Sodium Nitrate (NaNO₃), Sodium Bromide (NaBr), Sodium Sulfate (Na₂O₄S) and Sodium Phosphate (Na₃PO₄) in 1 L of 18.2M Ω -cm deionised water (DIW). From the stock solution seven dilutions were made (0.2, 0.5, 1, 2.5, 5, 10 and 15 ppm) to be used as calibration standards.

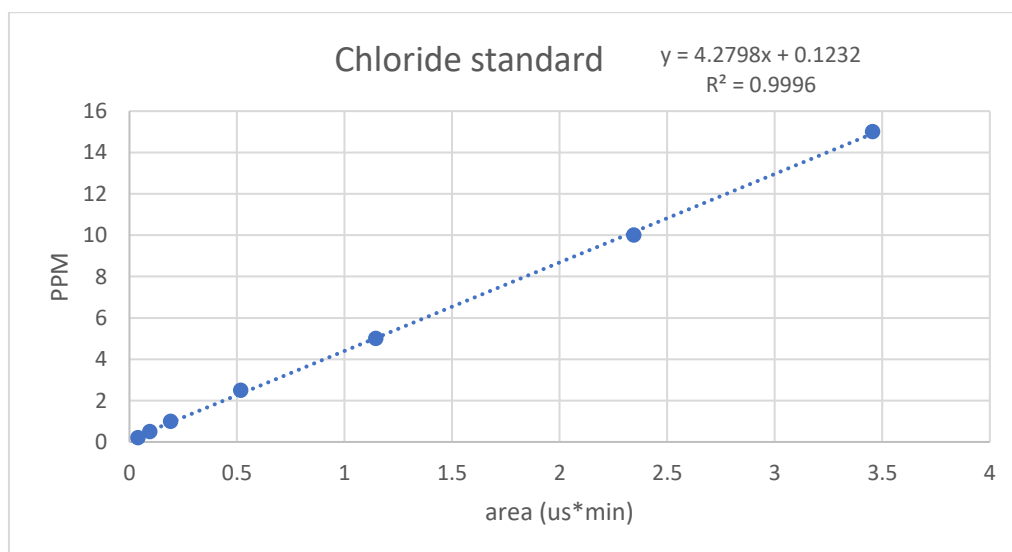


Figure 2.8 Scatter graph of the chloride standard prepared for anion analysis.

2.4.2.3 Cation standards:

1000 ppm (mg/L) cation stock solution was prepared by dissolving a salt form of Ammonium Chloride (NH₄Cl), Sodium Chloride (NaCl), Potassium Chloride (KCl), Calcium Chloride (CaCl₂·2H₂O) and hexahydrate Magnesium Chloride (MgCl₂·6H₂O) in 1 L of 18.2M Ω -cm deionised water. From the stock

solution, seven dilutions were made (0.2, 0.5, 1, 2.5, 5, 10 and 15 ppm) to be used as calibration standards.

2.4.2.4 Anion (Dionex ICS 1100):

Samples were transferred into 0.5 ml vials using a calibrated pipette. Vials were loaded into the autosampler connected to Dionex ICS 1100. Samples were taken by the autosampler to the eluent stream and then to the separator column (IONPAC AS22 2x250 mm column), where each anion was separated based on a specific retention time. Sodium carbonate and sodium bicarbonate (Na_2CO_3 and NaHCO_3) were prepared to be used as an eluent. In the autosampler, vials were loaded in the following order: three DIW, seven calibration standards, 10 samples, 1 ppm standards, three DIW, 10 samples and so on. Field blank filters were analysed with the same treatment as the real samples, and all samples were corrected using the field blank filters results where field blank filters were treated as sample filters.

2.4.2.5 Cation (Dionex Integrion HPIC):

Samples were transferred into 1.5 ml vials using a calibrated pipette. Vials were loaded into the autosampler connected to Dionex Integrion HPIC. Samples were taken by the autosampler to the eluent stream and then to the separator column (dionex ionpac cg12a), which separates common cations through methanesulfonic acid (MSA) eluent. In the autosampler, vials were in the following order: three DIW, seven calibration standards, 10 samples, 1 ppm standards, three DIW, 10 samples and so on. Field blank filters were then analysed with the same treatment as the real samples, and all samples were corrected using field blank filters results, and correction ranged from 2% to 20% of measured WSI.

2.4.2.6 detection limit:

Method detection limit for ions were calculated from blank filters using E 1.

$$MDL = SD \times 3 \quad E1$$

SD = standard deviation of measured 15 blank filters

MDL of ions are presented in table 2.3.

Table 2.3 MDL of measured WSI

Ion	MDL mg/L
Sodium	0.043
Ammonium	0.048
Potassium	0.012
Magnesium	0.0021
Calcium	0.065
Chloride	0.33
Sulfate	0.23
Nitrate	0.177

2.4.3 Metal Analyses

2.4.3.1 filter extraction:

PM_{2.5} was extracted from samples collected on quartz filters by adding 10 ml of 68% ultrapure nitric acid (HNO₃, Romil) using microwave digestion vessels. Vessels were placed in Mars 6 microwave digestion system (CEM). A filter-membrane programme was used where the temperature increased to 200°C

(ramp time of 15 minutes) and was held for 15 minutes at this temperature before being cooled to 30°C. Once the digestion cycle was completed, the digestion acid samples were diluted to the 2% HNO₃ concentration (16.6- fold dilution) as required for use with ICP-MS, using acid-washed glassware with DIW. The 2% HNO₃ acid digest solution was then filtered using a 0.45 µm syringe filter into a new 15 ml centrifuge tube. The liquid was kept in the fridge at 4 °C until the time of analysis.

2.4.3.2 Blank filter and Standard:

Each batch of samples to be digested contained one vessel with just 10 ml HNO₃ to check for contamination sources in the acid and dilution process. Another vessel contained a blank filter to check the metal content of unused quartz filter, and it was treated using the same method as the samples. For quality control and testing of the repeatability of the instruments, a standard reference material (Media-NIST, particulate on filter) was performed with each set of extractions (Loyola et al., 2009; González et al., 2017).

2.4.3.3 Cleaning:

All microwave vessels were cleaned after every digestion run to prevent contamination between samples. Vessels were cleaned with DIW and placed in a clean oven at 70 °C to dry. When the vessels became dried, 10 ml of HNO₃ was added to each vessel. Vessels were placed in the microwave using cleaning programme (ramp for 15 minutes and hold for 10 minutes at 190 °C). After the microwave finished the cleaning cycle, vessels were cleaned with DIW and left in a fume hood to dry before using again. All volumetric glasses were put in acid bath after every run and washed with DIW before they were used again.

2.4.3.4 detection method and recovery %:

A total of 7 blank filters were analysed alongside the samples. These 7 filters results were used to calculate the method detection limit (MDL) using E2.2

$$MDL = (SD \times 3) + average \quad E(2.2)$$

Where, SD = standard deviation of the 7 filters, average = mean of the 7 filters

The NIST results were used to calculate the recovery percent for metals as shown in table 2.3:

Table 2.4 MDL and recovery percent of metals measured by ICP-MS.

metal	MDL (mg/L)	Recovery %
Mg	3.199353	83
Al	5.336609	50
K	n.a	47
Ti	0.083585	47
V	0.006167	76
Cr	0.175601	45
Mn	0.09566	100
Fe	3.526798	90
Co	0.00424	97
Ni	0.32155	150
Cu	1.301573	100

Zn	7.960087	100
As	n.a	88
Sr	0.050336	89
Cd	0.013948	98
Sn	5.334911	NA
Sb	0.022426	82
Ba	0.415992	NA
Ce	0.086369	77
W	n.a	NA
Pt	n.a	NA
Pb	0.137512	96

2.4.3.5 standards preparation:

9 concentrations of standards were prepared before running the ICP-MS using sigma-aldrich certified reference material. The levels and concentration of all metals are shown in the table 2.4.

Table 2.5 concentrations (ppm) of standard metals prepared in the lab for the ICP-MS analysis.

Standard level	0 (Blank)	1	2	3	4	5	6	7	8
As	0	0.1	0.5	1	2	5	10	20	50
Cd	0	0.1	0.5	1	2	5	10	20	50

Co	0	0.1	0.5	1	2	5	10	20	50
Cr	0	0.1	0.5	1	2	5	10	20	50
Cu	0	0.1	0.5	1	2	5	10	20	50
Fe	0	2	10	20	40	100	200	400	1000
Pb	0	0.1	0.5	1	2	5	10	20	50
Mn	0	0.1	0.5	1	2	5	10	20	50
Ti	0	1	5	10	20	50	100	200	500
V	0	0.1	0.5	1	2	5	10	20	50
Zn	0	1	5	10	20	50	100	200	500
Sr	0	0.1	0.5	1	2	5	10	20	50
Sb	0	0.1	0.5	1	2	5	10	20	50
K	0	1	5	10	20	50	100	200	500
Ba	0	0.1	0.5	1	2	5	10	20	50
Al	0	2	10	20	40	100	200	400	1000
Mg	0	2	10	20	40	100	200	400	1000
Ce	0	0.5	2.5	5	10	25	50	100	250
Pt	0	0.1	0.5	1	2	5	10	20	50
Se	0	0.1	0.5	1	2	5	10	20	50
Sn	0	0.5	2.5	5	10	25	50	100	250

W	0	0.5	2.5	5	10	25	50	100	250
Ni	0	0.1	0.5	1	2	5	10	20	50
Rb	0	0.1	0.5	1	2	5	10	20	50
Ca	0	1	5	10	20	50	100	200	500
Na	0	1	5	10	20	50	100	200	500

2.4.3.6 Instrument

All metals were analysed using Inductively Coupled Plasma Mass Spectrometry (ICP-MS).

2.5 Toxicity

The candidate proxy for toxicity in PM was measured using Oxidative Potential methods (more details in chapter one page 28). As the DTT assay shows the best correlation with health outcomes among other OP assays, DTT assay was used in this thesis.

One of the suggested mechanisms giving rise to the ability of PM to induce toxicity *in vivo* is production of reactive oxygen species (ROS). ROS are produced in the body through the reduction of oxygen (O₂) to superoxide anions (O₂⁻) which could form ROS (Wragg *et al.*, 2017; Rao *et al.*, 2020). In vitro the electron-transfer mechanisms are simulated by the ability of redox active species within/on the surface of PM to transfer electrons from DTT to oxygen. The rate of superoxide anion production by PM in the sample is measured from the rate of DTT consumption in the reaction, which is proportional to the redox-active species concentration in the PM samples (Gao *et al.*, 2017; Bates *et al.*, 2019).

The reagents used were:

- 5,5'-Dithiobis(2-nitrobenzoic acid), 99 % (DTNB)
- DL-Dithiothreitol, ≥ 98 % (DTT)
- Potassium phosphate dibasic, ≥ 98 % (k-buffer)
- Potassium phosphate monobasic, ≥ 98 % (k-buffer)

2.5.1 OP Assay development:

developing the DTT assay has passed by many attempts before the final methods was achieved. This section tells some of these ways tested in the lab.

The first try was as follows:

K-buffer with Ph 7.4 was prepared from Potassium phosphate dibasic and Potassium phosphate monobasic. DTT stock was prepared in DIW, and DTNB was prepared in Methanol. Dust from Arizona was used as the first sample to be tested. The method was

- 1- Incubate known mass of PM with 100 μ l of 0.5 or 0.1 potassium phosphate buffer and 340 μ l very pure water for 10 minutes at temperature 37 oC and Ph 7.4.
- 2- Add 100 or 50 μ l 1 mM DTT to start the reaction.
- 3- Stop at designated time (0, 10, 20 and 30 minutes) to add 5,5'-Dithiobis(2-nitrobenzoic acid).
- 4- Place the sample in spectrophotometer and record absorbance at 412 nm.
- 5- Calculate the consumption of DTT with time to get the value expressed as nmol DTT/min/ μ g.

First results showed good correlation between absorbance from the UV/Vis and time; however, the amount of DTT consumed was very high, which exceeded the recommended percent (25%) stated by (Cho *et al.*, 2005b) as shown in fig 2.9.

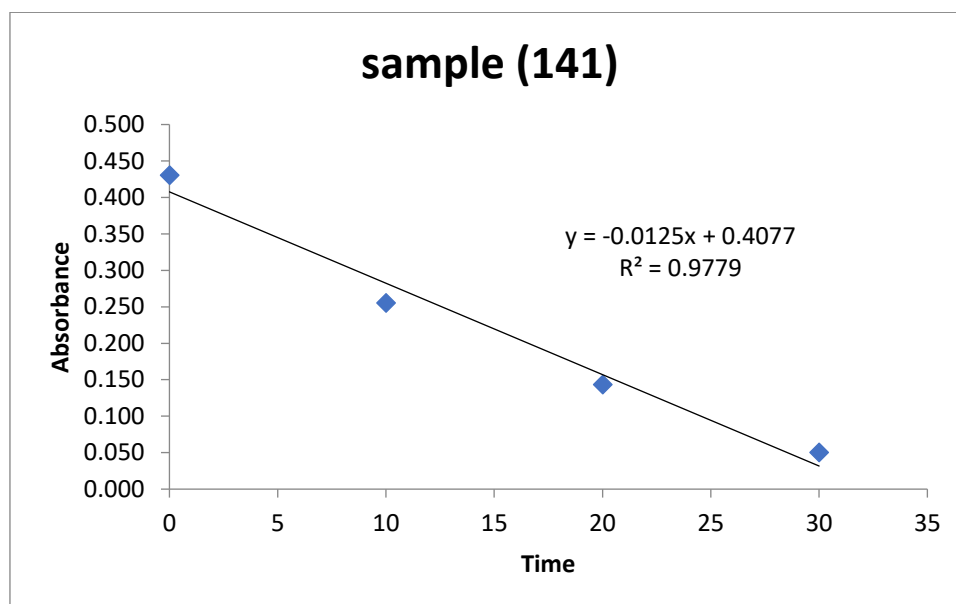


Figure 2.9 scatter graph illustrates the correlation between UV/Vis absorbance and time.

As this method did not meet requirements for DTT assay, more in-depth reading was done to find the correct way. Then it was found that DTT consumption needs to be tested against time rather than the absorbance of the UV/Vis. DTT consumption was tested against time as can be seen in fig 2.10, which showed the same issue of DTT high consumption.

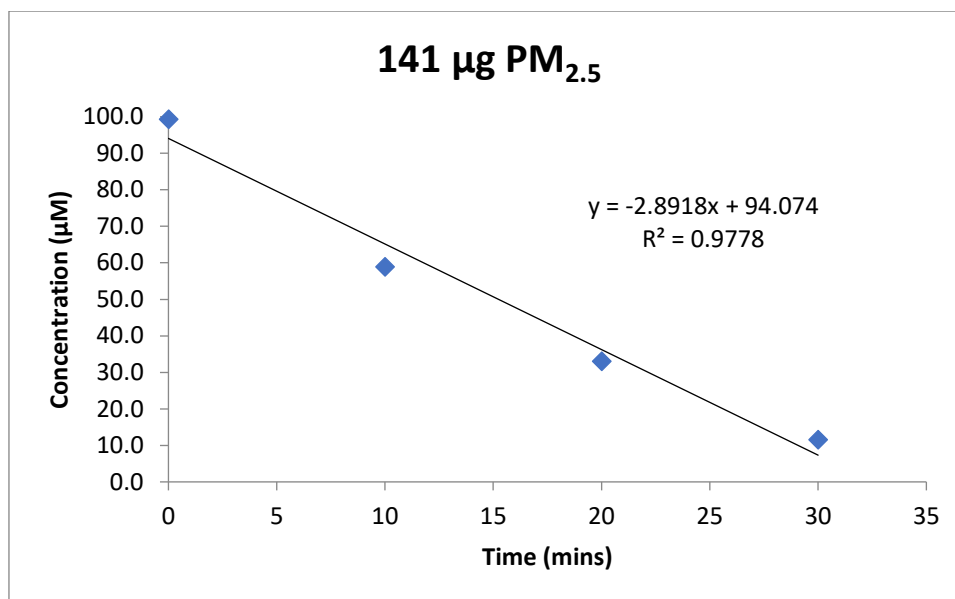


Figure 2.10 Scatter graph illustrates DTT consumed per time.

Many scholars have published that using trichloroacetic acid (TCA) to stop the reaction and then add Tris buffer with DTNB, helped them to get their results. TCA and Tris buffer were introduced to the DTT methods. **The second method** was as follow:

3.5 mL of the aerosol extract and 1 mL potassium phosphate buffer (0.5 mM) were transferred to an incubation vial. Then 0.5 mL of DTT (1 mM) was added, the DTT-buffer-sample mixture was incubated at 37 °C and continuously shaken (400 rpm). At specified times (4, 13, 23, 30, and 41 min) 100 µL of the incubated mixture was withdrawn to another centrifuge tube containing 1 mL TCA (1 % w/v), wrapped in aluminium foil to prevent possible light interference. Then 2 mL of Tris buffer (0.08 M with 4 mM EDTA) and 0.5 mL DTNB (0.2 mM) were added. The absorbance of this final mixture was then determined using UV-vis at 412 and 700 nm. 700 nm being the baseline absorbance for TNB. Unfortunately, this method did not work. The final solution, that is measured by UV/Vis, should turn into a yellow solution, but a colourless solution was obtained.

Because the second method did not work, the second method was slightly modified. The same reagents were used but instead of putting the whole sample in one tube, samples were tested in seven tubes. **The third method** was as follow: 0.7 mL of the PM extract was transferred into seven centrifuge tubes. 0.2 mL; 0.5 M potassium phosphate buffer and 0.1 mL; 1 mM DTT were added to each tube. Tubes were heated in a water bath at 37 °C and at designated time intervals (0, 3, 6, 9, 12, 15, and 20 min) 1 mL; 10 % v/v of TCA was added to quench the reaction. After all time points have been quenched 0.5 mL of this reaction mixture was combined with 25 μ L; 10 mM DTNB in 1 mL of TRIS buffer (0.4 M TRIS, pH = 8.9 in 20 mM EDTA). Absorption of the coloured solution was measured at 412 and 700 nm using UV-vis. The results showed a correlation but little variation between the time and absorption as shown in Fig 2.11.

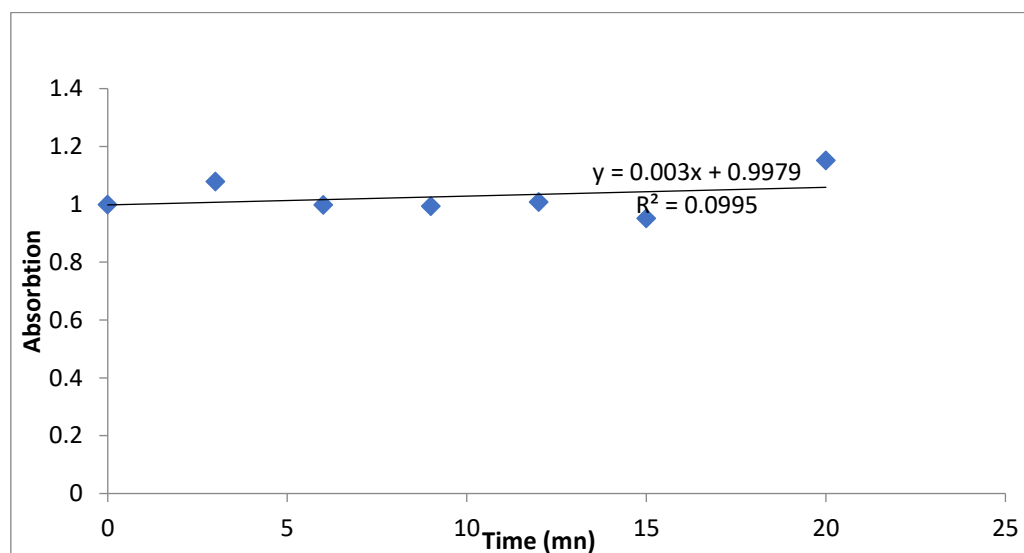


Figure 2.11 Scatter graph shows the slope of DTT consumption vs. time.

Many modifications were tested, including using dry incubator instead of water bath to maintain 37 °C for the reaction, wrapped tubes with foil to prevent

light interfere, and tested different samples with different concentrations. None of these modifications gave constant and realistic results compatible with the DTT assay criteria. Thus, criteria are DTT consumption needs to be no less than 2% and no more than 25% and coefficient of variation for triplication need to be less than 15% (Cho *et al.*, 2005b).

After reading and analysing many articles and contacting Dr. Vishal Verma (Verma *et al.*, 2007), it was found out that TCL and Tris buffer were not necessary in this assay, the amount of PM in the reaction should be the same for all samples, the reaction mixture needs to be 1 ml. all reagents were replaced, and at this moment an email was received from the company stated that DTT powder should be kept in fridge all the time not in the room temperature. The new method was tested many times and showed stable and strong correlation between time and DTT degradation.

2.5.2 Final Method:

2.5.2.1 Stock preparation:

- 1- 0.154 g of DL-Dithiothreitol, $\geq 98\%$ (DTT) was dissolved in 100 ml DIW to make 10 mM DTT stock. The stock was then kept in fridge in amber glass with a glass stopper. Just before DTT was used, the stock was diluted to 1 mM by transferring 5 ml from the stock to a 50 ml volumetric flask wrapped in foil to block light and then made up by DIW.
- 2- 0.396 g of 5,5'-Dithiobis(2-nitrobenzoic acid), 99 % (DTNB) was dissolved in 100 ml methanol to make 10 Mm DTNB stock. The stock was then kept in fridge in amber glass with a glass stopper. Just before DTNB was used, the stock was diluted to 0.2 mM by transferring 0.4 ml into amber glass and then 19.6 ml of DIW was added.

- 3- 8.71 g of dibasic potassium phosphate (K_2HPO_4) was dissolved in 100 ml of DIW to make 0.5 M of dipotassium phosphate. 1.701 g of monobasic potassium phosphate (KH_2PO_4) was dissolved in 10 ml of DIW to make 0.5 M monopotassium phosphate. The pH of dipotassium phosphate was adjusted by adding monopotassium phosphate until the pH stabilized at 7.40. The K-buffer stock was kept at room temperature in a glass bottle.
- 4- 0.0260 g of 9,10-Phenanthrenequinone, $\geq 99\%$ (PQN) was dissolved in 25 ml of Dimethyl sulfoxide (DMSO) to make 5 mM of PQN stock. The stock was kept in amber glass in the fridge. The stock was diluted directly before it was used to 0.05 μ M.

2.5.2.2 Filter extraction:

Depending on the PM mass loading of each filter, different numbers of punches ranged from 3-10 were taken from the Teflon filter in order to have ~ 20 μ g $PM_{2.5}$ in the reaction. E 2.3 was used to calculate how many punches were needed from each filter:

$$\frac{\frac{\text{Total PM on filter } (\mu\text{g}) \times \sum \text{SA of punches } (\text{mm}^2)}{\text{Filter SA } (\text{mm}^2)}}{\text{Final extract } V \text{ (mL)}} \times V \text{ of sample in reaction (mL)} \quad (\text{E 2.3})$$

Where SA = surface area

47 mm Teflon filters were used to collect $PM_{2.5}$ from Dammam, so E3 become:

$$\frac{\frac{\text{Total PM on filter } (\mu\text{g}) \times \sum \text{SA of punches } (\text{mm}^2)}{855 \text{ mm}^2}}{10 \text{ mL}} \times 0.7 \text{ mL} = \text{PM in reaction } (\mu\text{g}) \quad (\text{E 2.4})$$

Punches that were taken from the Teflon filter were placed in a 15 ml centrifuge tube. 5 ml of methanol was added to the tube using a calibrated automatic pipette. PM was extracted through sonication for 15 minutes. The extraction was

dried to about 1-2 ml by nitrogen blowdown. DIW was then added to the extraction to make up the final volume of the extraction to 10 ml. Finally, a 0.45 μm syringe filter was used to filter the extraction and move it to a new centrifuge tube. The extract was kept in the fridge until the time of the analysis which was done within 48 hours.

2.5.2.3 *Final DTT Assay:*

0.7 ml of the sample was mixed with 0.2 ml of K-buffer and heated in a water bath at 37 °C. 100 μl of 1 mM DTT was added to the sample and K-buffer mixture to form the reaction mixture. The reaction mixture was shaken well and then 100 μl of this reaction mixture was taken using a calibrated pipette and added to 0.7 ml of 0.2 mM DTNB in 1.5 ml amber glass vial to form the coloured mixture. The coloured mixture was immediately measured using dual-beam UV-vis. The reaction mixture was kept in the water bath, and then after various time points (10, 20, 30 and 40 minutes, plus the one taken at 0 minutes), 100 μL was added of 0.2 mM DTNB and measured immediately by UV-vis at 412 and 700 nm. Blank filters received the same treatment as the samples, and all samples were blank corrected. Also, PQN was used as a positive control by using the sample method, but instead of a sample a 0.05 μM of PQN was analysed as shown in fig 2.13. in order to check the validity, repeat and stability of the result, the coefficient of variation (%CV) was measured every day by repeating one random sample three times where %CV should be below 15%.

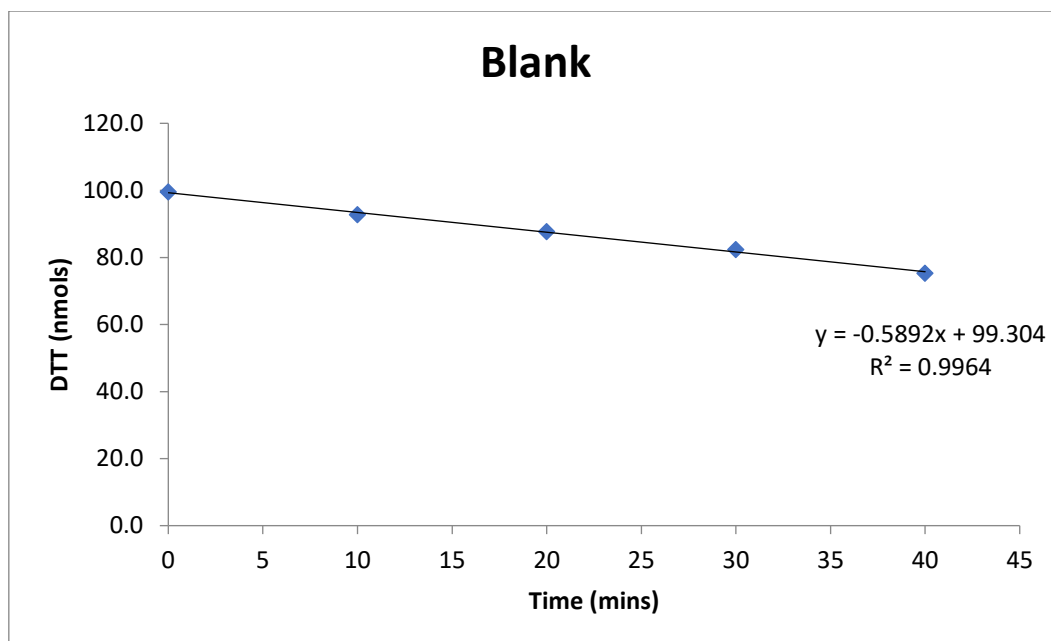


Figure 2.12 An example of scatter graph for the slope of DTT against time using DIW.

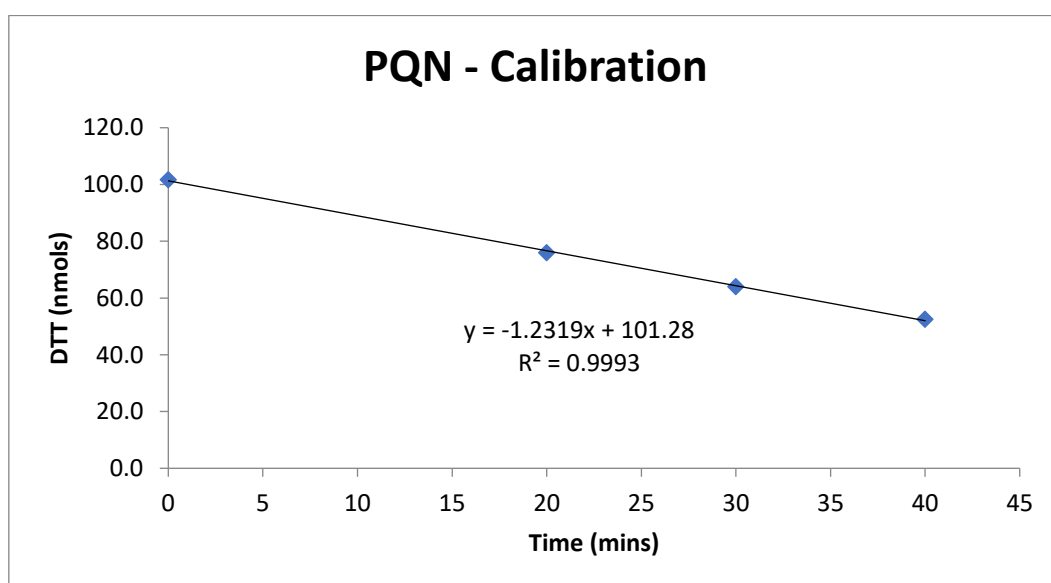


Figure 2.13 An example of scatter graph for the slope of DTT against time using PQN as a positive standard.

2.5.2.4 Calibration:

Various DTT concentrations were tested using DIW and K-buffer only, without heating in the water bath. 0.7 ml of DIW was mixed with 0.2 ml of 0.5

mM K-buffer in five centrifuge tubes. Then 100 μ l of different concentrations of DTT was added to each tube. These concentration were:

100 μ M: 5 mL in 50 mL DI

80 μ M: 4 mL in 50 mL DI

60 μ M: 3 mL in 50 mL DI

40 μ M: 2 mL in 50 mL DI

20 μ M: 1 mL in 50 mL DI

Also, 0 μ M of DTT was applied by adding DIW instead of DTT. 100 μ L was taken from each tube and added to 0.7 ml of 0.2 Mm DTNB. The coloured mixture was measured in the same way as samples using the same UV-vis at 412 nm and 700 nm. The 700 nm reading was subtracted from the 412 nm reading. The absorbance (x-axis) is then plotted against the DTT concentration (y-axis) to give the calibration curve:

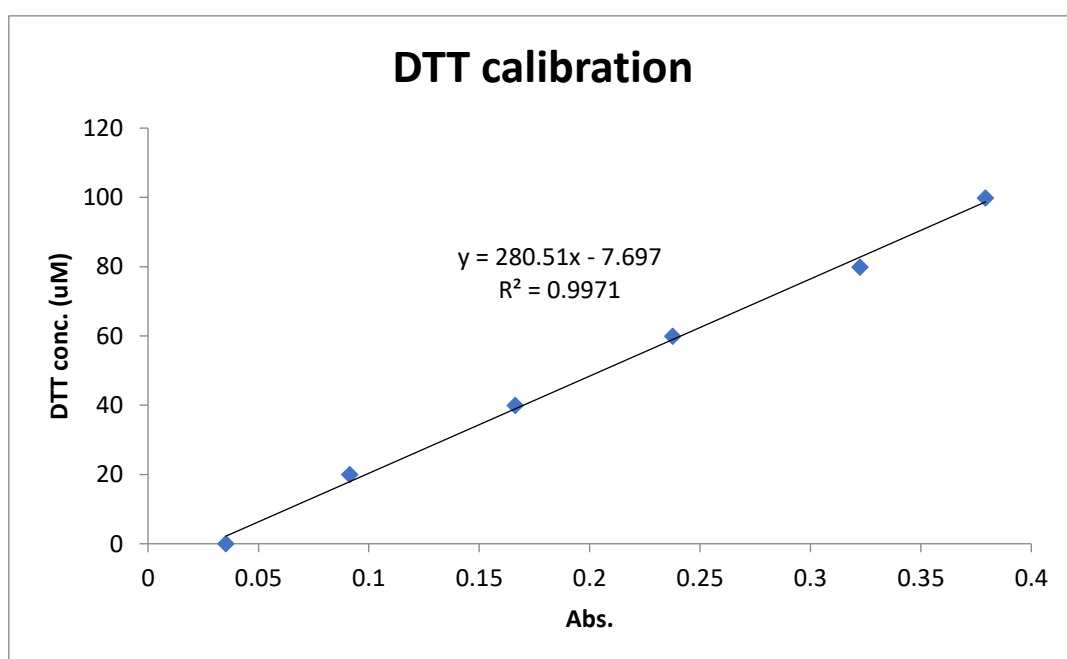


Figure 2.14 Scatter graph of DTT concentration vs. absorbance

The straight line equation in this graph was used to determine DTT concentration from absorbance:

$$\text{DTT concentration } (\mu\text{M}) = 280.51 * \text{absorbance} - 7.697.$$

The calibration curve was done for every new stock of DTT prepared.

2.5.2.5 Calculation:

OP activity for each sample is calculated based on DTT consumption rate, which is determined from the absolute value of the slope of the linear regression of DTT vs. time. The slope of the sample was corrected using the slope of the blank filter. For instance, the slope in the fig 2.15, which is for sample collected in the summer from Amanah location, is 1.38, and the slope for the blank in fig 2.12 is 0.59. after subtraction, the value of the sample will be 0.79. Thus, this slope is used to calculate the OP activity per air volume using the flow rate of the sampler, or the OP activity per mass volume using the concentration of PM collected on the same filter.

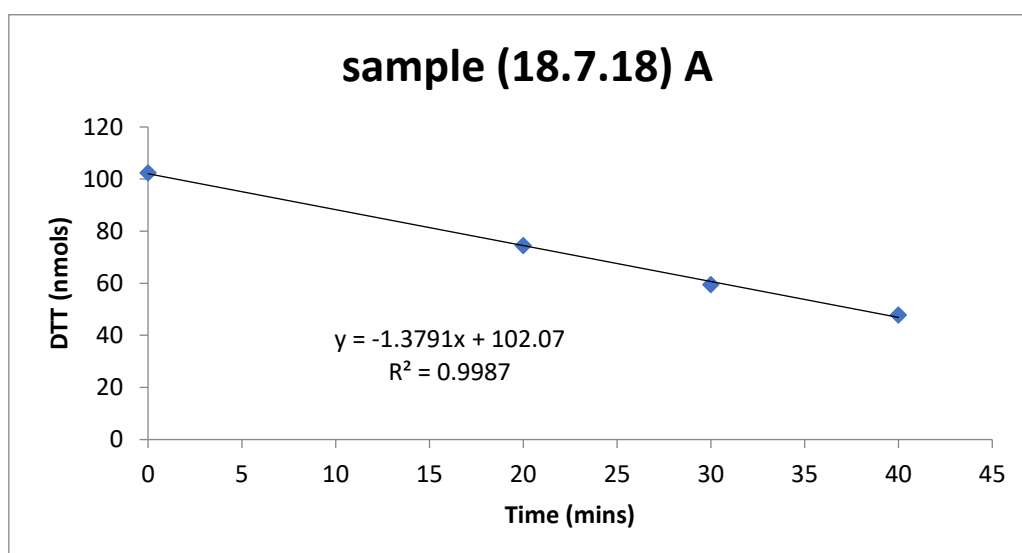


Figure 2.15 Scatter graph of slope of sample collected from Amanah on 18/07/2018.

Chapter 3 . Analysis of the air pollution climate in Dammam (2016-2019)

In this chapter, an analysis of NO₂, NO, NO_x, CO, O₃, SO₂ and PM₁₀ for the period between 2016 and 2019 is provided. Data were collected from two stations in Dammam. Results of this chapter provide diurnal, weekly and monthly pattern of the concentrations of these pollutants.

3.1 Introduction

Understanding the environment in any area is a key factor to protect human health. Air pollutants measurement is necessary to understand the environment of any area. Air quality is one of the most important environmental parameters and is the highest environmental threat to human lives (Sofia *et al.*, 2020). The emission of air pollutants from different sources is not constant as it increases and decreases based on human activities and the type of sources in the urban area. Knowing and studying air quality patterns and temporal variation is essential for air pollution control, protecting human health and examining the impact on people and the environment.

Many factors impact the temporal variation of air quality. The weather condition is one of the most important factors that play a critical role in increasing or decreasing concentrations of certain pollutants. Some pollutants are found at higher concentrations at the daytime in the presence of the sunlight while others are formed and accumulated at night-time. Also, wind speed and direction have an important role in driving pollutants from one place to another, bringing background/upwind components to the study area, and in the dispersion effect on the accumulation of pollutants in any area. The other factor is human activities. Much literature has reported that anthropogenic air pollution increases

when human activities increase, such as traffic (Bigi and Harrison, 2010; Bigi, Ghermandi and Harrison, 2012).

Very few studies have reported air pollution data for Saudi Arabia (SA). Alghamdi *et al.* (2014) reported the measurement of Ozone (O_3), nitrogen monoxide (NO) and nitrogen dioxide (NO_2) in Jeddah for the period from March 2012 to February 2013. In Alghamdi's work, O_3 showed a maximum level in summer while its minimum is in the winter. The authors attributed the high level of ozone in the summer compared to winter to the high temperature, clear sky and light wind in the summer, which are the favourable meteorological conditions for ozone. Ozone is also formed from VOC oxidation in the atmosphere; the longer daylight hours during the summer means more atmospheric oxidation reactions in the presence of NO, and hence more ozone formation. Ozone average concentrations were higher in the weekend (Friday) compared to weekdays (Saturday-Thursday) during all four seasons. The higher level of ozone in weekends was attributed to the low-level emission of NO in the weekends because of low traffic density in the weekends compared to weekdays. Ozone was found to reach its maximum in the afternoon for the daily pattern. NO_2 and NO also showed maximum concentration in the spring, and minimum level was the summer. NO_2 and NO were found to be lower during weekends compared to weekdays, owing to lower traffic density. For diurnal patterns, NO_2 and NO had their peak in the early morning (06:00 – 08:00), and another peak was observed only in the summer at midnight (00:00 – 02:00). Gasmi *et al.* (2017) studied NO_2 , NO and NO_2 daily pattern from 07 May to 30 July 2015 in Dharan city, about 10 km away from Dammam city (the main city in the eastern province of SA). In this study, NO has its maximum concentration at 0800 then

start to decline until it starts to increase around 2200. NO₂ has its maximum concentration about 2300 then decreases to reach its minimum at 0400 then increase again until 0800. The authors explained these peaks were highly correlated with traffic density. These two studies analysed pollutants measurements over a short period and thus may not be enough data to fully understand the air quality in SA.

Two studies reported air pollution data in SA over long periods. Alharbi, et al (2014) measured the concentrations of PM₁₀, CO, SO₂, H₂S, O₃ and NO₂ for the period from October 1999 to June 2004 in the city of Riyadh. The authors reported the annual trend for each pollutant. The largest annual concentration (17.2 ppm) of CO was in 1999 while its lowest (6.8 ppm) was in 2004, and the level of CO was below the SA standard level (35 ppm) for the whole study period. NO₂ highest annual concentration (29 ppb) was measured in 2003 and its minimum level (13.5 ppb) was in 2001. The annual Saudi's standard for NO₂ (50 ppb) was exceeded in 2003 only. O₃ showed a maximum annual concentration (28 ppb) in 2004 while its minimum (9 ppb) was recorded in 2001. Hourly O₃ for the study period did not exceed the Saudi standard (150 ppb). The average annual level of H₂S ranged from 7 – 15.7 ppb which were below the Saudi standard (140 ppb). SO₂ maximum annual concentration (46 ppb) was recorded in 2001 and its minimum (11 ppb) was recorded in 1999. The annual average concentration of SO₂ has exceeded the Saudi standard (20 ppb) during the period of study except for 1999 and 2004. The annual average concentration of PM₁₀ in Riyadh was above the Saudi standard (80 µg/m³) over the period of study. The lowest annual concentration (82 µg/m³) of PM₁₀ was in 2001 while the maximum (146 µg/m³) level was in 2003. In general, all measured pollutants during the study period

have indicated growing trends except H₂S and SO₂. In Yanbu, a highly industrialised city and a major seaport on the Red Sea, Khalil *et al* (2016) observed hourly data of SO₂, O₃, NO_x, PM_{2.5}, PM₁₀ and VOCs for six years from 2000 – 2005. Ozone and VOCs were higher in the spring and summer compared to fall and winter while NO_x was higher in the fall and winter with respect to spring and summer. Ozone showed relatively larger levels on weekends (Friday) compared to weekdays while other pollutants were higher on weekdays in agreement with the finding of Alghamdi *et al* (2014) in Jeddah. PM₁₀ and PM_{2.5} showed higher level in the summer compared to winter. The average hourly concentration of SO₂ had its maximum in the fall while its minimum was recorded in the winter.

Here, we report analysis of hourly air pollutants measurement for four years (2016-2019) from two measurement stations in Dammam, SA. Seasonal, weekly, and diurnal patterns were studied for criteria air pollutants (PM₁₀, CO, NO₂, NO, NO_x, O₃ and SO₂) and their relationship with meteorological conditions.

3.2 Data Analysis

Hourly Air quality data was obtained from the National Centre for Environmental Compliance (NCEC), Saudi Arabia for the period from 2016 – 2019, from two stations. The first station is located at the Corniche of Dammam (50° 120' 16" E, 26° 49' 10" N): the sampling station is inside the open car park of a recreation area on the Arabian Gulf.

The second station is located in the Rakkah area at (50° 17' 72" North, 26° 39' 73" West): sampling station located inside the courtyard of NCEC. These two

stations measure nitrogen dioxide (NO₂), nitric oxide (NO), nitrogen oxide (NO_x), carbon monoxide (CO), sulfur dioxide (SO₂), PM₁₀, ozone (O₃) and meteorological data including wind speed, wind direction, temperature, relative humidity and atmospheric pressure. After data was obtained, a primary quality assessment was performed, including data availability and the removal of unrealistic data. The results showed some unrealistic measurements, such as large concentrations of PM₁₀ e.g. 6000 µg/m³ for an hour, followed by 100 µg/m³ for the subsequent hour. Many gas phases measurements also recorded the same reading continuously for months. All these unrealistic measurements were consequently removed. The percentage of data that were removed from obtained four years data period is shown in table 3.1.

Table 3.1 Percent of measurements removed.

species	Corniche	Rakkah
	Percent removed	Percent removed
PM ₁₀	60.10	4.5
SO ₂	3.4	9.4
NO ₂	41.2	45.9
NO	na	45.9
NO _x	na	45.9
CO	4.2	9.1

O₃	22.7	1.1
----------------------	-------------	------------

3.3 Results and Discussion

The analysed measurements of the two stations will be presented in this section. Due to the significant differences between the measurements of the two stations, each station will have separate graphs for clarity of presentation.

3.3.1 Seasonal Pattern:

Hourly data was used to calculate monthly average concentrations for all species, and hence the annual cycle as shown in Fig 3.3 and 3.4.

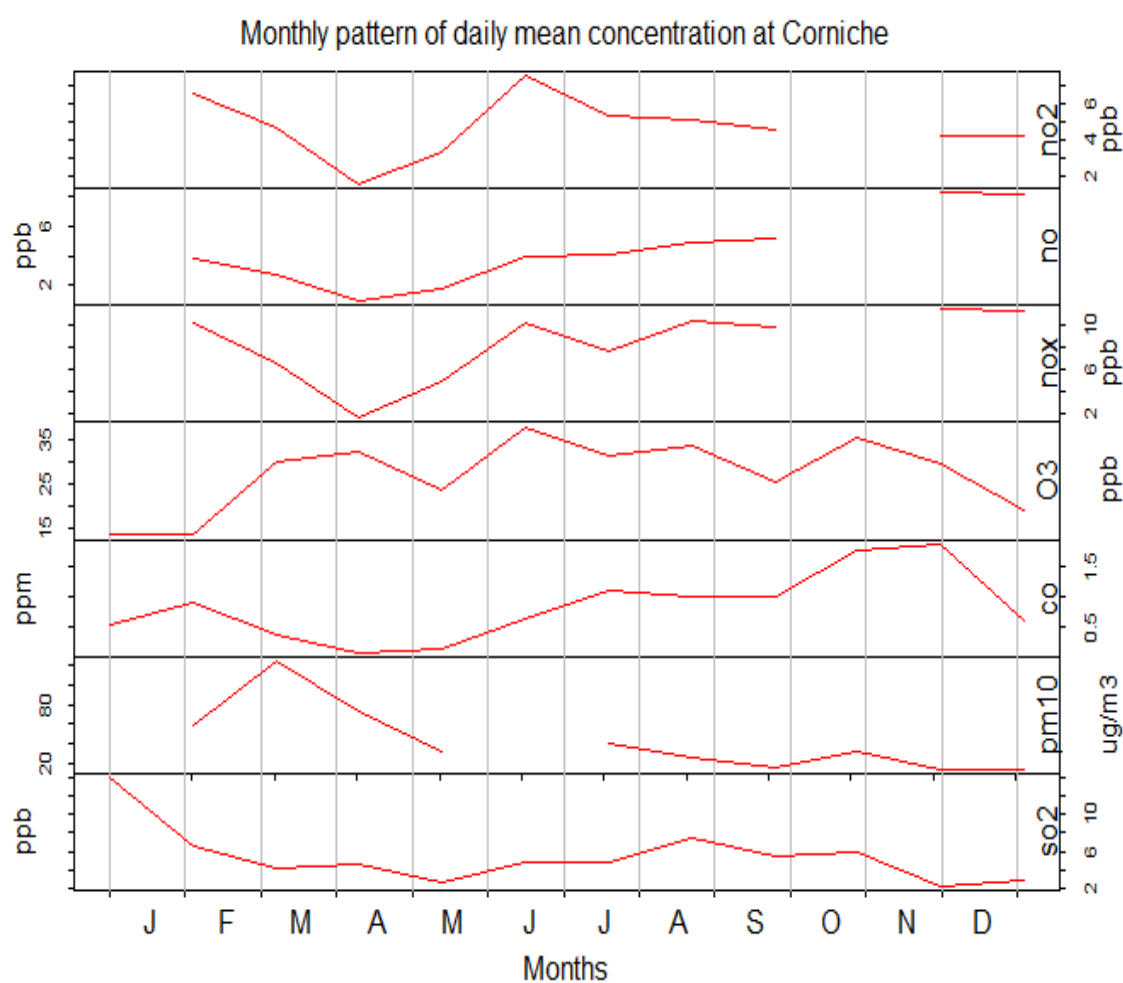


Figure 3.1 time series of annual cycle of pollutants from 2016 to 2019 from Corniche station.

In Corniche, NO₂ showed a maximum in June and a minimum in April, unlike the finding of Alghamdi et al (2014), who found the peak of NO₂ in the spring. The maximum concentrations of NO and NO_x were in December with another peak in summer and lower average monthly concentrations in April. The average daily concentration of CO was high in October and November and its minimum was in April. The O₃ pattern showed a maximum in summer and fall and lower concentrations in winter, similar to what has been found previously in Jeddah and Yanbu (Alghamdi *et al.*, 2014; Khalil *et al.*, 2016). PM₁₀ was high in the spring, where most dust storms occur, and low in the fall and winter while summer measurements were unavailable. SO₂ has its maximum in the January and small peak in August, and its minimum was in November and December unlike what was reported by Khalil *et al* (2016) in Yanbu where SO₂ was high in the fall compared to other seasons.

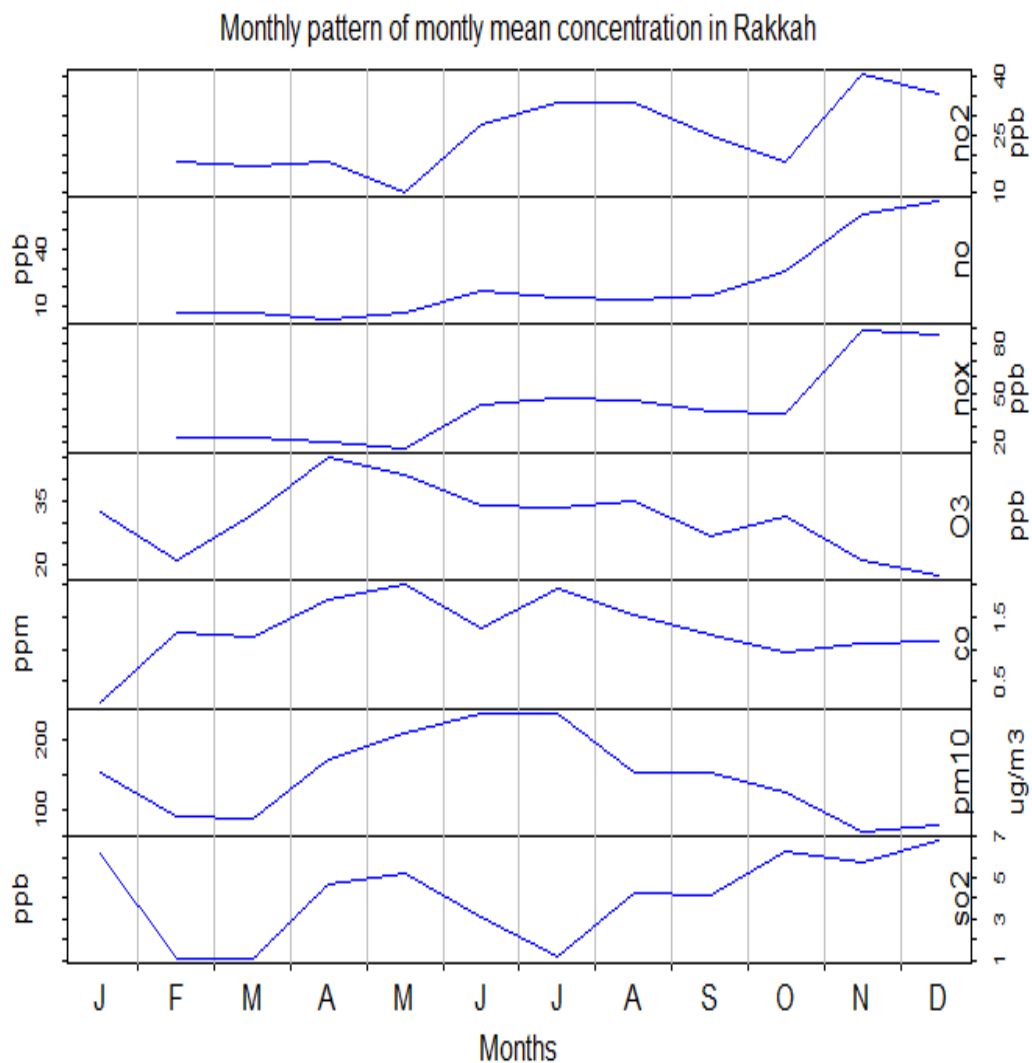


Figure 3.2 time series of annual cycle of pollutants from 2016 to 2019 from Rakkah station

In Rakkah, NO₂, NO and NO_x maximum was in winter, while their lowest average measurements were in spring. O₃ has its maximum in April, while its lowest monthly average measurement was in December. CO showed maximum in May and July its minimum in January. Summer (June and July) recorded the maximum average measurement for PM₁₀, unlike Corniche location, which had the maximum of PM₁₀ in spring. The maximum concentration of SO₂ was in December and its lower concentration was February and March.

The two locations have similarity in the maximum of NO and NO_x in December and SO₂ in the winter. Moreover, the two locations have similarity in the minimum average measurements of NO₂, NO, NO_x and SO₂ in the spring and O₃ in the winter suggesting the impact of regional rather than local sources.

3.3.2 Weekly patterns

It is very important to know that weekend in SA is Friday and Saturday.

Fig 3.5 and fig 3.6 present the weekly pattern of air pollutants was analysed from hourly measurements at Corniche and Rakkah stations.

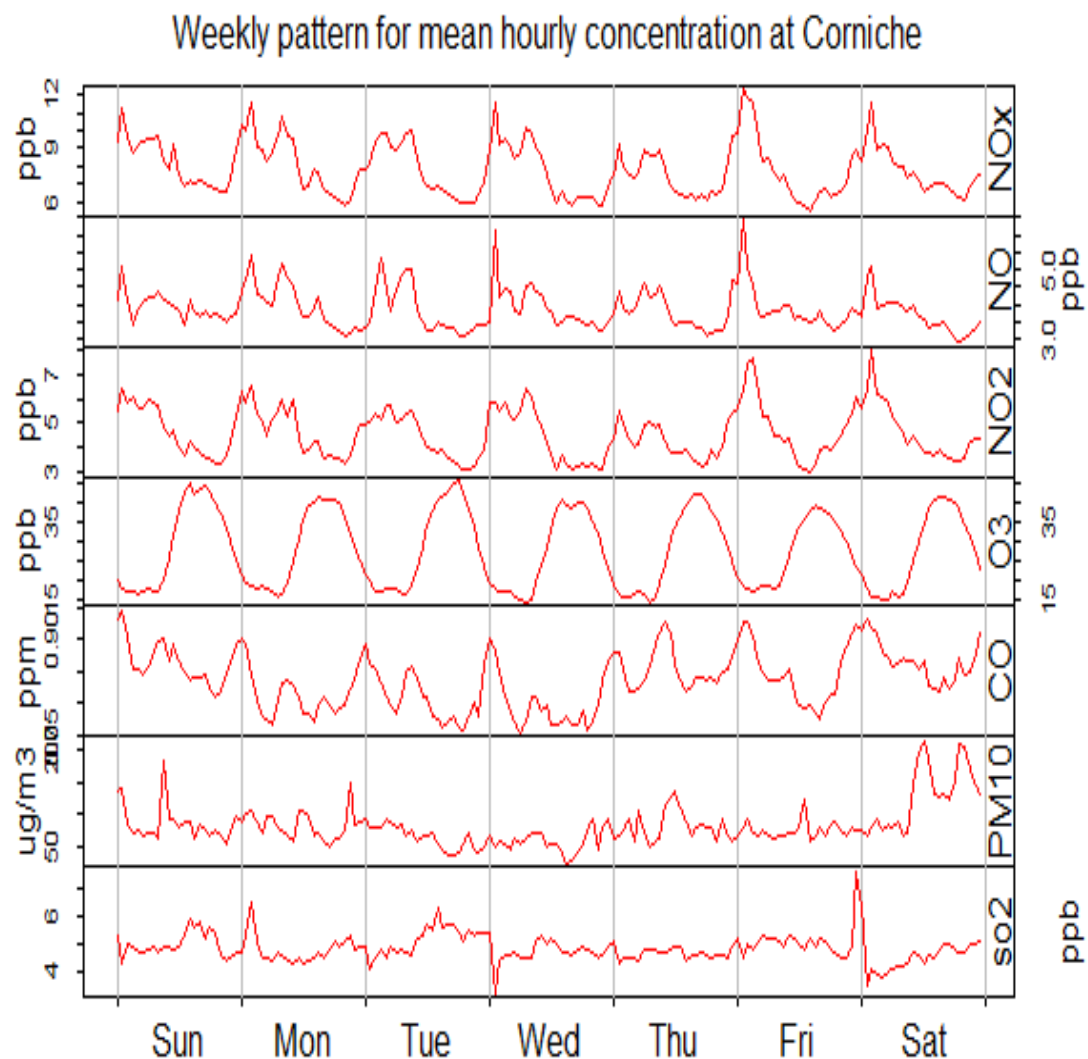


Figure 3.3 Weekly pattern for mean hourly concentration from Corniche station.

In Corniche, traffic-related pollutant CO shows its highest peak on Friday midnight, which could be because this recreation area receives more traffic in the weekend compared to weekdays. People usually go outside in Dammam at night because of heat during the day. NO₂, NO and NO_x have double-peaked patterns on weekdays, one after midnight and the other one around midday while in the weekend these pollutants have one peak after the midnight on Saturday and Friday with minimum average concentration in the midday of weekend. O₃ showed consistent patterns every day with approximately the same value of ozone in the weekdays and weekend in agree with Alghamdi *et al.* (2014) finding. Ozone has one peak in the late of the day followed by a minimum in the early morning. The ozone peaks are inverse to the nitrogen dioxide and nitrogen monoxide, indicating the impact of O₃ and NO photochemical reaction pollution (Bigi and Harrison, 2010; Bigi, Ghermandi and Harrison, 2012). PM₁₀ has a peak on Saturday and a flat pattern on other days. It is hard in SA to predict or connect PM to any activities as it is an arid area, and dust storms are common in this area. SO₂ average concentration shows a smooth daily pattern with its maximum peak on Friday night.

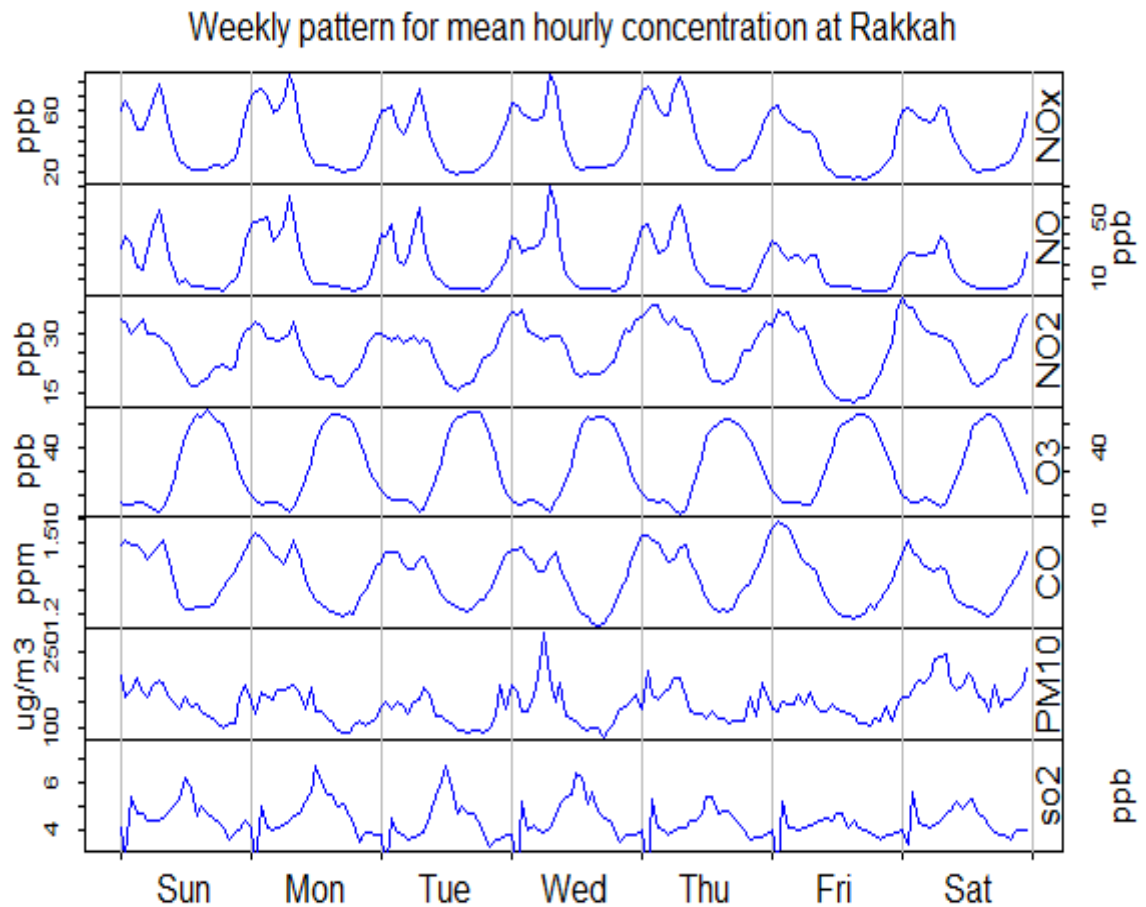


Figure 3.4 Weekly pattern for mean hourly concentration from Rakkah station.

In Rakkah, the traffic-related pollutants NO_2 , NO and CO showed almost the same pattern with a peak at midnight followed by a small decrease then another peak in the morning. The main traffic source to Rakkah is King Abdulaziz road which is the road that connects the city to the seaport. This road is used mainly by trucks and heavy-duty vehicles. In SA, small cars' fuel is gasoline, while trucks and heavy-duty vehicles mainly use diesel fuel. This road is located to the northwest of Rakkah station. Friday showed one peak in the midnight, and it is the day that is like Sunday in the UK and European countries where most companies and factories are close in this day. Ozone showed the same pattern every day, and its peaks are inverse with the peaks of NO as

mentioned earlier. PM₁₀ has its peak on Wednesday, and in Rakkah, it indicates the impact of rush hours with a maximum during rush hours and minimum in the night. SO₂ has its maximum in the late of days during weekdays and almost flat pattern on the weekend.

The average concentration of pollutants at Rakkah station were significantly higher than that at Corniche station except for SO₂, as can be seen in Table. Measurements from Rakkah station showed clearer pattern of traffic-related pollutants than that from Corniche station measurements.

Table 3.2 Mean daily concentration of pollutants at Corniche and Rakkah stations and p value (using paired t.test) comparing these pollutants between the two locations.

pollutant	Corniche	Rakkah	P value
NO ₂ (ppb)	4.5	25	< 0.01
NO (ppb)	3.8	19.1	< 0.01
NO ₂ (ppb)	7.8	41.5	< 0.01
CO (ppm)	0.8	1.3	< 0.01
O ₃ (ppb)	28	32	< 0.01
PM ₁₀ (µg/m ³)	82	143	< 0.01
SO ₂ (ppb)	4.8	4.4	< 0.01

3.3.3 Diurnal pattern:

The diurnal pattern was analysed by hourly averaging the pollutants measurements and presented in graphs showing each pollutant's average concentration for 24 hours in fig 3.7 and 3.8.

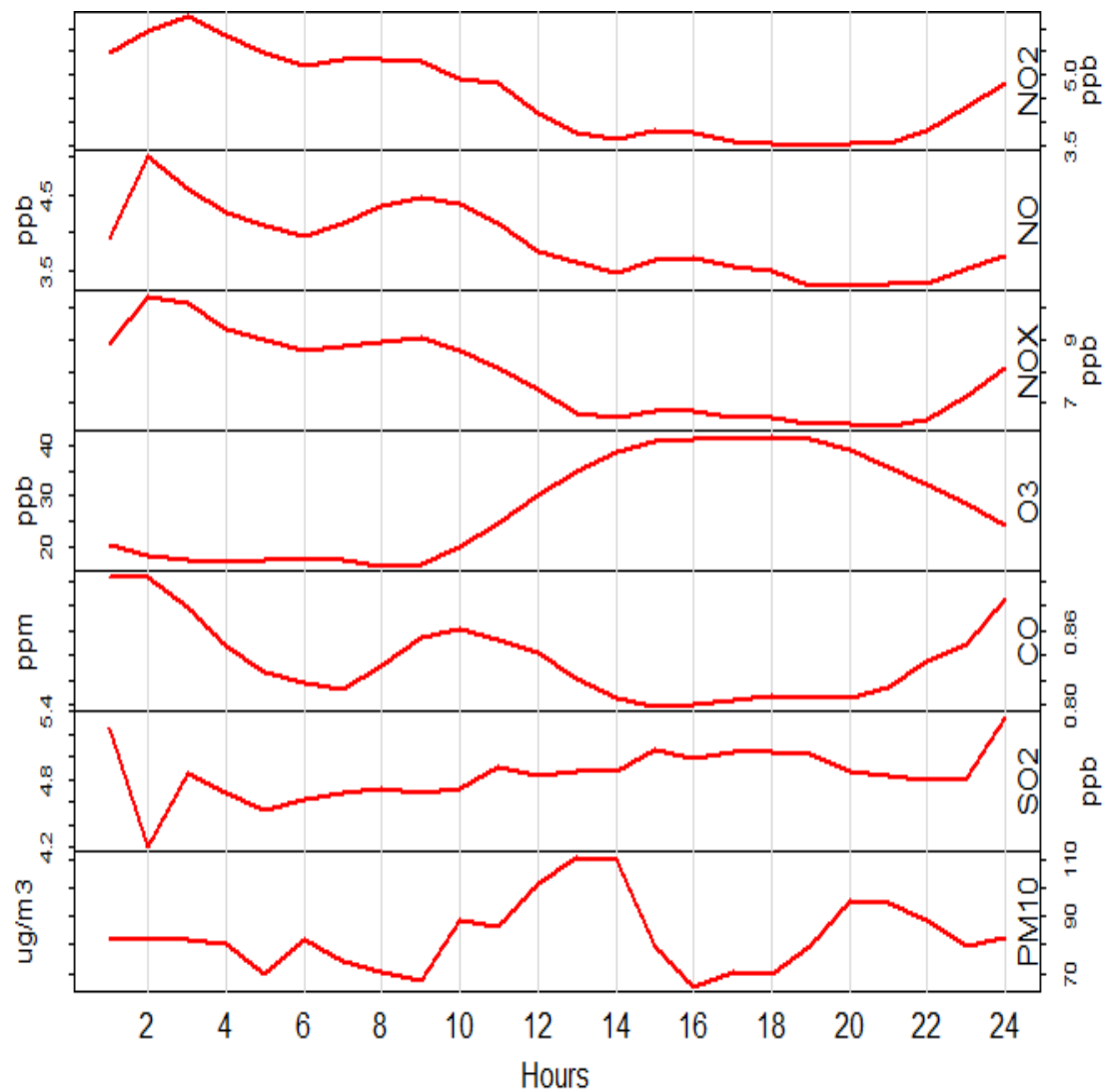


Figure 3.5 Diurnal pattern for mean hourly concentration from Corniche station.

In Corniche, NO_2 , NO , and NO_x have their maximum at 0200 then reduced gradually then have small increase at about 0900 in agree with Gasmi *et al.* (2017) finding and unlike Alghamdi *et al.* (2014) results. NO_2 and NO high concentrations are usually observed when there is an interaction between the dispersion condition and strong source (traffic) (Bigi and Harrison, 2010). Also, nitrogen dioxide and nitrogen monoxide are emitted from diesel vehicles. The occurrence of peaks could be due to trucks and heavy-duty vehicles that usually use diesel fuel at this time. In SA, trucks and heavy-duty vehicles are not allowed to be driven inside cities during rush hours 0500-0800, 1200-1300 and 1700-

2200. The pattern of these pollutants almost agrees with this role as peaks occur in the early morning and have their minimum late in the day and start to increase again at 2200. CO has a maximum average concentration at 0200, which could be for the same reason trucks movement, and it has another smaller peak at 0900, which is the rush hour for people going to their work using their gasoline cars. The ozone pattern was almost the inverse of nitrogen dioxide and nitrogen monoxide, suggesting the loss of NO in the ozone reaction. PM₁₀ showed two peaks, one around 1300 and the other one around 2000, which would be due to the movement of trucks in the daytime and present of dispersion condition. SO₂ has a steady increase from 0500 until 1800, then small decrease was observed and starts to increase again to reach its maximum at midnight. SO₂ declined after midnight to reach its minimum at 0200.

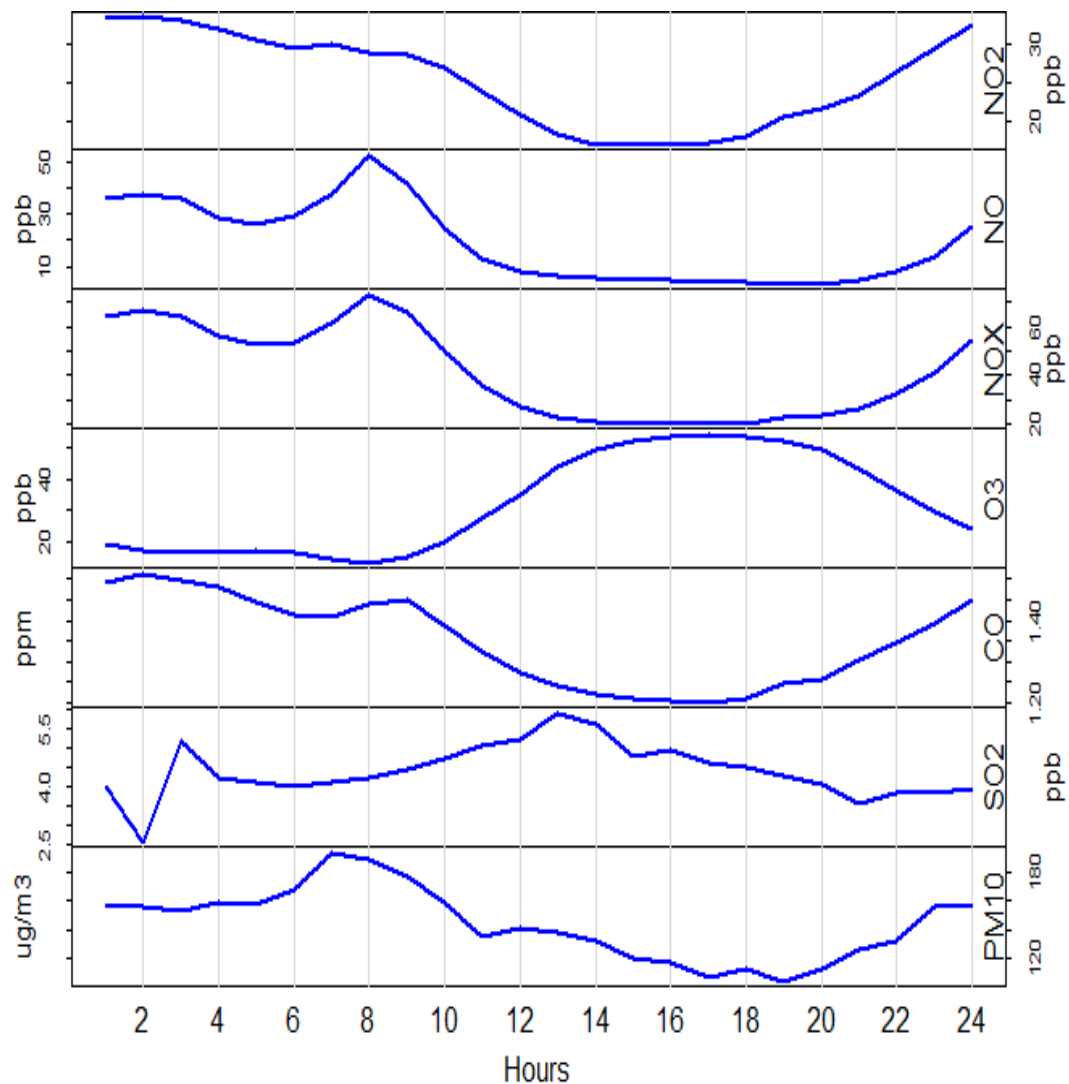


Figure 3.6 Diurnal pattern for mean hourly concentration from Rakkah station.

In Rakkah, all pollutants except SO_2 and PM_{10} showed the same pattern as Corniche station. SO_2 has its maximum average concentration around 1300 then decrease gradually to its minimum level in the early morning. The same has been reported by Bigi and Harrison, (2010) suggesting this peak more properly driven by elevated sources rather than local or nearby sources. PM_{10} has a maximum average concentration around 0700 indicating the effect of traffic rush hour.

3.3.4 The effect of wind speed and direction on pollutants in Dammam:

Polar plots were created to assess the effect of wind direction and speed on the concentration of pollutants. All polar plots were generated using 'openair'

package in R (Carslaw, 2015). Polar plots for NO_2 in fig 3.9 a and b illustrate those high concentrations of NO_2 at Corniche station were seen when the wind came from the southeast while the high concentration of NO_2 at Rakkah station were seen when the wind came from the west and northwest.

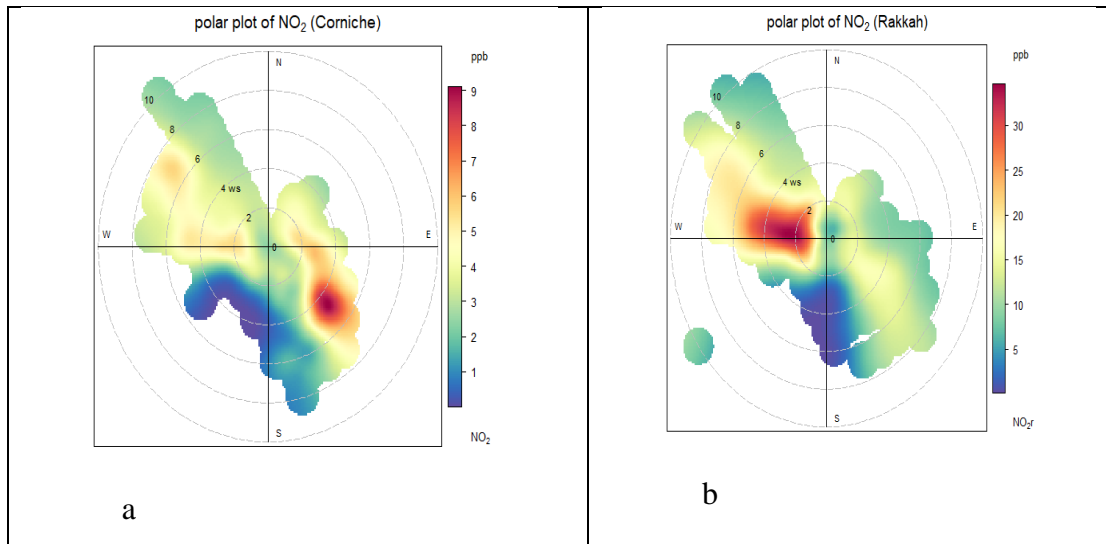


Figure 3.7 Polar plot of NO_2 from a) Corniche and b) from Rakkah stations.

From the map in Fig 3.10, it seems that both stations record high concentration of nitrogen dioxide when the air comes from the same sources. King Abdulaziz Seaport and King Abdulaziz road (red line) could be the main sources for emitting NO_2 in these locations, as mentioned above.

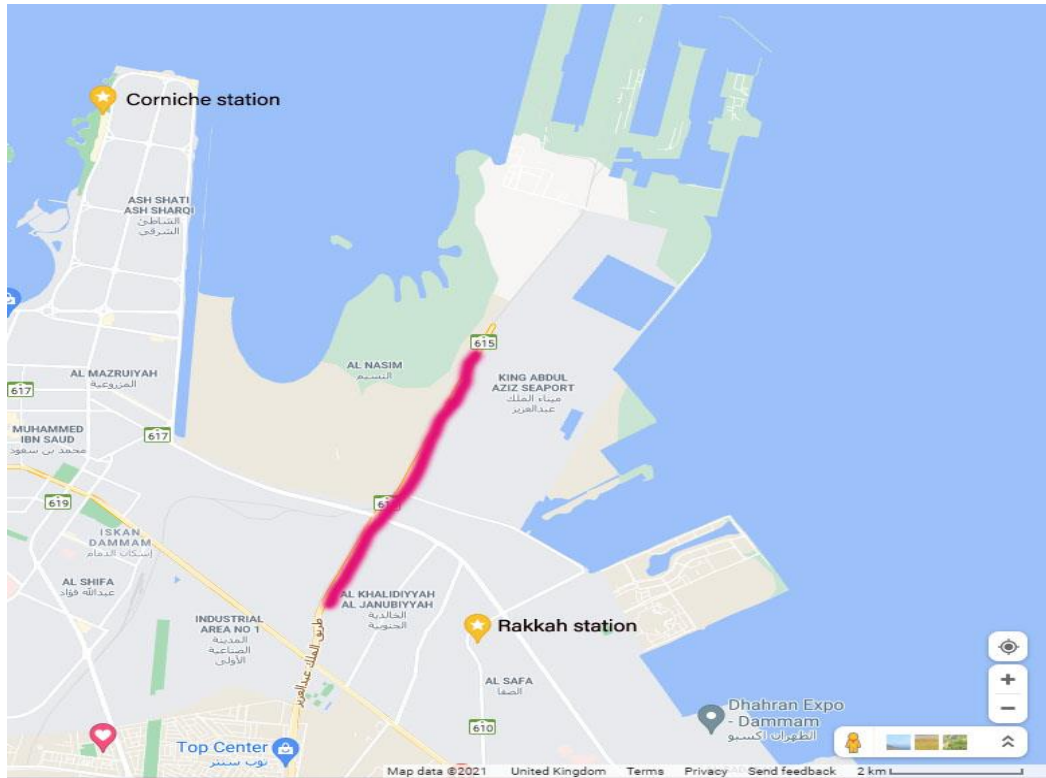


Figure 3.8 Map shows the location of Corniche and Rakkah stations and possible sources of pollutants

The polar plot for NO at Rakkah station illustrates the same source as NO₂ with the same trend as shown in Fig 3.11 b. however, NO at Corniche station showed important sources to the northwest besides the same sources as NO₂ from the southeast, as shown in Fig 3.11 a. To the north of Corniche station is the Arabian Gulf, meaning the NO in this location could be from ships.

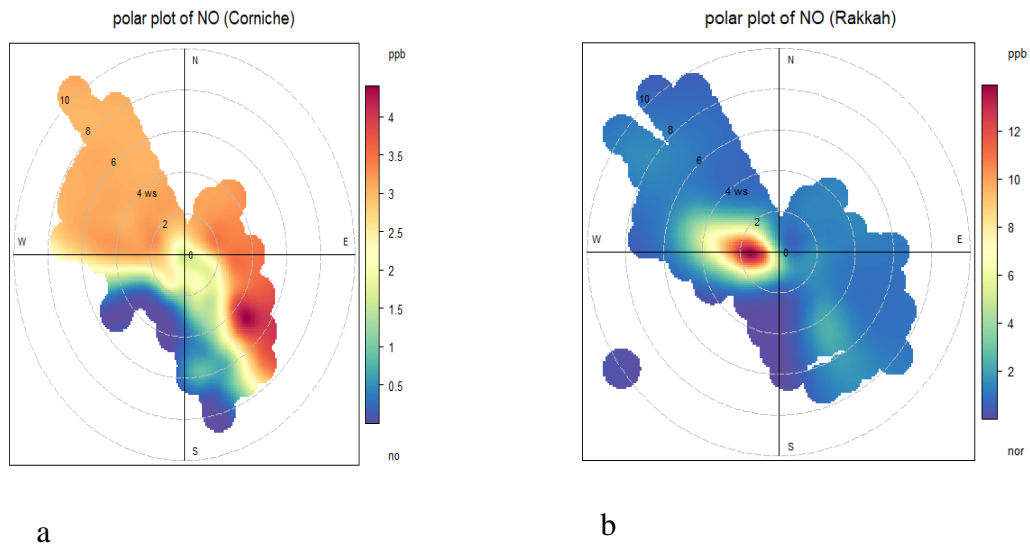


Figure 3.9 Polar plot of NO from a) Corniche and b) Rakkah stations.

Bigi and Harrison (2010) suggested that because SO_2 was high around midday, the sources could be far from the station. It was shown on Fig 3.8 that SO_2 increased in Rakkah after the midday. The polar plot of SO_2 from Rakkah station explained this suggestion, as Fig 3.12 showed high SO_2 came from west when the air speed was high.

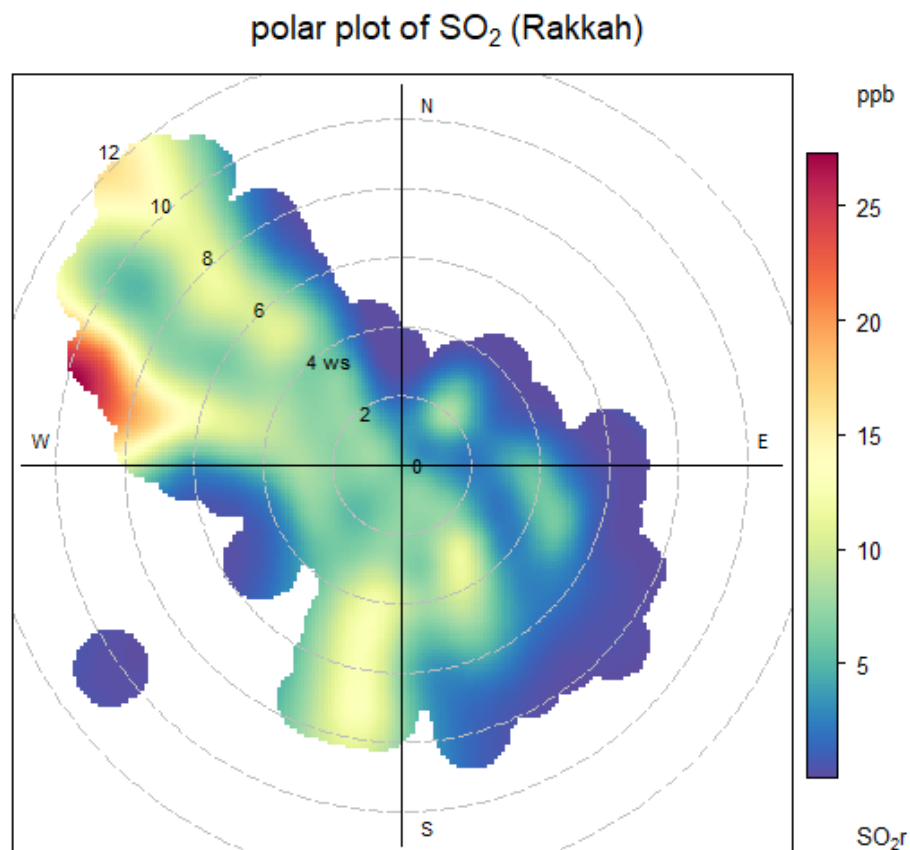


Figure 3.10 Polar plot of SO₂ from Rakkah station.

3.4 Conclusions

In general, concentrations of all pollutants were higher at the Rakkah station than those measured at the Corniche station. NO₂, NO and NO_x levels were higher in the winter compared to other seasons. O₃ was higher in hot months with respect to cold months. Carbon monoxide was higher in the summer than that in other seasons. SO₂ was higher in the winter than in other seasons. The weekly pattern of pollutants showed the effect of traffic emission on air quality, especially in Rakkah. CO has a maximum concentration during the weekend comparing to weekdays. The increase in CO on the weekend was because the Corniche area has more traffic during the weekend than on weekdays. Ozone at both locations showed the same pattern every day. This

analysis shows the impact of traffic on traffic-related pollutants level in Dammam. In some literature, NO_2 and NO were reported to be high in the morning and afternoon during rush hours, while in Dammam, these pollutants were higher in the night when trucks were allowed to be driven inside the city. PM_{10} showed its maximum concentration in hot months impacted by the frequent occurrence of dust storms in these months compared to cold months. However, the maximum mean hourly concentrations of PM_{10} were high in the morning and afternoon illustrating the influence of rush hours on PM_{10} level in Dammam.

Chapter 4. Chemical characteristics and source apportionment of particulate matter (PM_{2.5}) in Dammam, Saudi Arabia

PM_{2.5} mass concentration, composition and sources are presented in this chapter. PM_{2.5} mass, metals, water soluble ions and organic and elemental carbon are presented here for the winter and summer campaigns and for the two locations in Dammam. Also, PMF results for the sources of PM are discussed in detail. In addition, in this part, data is split into dust storm and non-dust storm samples and show the impact of dust storms on air quality and sources of PM in Dammam.

4.1 Introduction

Acute and chronic exposure to fine particles has been linked with several human health impacts, including cardiovascular diseases, respiratory disorders, mortality and morbidity (Rai et al., 2016; Shi et al., 2019; Hama et al., 2020). The world health organization (WHO) said more than 91% of population in 2016 was exposed to air quality that exceed the WHO guidelines, and that in the same year the outdoor ambient air pollution was estimated to cause more than four million premature deaths in the world (WHO, 2018b). Understanding the characteristics and sources of airborne particulate matter (PM) is essential to mitigate its impacts on public health, climate, agriculture and economy.

PM mass is not the only factor in measuring its ability to induce public health. Ambient particulate matter with a diameter of less than 2.5 μm (PM_{2.5}) typically comprises a mixture of chemical components originating from multiple sources (Allan *et al.*, 2010; Geng *et al.*, 2017). The size and chemical composition of PM are thought to be the primary toxic factors to humans, as smaller particles are more toxic than the same mass of large particles (Crilley et

al., 2017). Studying the composition and sources of PM_{2.5} is critical for understanding the capability of these substances while harming people and the environment. Moreover, it has been suggested that low-toxicity outcomes are derived from soil dust, sodium chloride and ammonium nitrate, although they make up the most of PM bulk (Borm *et al.*, 2007a; Kundu and Stone, 2014). In contrast, transition metals that make up a small portion of the total PM mass cause high-toxicity outcomes (Sørensen *et al.*, 2003; Borm *et al.*, 2007a; Kundu and Stone, 2014). Therefore, knowing PM composition in details can help to understand different toxicity from different composition, as a result, helps improving policies to target most toxic components to reduce health impact most effectively from poor air quality.

PM composition may include organic and elemental carbon, metals, silicate, carbonate and ions, and it may combine both primary species emitted directly to the atmosphere and secondary species formed in it (Contini *et al.*, 2010; Hama *et al.*, 2020). The chemical composition of PM in any area is related to its sources, and to subsequent atmospheric processing- evaporation/condensation, and chemical reactions. These processes affect different components to different extents, depending upon the nature of the particles and the post-emission atmospheric environment. Carbonaceous particles are present in the PM in a considerable fraction, representing 21–78% of PM_{2.5} mass, and they have critical environmental and public health impacts including cardiovascular mortality and morbidity (Pio *et al.*, 2011; Grivas *et al.* 2012). Metals are emitted into the atmosphere from natural (volcanic activities and soil dust) and anthropogenic sources (fossil fuel composition, vehicle emission and industrial activities), although their relative importance varies substantially with

the species considered. Metals are typically stable within the atmosphere following emission, and they may accumulate in the human body, damaging internal organs even at low concentrations like Pb, Cd, As and Cr (Lee et al., 2007; Park and Dam, 2010; González et al., 2017).

In general, sources of PM are natural and anthropogenic. These two sources are subdivided into many factors, including soil and sea salt as natural and industrial emissions, biomass burning and oil combustion as anthropogenic sources. Distinguishing between these sources is not easy, especially in the urban environment. Still, several methods may be used to evaluate the contribution of various sources to PM. One such method is the enrichment factor (EF) established by Taylor (1964), which is a mathematical equation used to differentiate between the potential natural or anthropogenic sources of PM composition by comparing the ratio of the concentration of an element in the air sample with a reference element (like Al or Fe) that is believed to be entirely from crustal sources. By using this method, it is possible to compare the relative amount of a measured element with typical crustal background values (Duan et al., 2006; Haritash and Kaushik, 2007; Murillo-tovar, 2011; Chen et al., 2015). Another way to distinguish between different PM sources is the receptor-model-based source apportionment (Sharma and Mandal, 2017). Receptor modelling uses measurements of PM chemical composition as critical factors to differentiate between sources (Pant and Harrison, 2012). The positive matrix factorisation (PMF) implementation from the United States Environmental Protection Agency (USEPA) (US-EPA, 2014) is one of the most common models for estimating the contribution of each source to PM.

The air quality in Saudi Arabia (SA) is negatively impacted by the prevailing incidence of dust storms and anthropogenic sources from petroleum industries, constructions and a rapidly increasing number of vehicles (Farahat, 2016; Lihavainen et al., 2017). Due to the hot weather, arid lands and dust storms, the average PM concentration in SA is higher in hot months than in cold months (Alharbi et al., 2015; Munir et al., 2017). In Makkah, the average mass concentration of PM_{2.5} in the summer was 88.3 µg/m³ while it was 67.6 µg/m³ in the winter (Nayebare *et al.*, 2018), in Riyadh, the PM_{2.5} average mass concentration was 104 µg/m³ and 76.3 µg/m³ in the summer and winter respectively (Rushdi *et al.*, 2013), and in Hada al-Sham (rural area) the average mass concentration of PM_{2.5} was 37 µg/m³ in the summer and 30 µg/m³ in the winter (Lihavainen *et al.*, 2016). The most abundant PM_{2.5} composition in SA is crustal elements, followed by secondary inorganic ions (NH₄⁺ and SO₄⁻) (Alharbi et al., 2015; Nayebare et al., 2016; Bian, 2018). Nayebare et al. (2016) studied the source of PM_{2.5} in Rabigh, SA. The 24-hour PM_{2.5} samples were collected on PTFE filters using a low volume air sampler in a residential area from 6th May to 17th June 2013. Samples were analysed for mass concentration, black carbon, water soluble ions and trace elements. The contribution of sources to PM_{2.5} in Rabigh was predicted using the PMF model (version 5.0.14). The authors reported five possible sources of PM_{2.5}, identified as crustal, heavy oil combustion, industrial dust, vehicle emissions and sea spray. In Jeddah, Khodeir et al. (2012) investigated the composition and sources of PM_{2.5} by collecting 24-hour samples on Teflon filters at seven sites from June to September 2011. Filters were analysed for trace elements using dispersive energy X-ray fluorescence. Five factors were identified for trace PM_{2.5} elements in Jeddah,

including crustal, oil combustion, traffic, industrial mix-1 (welding, fine sanding and other metal cutting activities) and industrial mix-2 (polishing and air plastic burning). The crustal factors represented 40% and 51% of the $PM_{2.5}$ sources found in previous studies. Both studies collected samples in hot months only which may be the reason of the high contribution of crustal elements. Moreover, oil combustion, industrial, and traffic factors were all identified as $PM_{2.5}$ components in both studies. However, sea salt was not identified in Jeddah, although it is a coastal city. The industrial mix-2 factor in Jeddah was rich in Cl and Na with Ca, but the absence of Mg made the authors decide that this was not from a sea salt source.

Dammam is an urban city located on the east coast of SA. The Arabian Gulf surrounds it to the east and Ad-Dahna desert to the west. Dammam is home to more than three million people and is characterised by rapid urbanisation growth and vehicular traffic. The weather in Dammam is hot, with high humidity throughout the entire year. Usually, temperatures reach $50^{\circ}C$ in the summer, but the temperature range during the winter goes from $0^{\circ}C$ to $25^{\circ}C$. Cars are the only means of transportation, and the city has different industrial and commercial activities. This study is the first to investigate $PM_{2.5}$ composition and sources in urban and urban background locations in Dammam.

4.2 Materials and Methods

4.2.1 Sampling:

Daily (24-hour period) $PM_{2.5}$ samples were collected at two locations in Dammam, SA, over two periods of two months each, January/February and July/August 2018. The first location was on the roof (about 15 m high from ground) of the Amanah building, which is in the city centre of Dammam, which

characterised by high traffic and commercial activities. The second location was on roof (about 15 m high from ground) the Public Health college building roof inside the campus of Imam Abdulrahman bin Faisal University. The PM_{2.5} samples were collected in parallel on pre-baked 100% pure quartz filters and pre-weighed Teflon filters with a 47 mm diameter at each location using MiniVol samplers. Two samplers were utilised at the Amanah location, and two samplers were utilised at the university location simultaneously in both campaigns. A total of 39 daily samples were collected on each Teflon and Quartz filters for each location and each sampling seasons.

Field blanks were collected prior to, in the middle of and at the conclusion of each sampling period and locations. Filters were stored in petri dishes and frozen directly after collection and shipped frozen to Birmingham for laboratory analysis.

4.2.2 Laboratory Analyses:

4.2.2.1 Organic Carbon (OC) and Elemental Carbon Analysis (EC):

The total organic carbon loading, separated into organic (OC) and elemental (EC) carbon fractions was determined by analysing samples collected on the quartz filters by measuring the amount of carbon that evolved from the filter samples as a function of temperature. Organic and elemental carbon were measured using a DRI Model 2015 Multiwavelength Thermal/Optical Carbon Analyser using the EUSAAR2 protocol (Crilley et al., 2015; Vodička et al., 2015). Before the samples were analysed, lab blank calibrations was performed daily. Device control calibration using sucrose was performed every second day following the DRI manual, and all sucrose's results were constant. All results

were corrected using field blank filters which was $0.5 \mu\text{g}/\text{cm}^2$ for OC and $0 \mu\text{g}/\text{cm}^2$ for EC.

4.2.2.2 *Water Soluble Ions (WSI):*

Each quartz filter was extracted in 5 ml of $18.2\text{M}\Omega\text{-cm}$ deionised water using 15 ml centrifuge tubes. Extraction solutions were refrigerated until the time of analysis. All field blank filters were extracted and treated like samples. Water soluble ions were analysed via a Dionex ICS 1100 ion chromatograph fitted with the IONPAC AS22 2×250 mm column to measure anions, while DionexTM Integrion HPIC fitted with (DionexTM ionpac cg12a) column for cations. For quality control, certified reference material (CRM) was used for cation and anion standards. Additional details are described elsewhere (Song et al., 2020). All results were corrected using field blank filter results, and correction ranged from 2% to 20% of measured WSI.

4.2.2.3 *Metal Analysis:*

$\text{PM}_{2.5}$ was extracted from samples collected on quartz filters by adding 10 ml of 68% ultrapure nitric acid using microwave digestion vessels. Vessels were placed in a Mars-6 Microwave Digestion System (CEM). The digestion acid samples were diluted with 2% HNO_3 concentration (16.6-fold dilution) required for using inductively coupled plasma mass spectrometry (ICP-MS).

Metals were measured using ICP-MS. For quality control and testing of the repeatability of the instruments, a standard reference material (Media-NIST, particulate on filter) was performed with each set of extractions (Loyola et al., 2009; González et al., 2017). Extraction efficiency was high (more than 80%) for most elements, except for Al and Ti. All results were corrected using field blank

filter results which ranged from 0% (no target compounds were detected) to 10% of measured metals.

4.2.3 Data Approaches:

4.2.3.1 The enrichment factor:

EF is the ratio of the concentration of two elements in the sample (C_i/C_n), where C_i is the concentration of the metal of interest and C_n is that of the reference metal, divided by the related ratio of the concentration of the same metal of interest and reference in crustal background material (Megido *et al.*, 2017) based on equation 4.1:

$$EF = \frac{(C_i/C_n)_{sample}}{(C_i/C_n)_{background}} \quad (4.1)$$

Where C_i is the concentration of metal of interest, and C_n is the concentration of the reference metal. Aluminium (Al) was used as the reference metal in this work-consequently the enrichment factors determined reflect the approximation that all measured Al is entirely crustal in origin (Perrone *et al.*, 2009).

4.2.3.2 Source Apportionment:

PM sources in Dammam were quantified by the EPA implementation of positive matrix factorisation (PMF) analysis (version 5.0.14). PMF is a model that uses mathematical approaches to estimate the contribution of different sources based on their unique fingerprint. Many researchers have used PMF to determine the sources of PM. A data matrix X of i (number of samples) by j (chemical species) is calculated in the presence of uncertainty (u). PMF solves the chemical mass balance (CMB) between source profiles and species concentrations through the number of p factors, based on equation 4.2:

$$X_{ij} = \sum_{k=1}^p g_{ik}f_{jk} + e_{ij} \quad (4.2)$$

Where (X) is the matrix of the number of samples (i) each composed of the number of chemical species (j), (p) is the number of factors and the mass concentration (g) of each species contributing to each sample (i) multiplied by each factor (k). (e_{ij}) is the residual for each species. Uncertainty of each species was calculated using equation 4.3 (Prendes *et al.*, 1999):

$$Unc = \sqrt{(Error\ Fraction \times concentration)^2 + (0.5 \times MDL)^2} \quad (4.3)$$

MDL is the method detection limit. The error fraction was calculated by dividing the standard deviation of the measured reference material, treated as samples, by the average of these measured materials. This equation was preferred in this work since it takes account of the reproducibility of samples and sampling error. Also, this equation considers the laboratory technique precision errors where detection limit is considered (Prendes *et al.*, 1999). PMF does not accept zero or negative values. The concentration of species below MDL was replaced by half of the MDL following Polissar *et al.* (1998), which is the geometric mean of measured species. The uncertainty assigned to species whose concentration was below the MDL was calculated using equation 4.4, which corresponds to four times the mean geometric value of the species concentration (Polissar *et al.*, 1998; Reff *et al.*, 2007; Kim *et al.*, 2012):

$$Unc = \frac{5}{6} \times MDL \quad (4.4)$$

There are no specific criteria for choosing the number of factors in PMF. In this case, the model was initially instructed to run four factors initially. Then, the number of factors was increased step-wise until nine factors were included.

4.3 Results and Discussion

4.3.1 PM_{2.5} Mass Concentration:

In Table 4.1, the mean and standard deviation of concentration of PM_{2.5}, metals, water soluble ions, OC and EC within PM_{2.5} are shown for the Amanah and University sites for the winter and summer measurement campaigns of 2018.

Table 4.1 Mean concentrations and standard deviation of PM_{2.5}, metals, water soluble ions, OC and EC at Amanah and University sites during the winter and summer 2018 campaigns.

Species	Winter		Summer	
	Amanah	University	Amanah	University
	Mean ± SD	Mean ± SD	Mean ± SD	Mean ± SD
PM _{2.5} (µg/m ³)	63.9 ± 49.1	54.2 ± 31.6	121.2 ± 66.9	114.7 ± 65.6
Metals (ng/m ³)				
Al	2420 ± 2358.7	2229.7 ± 2656.8	3399.3 ± 3687.6	3909.9 ± 4383.8
Ti	76.6 ± 92.9	71.3 ± 107.0	178.6 ± 209.3	189.7 ± 209.6
Mn	25.6 ± 26.6	19.5 ± 22.0	52.1 ± 48.3	56.7 ± 51.6
Fe	1053.8 ± 1381.5	955 ± 1353.0	2512.6 ± 2536.4	2818.5 ± 2768.4
Co	0.7 ± 0.7	0.6 ± 0.7	1.6 ± 1.6	1.7 ± 1.6
Cu	372.3 ± 373	220.5 ± 193.4	81.5 ± 95.7	63.3 ± 75.1
Ni	17 ± 21.5	19.5 ± 21.6	36.4 ± 23.4	26.9 ± 17.7
V	8 ± 4.0	7.7 ± 4.2	14.5 ± 8.2	18.1 ± 8.3
As	0.6 ± 0.5	0.7 ± 0.4	0.9 ± 0.7	0.7 ± 0.7
Sr	14.6 ± 14.5	13.1 ± 17.5	30.4 ± 28.8	34.6 ± 30.9
Sn	27.3 ± 14.9	31.1 ± 26.4	99.5 ± 49.2	117.7 ± 39.4
Sb	5.5 ± 6.8	3 ± 4.5	2.9 ± 3.1	2 ± 1.6

Ba	20.9 ± 20.6	37.7 ± 78.5	30.1 ± 23.9	82.9 ± 79.9
Pb	30.8 ± 45.4	26.7 ± 35.3	36.5 ± 48.0	36.2 ± 70.4
WSI				
(µg/m ³)				
Na ⁺	0.4±0.2	0.4 ± 0.2	0.6 ± 0.4	0.9 ± 0.5
NH ⁴⁺	3.9±3.0	4.1 ± 3.8	4.4 ± 2.2	5 ± 2.2
K ⁺	0.17±0.1	0.1 ± 0.1	0.2 ± 0.1	0.2 ± 0.2
Mg ²⁺	0.16±0.16	0.2 ± 0.2	0.3 ± 0.2	0.5 ± 0.3
Ca ²⁺	1.6±2.4	1.9 ± 3.2	4.5 ± 3.9	6.2 ± 5.2
Cl ⁻	0.54±0.2	0.6 ± 0.5	0.8±0.5	0.8 ± 0.5
SO ₄ ²⁻	7±3.5	87 ± 5.0	13.2±4.9	15.6 ± 6.5
NO ₃ ⁻	3.4±2.1	3.9 ± 2.5	2.7±1.4	2.8 ± 1.2
OC and EC				
(µg/m ³)				
OC	6.3±3.0	6.2 ± 2.9	7.8 ± 3.9	8 ± 4.2
EC	1.8±0.8	2 ± 0.7	1.9 ± 1.4	2 ± 1.4

The mean mass concentration of PM_{2.5} was similar at the two locations for both the winter and summer campaigns. The mass of PM_{2.5} concentration in the summer was nearly twice that in the winter, as shown in Table 4.1. In winter, the PM_{2.5} mass concentration was below the World Health Organisation (WHO) guidelines for maximum PM_{2.5} concentration in 24 hours (25 µg/m³) (WHO, 2021), in three days and four days at Amanah and University, respectively. Both locations were above the WHO guidelines for the maximum PM_{2.5} concentration per 24-hour during all sampling periods in the summer. The mean PM_{2.5} concentration in the Dammam samples during the winter was lower than those observed during the summer, consistent with results from three other Saudi Arabian cities. In this study, the mean of PM_{2.5} concentration in Dammam in summer (118 µg/m³) was 1.9 higher than that observed in the winter (60 µg/m³).

Similarly, in Riyadh and Makkah (Rushdi et al., 2013; Nayebare et al., 2018), the $PM_{2.5}$ concentration in the summer samples was 1.4 times higher than that observed in the winter. In Huda Al-Sham, a rural area about 60 km to the east of Jeddah ((21.802° North, 39.729° East), the $PM_{2.5}$ concentration in the summer was 1.2 times higher than that observed in the winter (Lihavainen et al., 2016). This finding confirms the association between summer and the increase in $PM_{2.5}$ concentration in SA, which may be attributed to dry weather that leads to dust storms and increases air to loft particles from the ground to the atmosphere.

The timeseries of $PM_{2.5}$ mass concentration between the two locations explored in this study was strongly correlated and concentrations tracked each other (Fig 4.1), indicating a regional pattern of $PM_{2.5}$ abundance, and those local sources, specific to just one of the sampling locations, had a minimal impact on $PM_{2.5}$ concentrations.

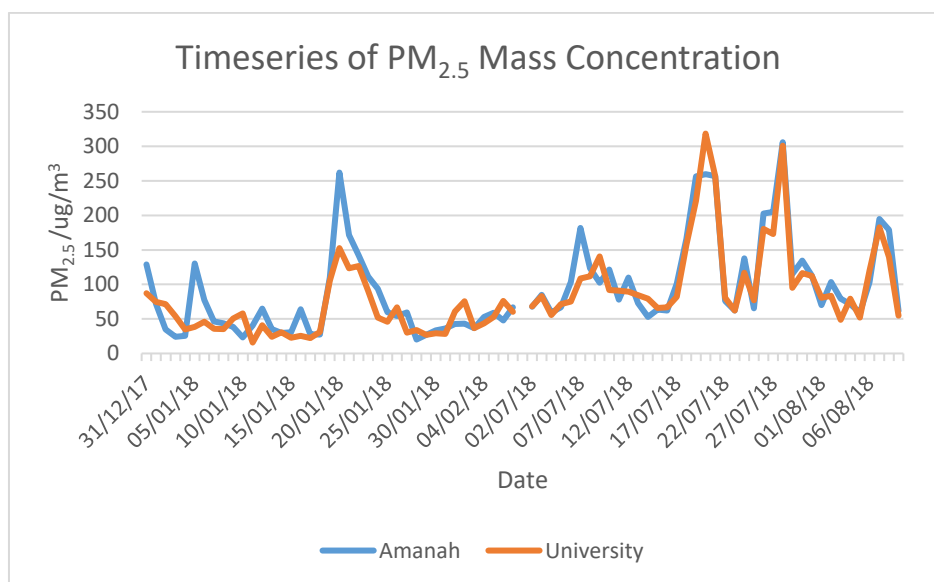


Figure 4.1 The $PM_{2.5}$ concentration ($\mu g/m^3$) timeseries for Amanah (blue line) and University (orange line) sites during the summer and winter sampling 2018 seasons.

4.3.2 Organic Carbon and Elemental Carbon (OC and EC):

Both OC and EC concentrations were similar at the Amanah and university sites (Table 4.1). The mean OC concentrations were higher in the summer than in the winter at both locations (to a statistically significant extent using a paired t.test, $P < 0.05$). The mean EC concentrations showed no significant seasonal variation (using a paired t.test), similarly to observation of Grivas et al. (2012). It is apparent from Fig 4.2 that OC and EC at both locations tracked each other, suggesting a relatively similar background loading from regional sources (such as industries) rather than local ones (such as local road traffic).

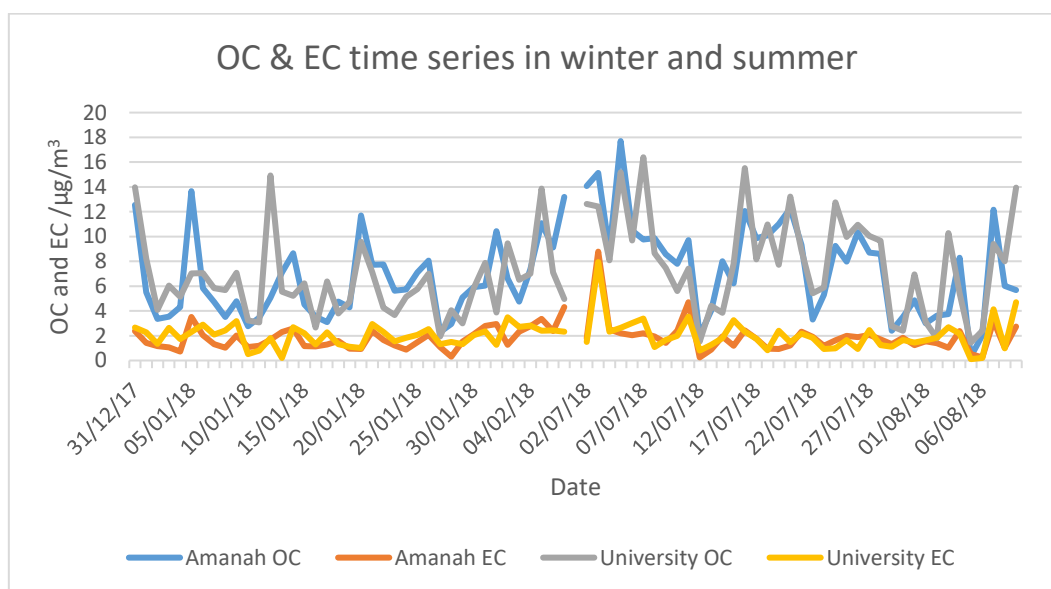


Figure 4.2 The OC and EC time series in the PM_{2.5} mass for Amanah (blue and orange lines) and university (grey and yellow lines) sites during the summer and winter sampling 2018.

4.3.2.1 OC/EC Ratio:

EC is emitted directly as a primary pollutant from the combustion of carbonaceous matter, whereas OC can be emitted directly into the atmosphere (primary OC) or can be formed in it through the reaction of other organic matter with oxidants and subsequent condensation onto PM (Pio et al., 2011; Grivas et

al., 2012; Zhao et al., 2013). The OC/EC ratio may be used as a tracer to evaluate the sources of carbonaceous matter in the atmosphere (Pio et al., 2011). An OC/EC ratio below 1.0 is indicative of samples impacted by diesel emission, OC/EC ratios of around 1.0 are associated with oil combustion sources, and higher OC/EC ratios (with an average of 3.4) are associated with gasoline combustion emission sources (Chow et al., 2011; Pio et al., 2011; Grivas et al., 2012). The OC/EC ratio was higher during the summer than during the winter at both locations. A paired t.test illustrated no significant difference between Amanah and university locations in the two seasons, which provides more evidence of the regional impact of common sources on PM concentrations than local sources.

In the winter, the OC/EC mean ratio was 3.9 and 3.2 for Amanah and University sites, respectively. In the summer the OC/EC mean ratio was 4.8 at Amanah and 5.2 at University location. In both locations and seasons OC/EC ratios were above 3.0. Such a value indicates the impact of gasoline, which is the primary fuel used in Saudi Arabian cars and accounts for 69% of consumed transportation fuel (Howarth et al., 2020).

4.3.3 Water Soluble Ions (WSI):

During the winter, the most abundant WSI measured was SO_4^{2-} followed by NH_4^+ and NO_3^- at both locations. However, during the summer, Ca^{2+} was the second most abundant ionic species after SO_4^{2-} . The Ca^{2+} ionic species had a higher mean concentration than NH_4^+ and NO_3^- potentially because of the influence of crustal-derived components during the summer from dust storms. The mean total WSI mass analysed during the winter was $17.2 \mu\text{g}/\text{m}^3$ at Amanah and $20 \mu\text{g}/\text{m}^3$ at the university. In comparison, the mean total measured ion

concentrations during the summer were $26.8 \mu\text{g}/\text{m}^3$ and $32.2 \mu\text{g}/\text{m}^3$ at Amanah and University, respectively. Even though the mean total measured WSI concentration was higher during the summer than during the winter, the contribution of the WSI to the total $\text{PM}_{2.5}$ mass was higher during the winter at both locations. The total ion contribution to the $\text{PM}_{2.5}$ mass during the winter was 33.2% and 41% at Amanah and University, respectively. During the summer, the total ion contribution was 25.8% at Amanah and 33.2% at the university location Fig. 4.3. The lower contribution of total ions during the summer compared to the winter could be due to the high $\text{PM}_{2.5}$ concentration caused by a higher incidence of dust storms during summer.

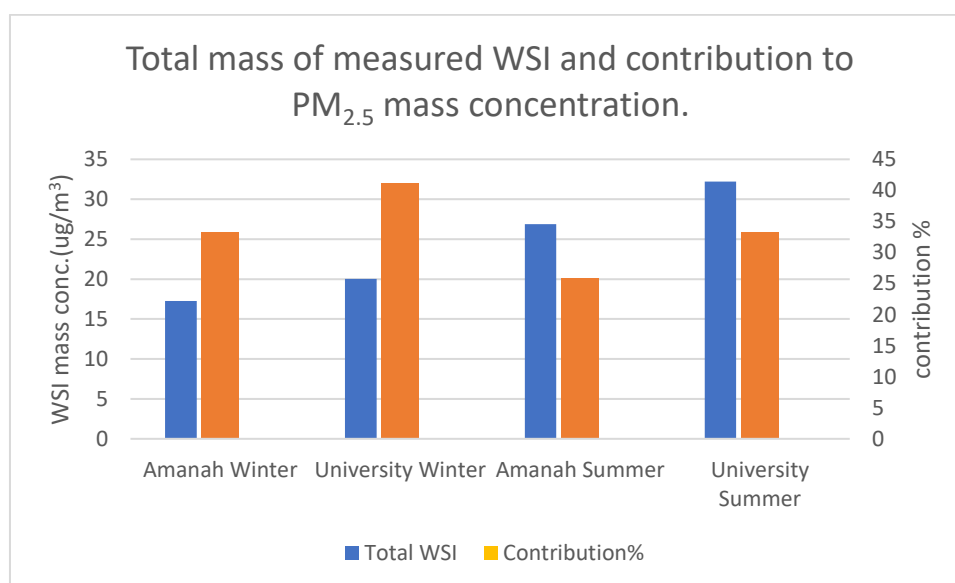


Figure 4.3 Total measured WSI mass and the percentage contribution of such ions to $\text{PM}_{2.5}$ mass for Amanah and University sites during summer and winter 2018.

SO_4^{2-} , NH_4^+ and NO_3^- were the most abundant WSI species, representing more than 80% of the total measured WSI during the winter and more than 75% during the summer at both locations. The high contribution of these three secondary inorganic species has also been found in previous works. In Guiyang,

southwest China, Xiao et al. (2020) found that SO_4^{2-} , NH_4^+ and NO_3^- accounted for 80.05% of the measured WSI. Also, Yang et al. (2020) reported that these three species accounted for 80.2% of measured WSI in Zhengzhou, China. In Delhi, India, SO_4^{2-} , NH_4^+ , NO_3^- and Cl^- contributed to more than 70% of $\text{PM}_{2.5}$ mass (Sharma and Mandal, 2017). In Veneto, Italy, these three species account for 75%–97% of WSI (Masiol et al., 2015). SO_4^{2-} , NH_4^+ and NO_3^- are secondary inorganic species that form in the atmosphere depending on the gas-to-particle transformation of their precursors (SO_2 , NH_3 and NO_x) under certain conditions (Xiao et al., 2020; Yang et al., 2020; Su et al., 2021).

4.3.4 Crustal and Trace Metals:

Overall, a paired t.test showed that there was no significant difference between the mean metal concentrations at Amanah and University locations in either of the two seasons (Table 4.1). On average, crustal elements, such as Al, Fe and Ti, were more abundant than other elements, as expected in arid areas. These three elements represented more than 88% and 94% of the average metal mass concentrations found during the winter and summer seasons, respectively, indicating the substantial impact of crustal elements on the $\text{PM}_{2.5}$ mass in Damman. Concentrations of all other metals analysed were below 100 ng/m^3 , except for Cu at both locations in the winter (Table 4.1). Both Co and As had mean concentration below 1 ng/m^3 at both locations during the winter. During the summer, all non-crustal metals had a mean concentration below 100 ng/m^3 , except for Sn at the university location. Nonetheless, only As mean concentration below 1 ng/m^3 at both locations, as shown in Table 4.1. The seasonal variation for trace elements is indicative that they were higher during the summer than during the winter at both locations. Nonetheless, Cu and Sb reached higher

concentrations during the winter than in the summer ($P < 0.05$). Cu and Sb are connected to traffic emissions (Loyola et al., 2009; Park and Dam, 2010; González et al., 2017). The sample collection obtained during the summer was related to the vacation period, when the number of vehicles was lower than during the winter.

The mean measured total mass of metals was higher during the summer than during the winter. During the winter, the mean total mass of metals was $4 \mu\text{g}/\text{m}^3$ and $3.6 \mu\text{g}/\text{m}^3$ at the Amanah and university sites. During the summer, the mean total mass of metals was $6.5 \mu\text{g}/\text{m}^3$ at Amanah and $7.4 \mu\text{g}/\text{m}^3$ at the University site. However, the opposite pattern was observed for the contribution of metals (combined) to the total $\text{PM}_{2.5}$ mass, where the total metal contribution during the winter was higher than that observed during the summer. The mean contributions of metal species to the total $\text{PM}_{2.5}$ mass was 6.3% and 6.7% at the Amanah and university sites during the winter, respectively. During the summer, the mean total metal contribution at Amanah was 5.3% and 6.4% at the university location, as shown in Fig 4.4.

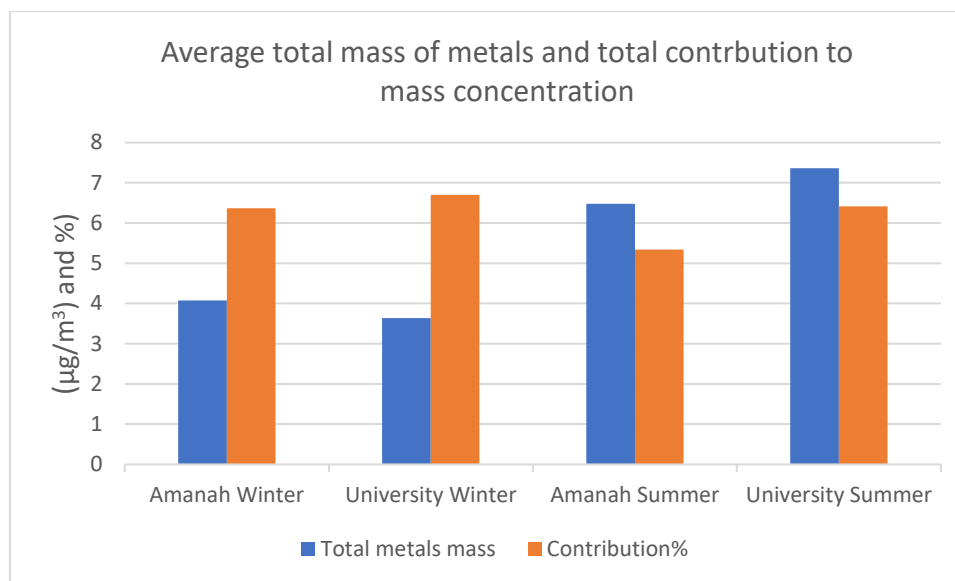


Figure 4.4 Mean mass (blue bars) and percentage contribution (orange bars) of total measured metals for Amanah and university sites during summer and winter 2018 sampling seasons.

4.3.5 Mass Closure:

The mass closure for $PM_{2.5}$ in Dammam was evaluated as the sum of the mass concentrations of the oxides of Al (Al_2O_3), Fe (Fe_2O_3), Mn (MnO), Ti (TiO_2), Ca ($CaCO_3$) and OM ($OM = OC \times 1.6$ (Squizzato *et al.*, 2016; Masiol *et al.*, 2020)) in addition to concentrations of other measured species, including other ions measured in this work (Mg^{2+} , Na^+ , K^+ and Cl^-) and other metals measured in this work (Co, Cu, Ni, V, As, Sr, Sn, Sb, Ba and Pb). It was not possible to quantify the mass concentration of Si (hence SiO_2), so Si was estimated from Al mass concentration assuming $Si = Al \times 3.83$ (M. R. Perrone *et al.*, 2016). Thus, the “crustal” category presented here is the sum of Al_2O_3 , Fe_2O_3 , MnO, TiO_2 , $CaCO_3$ and estimated SiO_2 . The unexplained mass (termed “others” in Fig 4.5), which are unmeasured species or aerosol bound water, was calculated as the difference between gravimetrically determined total $PM_{2.5}$ mass and the sum of measured components (estimated in the case of (SiO_2) mass. In the winter, the crustal components represented 38% and 40% of the average $PM_{2.5}$ mass concentration in the Amanah and University locations,

respectively (Fig 4.5). Secondary inorganic aerosols (ammonium, sulfate and nitrate) represented 22% and 30% of the average $PM_{2.5}$ mass in the Amanah and University, respectively. Organic matter contributed 16% and 18% followed by elemental carbon (3% and 4%), other ions (2% and 3%), and other metals (1% and 1%) at each location. Non-measured components (others), which could be volatile organic compound, represented 18% and 4% of $PM_{2.5}$ at the Amanah and the University, respectively (Fig 4.5). In the summer, the contribution of crustal components increased from 38% at the Amanah site to 52%, and from 40% at the University to 50%, indicating the impact of greater occurrence of dust storms. Secondary inorganic aerosols were the second largest component (after crustal) of the average mass closure of $PM_{2.5}$ contributing to 17% and 20% in the Amanah and University, respectively. The organic matter contribution to the average mass closure decreased in the summer from 16% to 10% at the Amanah site, and from 18% to 11% at the University site. Elemental carbon contributions reduced from 3% and 4% in the winter to 2% in the summer in both locations. The contribution of other ions was 2% at both locations, and other metals were responsible for 1% of $PM_{2.5}$ mass concentration at both sites (considering their elemental masses only, not oxides). The unexplained mass in the summer was 16% at the Amanah and 14% at the University location (Fig 4.5).

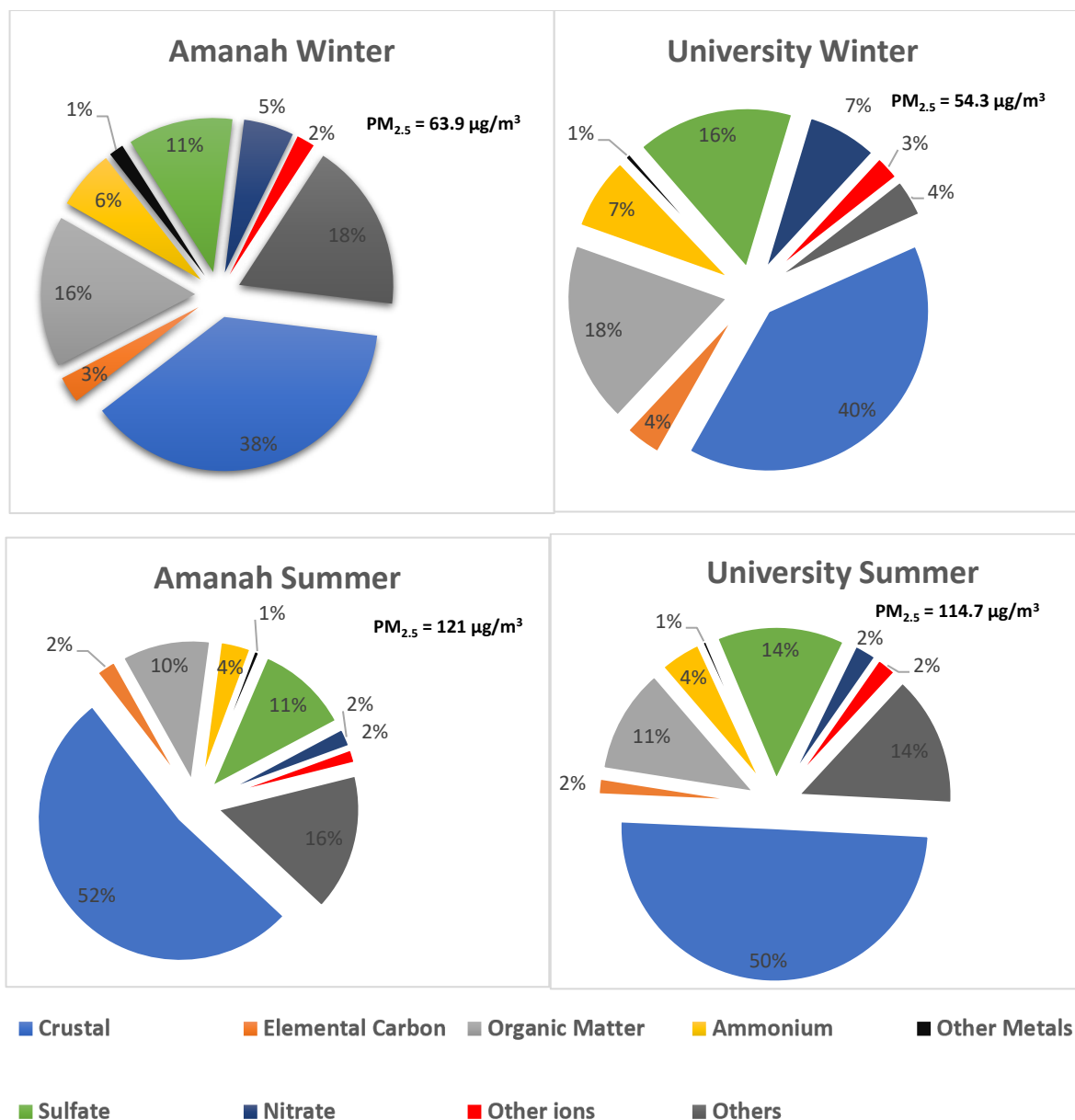


Figure 4.5 Major chemical components of $PM_{2.5}$ in Damman collected in the winter and summer of 2018 where “Crustal” is the sum of Al_2O_3 , Fe_2O_3 , MnO , TiO_2 , $CaCO_3$ and estimated SiO_2 , “Other Ions” is the sum of Mg^{2+} , Na^+ , K^+ and Cl^- , “Other Metals” is the sum of Co, Cu, Ni, V, As, Sr, Sn, Sb, Ba and Pb.

4.3.5 $PM_{2.5}$ Sources in Damman:

4.3.5.1 Enrichment Factor:

If the EF value is equal to or close to 1.0, a given element can be assumed to be generated mainly from the same source as the reference material, in this case Al (i.e., the crustal source). On the other hand, if the EF is higher (with an

indicative threshold EF of 10), the element can be assumed to be generated predominantly from anthropogenic sources (Duan et al., 2006; Murillo-tovar, 2011; Chen et al., 2015). For EF values between 1 and 10, elements can be considered to exhibit a mix of natural and anthropogenic sources (Megido et al., 2017). The EF results are provided in Fig 4.6.

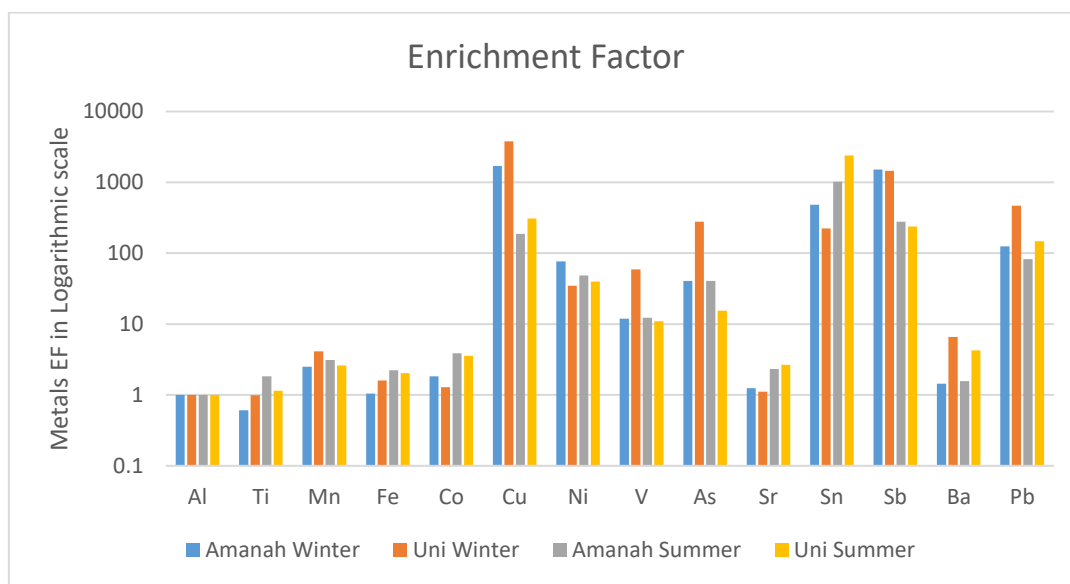


Figure 4.6 Enrichment factor for PM_{2.5} concentration for Amanah and University sites during summer and winter 2018 sampling seasons.

Metals with EF > 10 were Cu, Sb, Pb, Sn, As, V and Ni, indicating that these elements were generated overwhelmingly from anthropogenic sources in these samples. During the summer, Mn and Co reached EF values between 3.0–5.0, indicating that these elements were produced from both natural (crustal) and anthropogenic sources. At the university site, Ba reached EF values of 6.5 in the winter and 4.2 in the summer, whereas at the Amanah site, the EF values for Ba were close to 1.0 in both seasons, suggesting anthropogenic sources near the University site. The EF values for the other elements were below or close to 1.0, suggesting that these elements were mainly of crustal origin. The highest EF value observed was for Cu during the winter at the university site (more than

3,700), followed by Sn during the summer at the university location (more than 2,300). The Al concentration during the summer was higher than during the winter at the two sites due to more frequent dust storms and haze conditions during the summer. The higher Al concentration could underestimate the EF value for some elements, especially during dry deposition (Chester, 1999). As a result, Cu and Sb showed higher EF values during the winter than during the summer. Half of the 14 elements found in this study were from anthropogenic sources. In the literature, the elements with high EF in this study (Cu, Sb and Pb) have been linked with traffic emission (Pant and Harrison, 2012). Previously, As, V and Ni have been related to oil combustion and industrial activities (Megido et al., 2017; Tan *et al.*, 2017).

4.3.5.2 Source Apportionment Using PMF:

PMF analysis was undertaken on the entire dataset, combining all filter analysis results for both locations and seasons. The six-factor solution was identified to provide the best source solution for this study, as it had the minimum difference between Q (Robust) and Q (True), that compares the predicted concentration by PMF and the actual measurement of the same species (Reff et al., 2007), and the closet $Q_{(True)}/Q_{expected\ value}$ (1.4) of the optimal solution value (1.0). Moreover, the six-factor solution had the highest coefficient of variation between the predicted and measured $PM_{2.5}$ ($r^2 = 0.859$). Furthermore, the six-factor solution provides the most realistic interpretation of the sources at the locations. The factor source profiles for the six-factor solution are shown in Fig 4.7. In the following sections, we discuss the characteristics and identities of each factor.

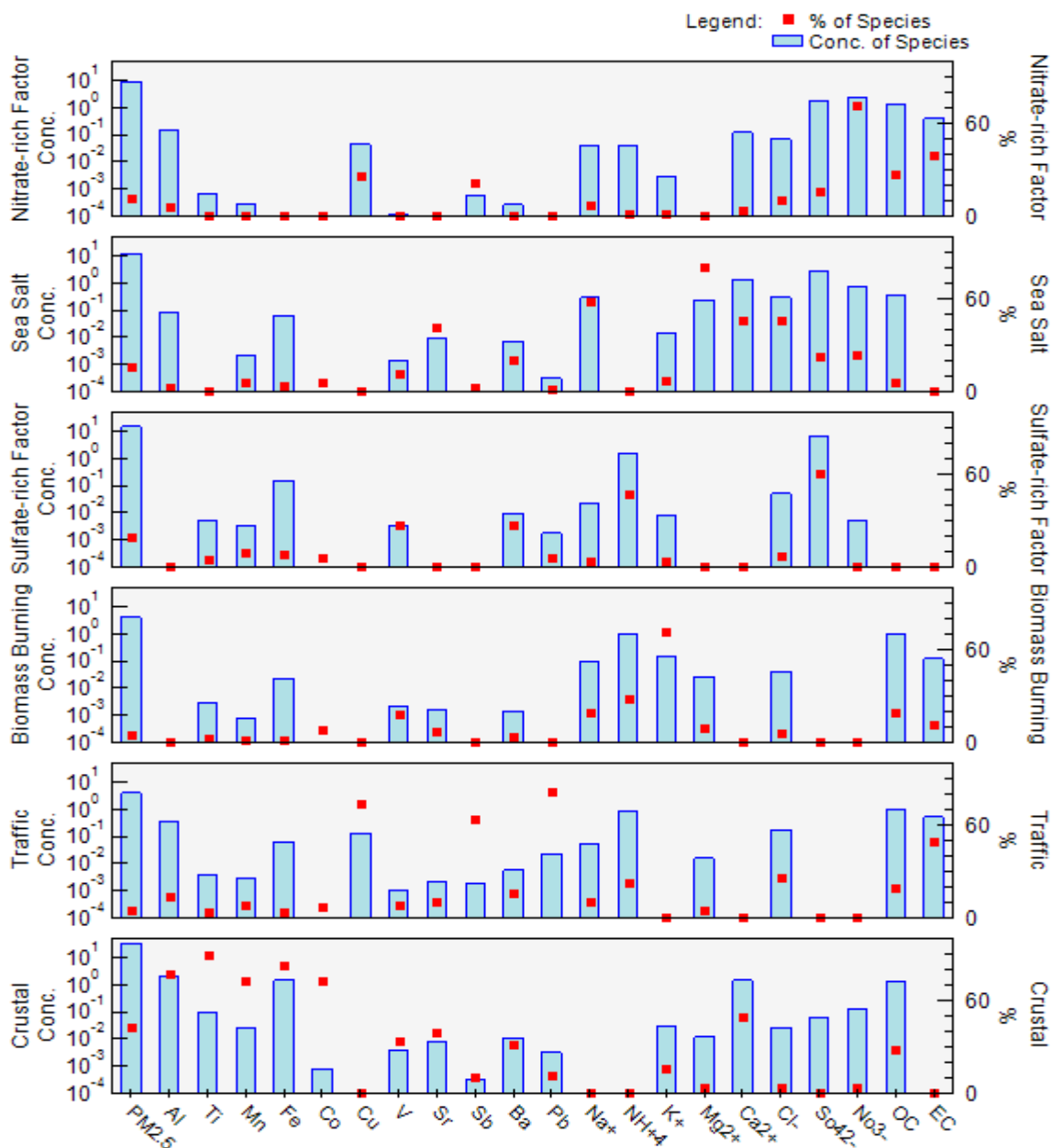


Figure 4.7 Factor profiles for the factors identified with the PMF analysis. Blue bars refer to the concentration ($\mu\text{g}/\text{m}^3$), whereas red squares refer to the percentage contribution of each species.

Table 4.2 percentage contribution of each species to different factors.

	Nitrate-rich factor	Biomass Burning	Crustal	Sea Salt	Traffic	Sulfate-rich factor
PM _{2.5}	12.02	5.24	43.19	15.64	5.03	18.87
Al	5.82	0.00	77.07	3.07	14.04	0.00
Ti	0.57	2.54	88.92	0.00	3.54	4.43
Mn	0.83	2.03	72.60	6.44	8.52	9.59
Fe	0.00	1.23	82.71	3.58	3.67	8.82
Co	0.00	8.27	72.64	5.62	7.02	6.45
Cu	25.76	0.00	0.00	0.00	74.24	0.00
V	1.04	18.03	33.98	11.14	8.48	27.34
Sr	0.00	7.67	39.93	41.39	10.82	0.19
Sb	21.84	0.33	11.07	3.24	63.52	0.00
Ba	0.74	4.00	31.60	20.35	16.62	26.69
Pb	0.00	0.00	11.17	1.10	81.74	5.99
Na ⁺	7.65	19.07	0.00	58.03	10.97	4.28
NH ₄ ⁺	1.23	28.10	0.00	0.00	23.07	47.59
K ⁺	1.64	71.40	15.61	7.57	0.00	3.78
Mg ²⁺	0.00	9.46	4.20	80.95	5.40	0.00
Ca ²⁺	3.99	0.00	49.44	46.57	0.00	0.00
Cl ⁻	10.38	6.08	4.14	45.68	26.20	7.52
SO ₄ ²⁻	16.22	0.00	0.53	23.15	0.00	60.10
NO ₃ ⁻	71.90	0.00	3.86	24.07	0.00	0.18
OC	27.25	18.85	27.97	6.55	19.38	0.00
EC	39.27	11.62	0.00	0.00	49.11	0.00

4.3.5.2.1 Factor One:

This factor was dominated by NO₃⁻ (71.9% of which was this factor), EC (39.2% of which was this factor), OC (27.2% of which was this factor), Cu (25% of which was in this factor) and Sb (21.8% of which was in this factor) (Fig 4.7).

Nitrate is a secondary particle component formed in the atmosphere from the oxidation of NO_x, which in turn is emitted from many sources, such as ships, biomass burning and agricultural activities (Tan et al., 2017; Dadashazar et al., 2019). This factor may contain contributions from shipping activities in the Arabian Gulf, as ships added 4% to 12% to particulate nitrate in the coastal area (Dai and Wang, 2021). Another contribution to this factor would be from power plants and traffic emissions because they are responsible for more than 55% and 25% of the NO_x emission in SA (European Commission, 2018). The timeseries

of this factor (Fig 4.8) showed a same trend for both sites, indicating regional rather than local sources, and the level of this factor was higher in the winter than that in the summer as low temperature increases the formation of NO_3^- (Kim and Hopke, 2012). This factor contributed to 12% of the $\text{PM}_{2.5}$ in Dammam.

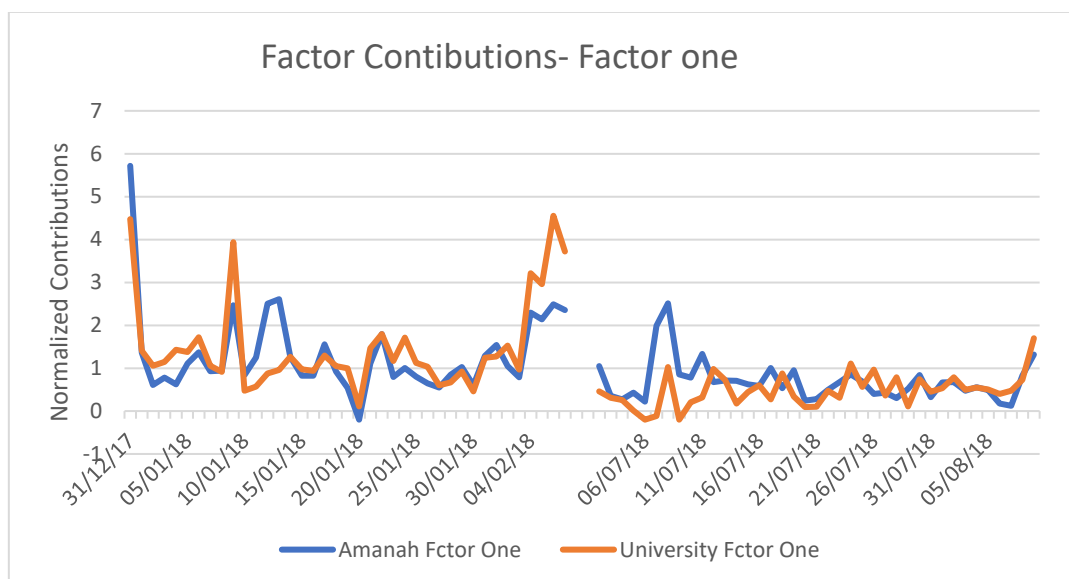


Figure 4.8 Timeseries of the contribution of Factor one.

4.3.5.2.2 Factor Two:

This factor was dominated by Mg^{2+} (80.9% of which was in this factor), Na^+ (58% of which was in this factor), Ca^{2+} (46.5% of which was in this factor), Cl^- (45.6% of which was in this factor), which are typically sea salt. The “sea salt” factor was estimated by PMF to contribute to 15.6% of $\text{PM}_{2.5}$ in Dammam.

4.3.5.2.3 Factor Three

The third factor contributing to the $\text{PM}_{2.5}$ in Dammam was rich with sulfate and ammonium. This factor was dominated mostly by SO_4^{2-} (60% of which was in this factor), NH_4^+ (47% of which was in this factor) and V (27% of which was in this factor), as can be seen in Fig 4.7. Sulfate and ammonium are mainly secondarily formed in the atmosphere from SO_2 and NH_3 (Liu, Liu, *et al.*, 2014; Tan *et al.*, 2017). The element V is commonly linked to oil combustion,

including shipping oil combustion (Cesari et al., 2014; Dadashazar et al., 2019). This factor was most likely associated with two primary sources: power plants, i.e. oil combustion (Kim et al., 2004; Tsai et al., 2013; Nayebare et al., 2016; Rai et al., 2016) and shipping emissions (Cesari et al., 2014, 2016; Dadashazar et al., 2019). Oil combustion is the primary fuel used in SA to generate electricity. Also, Dammam is located on the Arabian Gulf, which receives many ships exporting oil from SA to the world, and others bringing goods from around the globe to SA and other Arabian Gulf countries and Iran. This factor was responsible for 19% of the PM_{2.5} in Dammam.

4.3.5.2.4 Factor Four:

This factor was dominated by K⁺ (71.4% of which was in this factor), NH₄⁺ (28.1% of which was in this factor), OC (18.8% of which was in this factor) and EC (11.6% of which was in this factor) (Fig 4.7). This factor was believed to be related to biomass burning due to the high abundances of K⁺, OC and EC (Cesari et al., 2014, 2016; Dadashazar et al., 2019). The contribution of biomass burning found here, while not negligible, is lower compared to other studies worldwide, which found appreciable and higher contribution with biomass burning accounted for 9%–24% of the PM mass (Kundu and Stone, 2014; Rai et al., 2016; Dadashazaret al., 2019; Liu et al., 2020). There could be two main sources for this factor. The first is agricultural activities on palms' farms located some 15 km to the northwest of Dammam. Stubble is burned off after harvest and before planting crops to improve the agricultural land and to kill the Red Palm Weevil and palms infected by it, protecting the uninfected ones. This location was inspected by pollution rose analysis using the openair package in R (Carslaw, 2015), as shown in Fig 4.9. More than 30% of this factor was

explained by the farm area and impacted both locations. The second one could be related to waste incinerators, as suggested by (Kim and Hopke, 2004; Lomoziket al., 2004; Cheng et al., 2015). Waste incinerators exist in different areas around Dammam, mainly in the northwest and southwest areas of the city. According to the PMF analysis, this factor was estimated to be the source of 5.2% of the PM_{2.5} in Dammam.

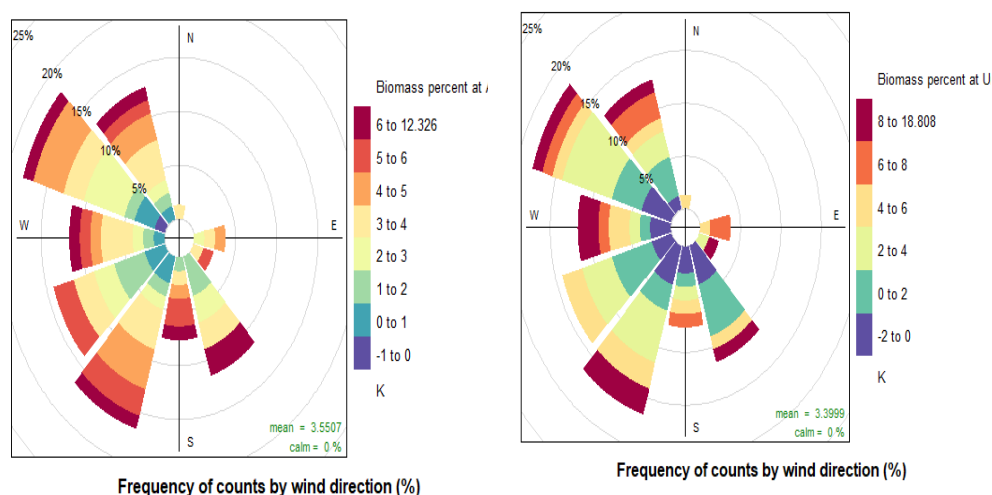


Figure 4.9 Pollution rose graph of the biomass burning factor at the Amanah (left) and the university (right).

4.3.5.2.5 Factor Five:

This factor was dominated by Pb (81.7% of which was in this factor), Cu (74.2% of which was in this factor), Sb (63.5% of which was in this factor), EC (49.1% of which was in this factor), Cl⁻ (26.2% of which was in this factor) and OC (19.3% of which was in this factor), as can be seen in Fig 4.7. These elements are used as markers for traffic sources attributed to PM, including tailpipe emission, brake abrasion and re-suspension of road dust (Pant and Harrison, 2012; Srivastava et al., 2018). EC is considered a typical marker for

vehicle exhaust emission, while elements like Cu, Mn, Zn and Pb are associated with vehicle wear particles (Thorpe and Harrison, 2008; Crilley et al., 2017).

Traffic is a common PM source of pollution reported in almost all studies of PM apportionment sources. The timeseries of this factor (Fig 4.10) illustrated the variation between the two locations, suggesting the impact of local sources (vehicle emission). This factor was estimated by the PMF analysis to be the source of 5% of PM_{2.5} in Dammam.

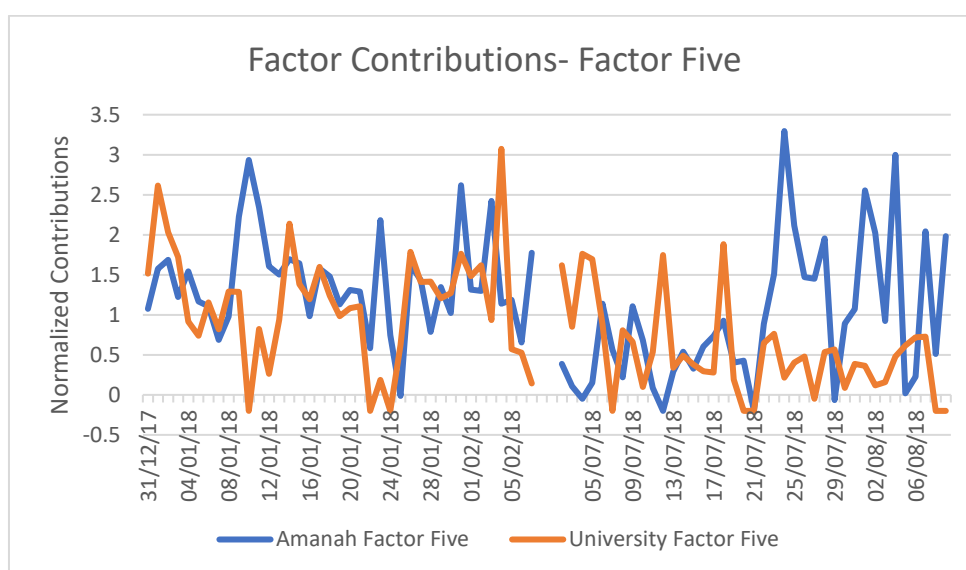


Figure 4.10 Timeseries of the contribution of Factor Five.

4.3.5.2.6 Factor Six:

This factor was mostly dominated by Al (77% of which was associated with this factor), Ti (88.9% of which was associated with this factor), Mn (72.6% of which was associated with this factor), Fe (82.7% of which was associated with this factor) and Ca²⁺ (49.4% of which was associated with this factor), as can be seen in Fig 4.7. These elements are typically crustal (Lomozik et al., 2004; Liu et al., 2014; Crilley et al., 2017). The crustal contribution to PM with a high percentage is comparable to those reported in earlier studies by Nayebare et

al. (2016) and Kchih et al. (2015), developed in Rabigh, SA and Tunis, Tunisia, respectively. In those studies, it was found that crustal contributed 40% and 41% of $PM_{2.5}$, respectively. Both Rabigh and Tunis are surrounded by deserts and seas, similar to Dammam. The presence of Ca^{2+} and Sr suggests the influence of construction and cement work in the surroundings, as these two elements are associated with these activities (Bernardoni et al., 2011; Crilley et al., 2017). During the sampling campaign, many construction activities surrounded the sampling sites, explaining the abundant presence of Ca^{+2} and Sr in this factor. The timeseries of this factor (Fig 4.11) was similar to the timeseries of $PM_{2.5}$ mass concentration (Fig 4.1) and revealed the impact of dust storm on this factor. This factor contributed to more than 40% of the $PM_{2.5}$ in Dammam.

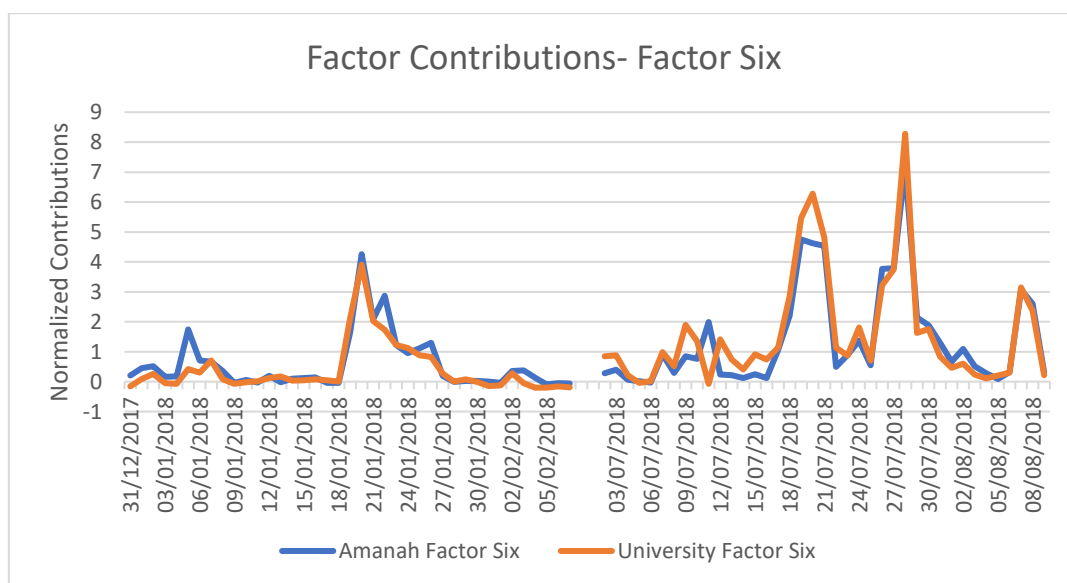


Figure 4.11 Timeseries of the contribution of Factor Six.

4.3.6 Impact of Dust Storms on $PM_{2.5}$ Composition and Sources:

The occurrence of dust storms is common in Saudi Arabia. There was one dust storm during the sampling collection in the winter and three dust storms in the summer. Here, winter dust storm periods were defined as any sample with

a PM_{2.5} mass concentration of more than 100 µg/m³ (4 out of 39 samples), and those from the summer had a PM_{2.5} mass concentration of more than 150 µg/m³ (7 out of 39 samples).

Table 4.3 The mean PM_{2.5} concentration and its composition in samples of non-dust storm and dust days.

Species	Winter		Summer	
	Non-dust storm samples	Dust samples	Non-dust samples	Dust samples
PM _{2.5} ($\mu\text{g}/\text{m}^3$)	45.4	137 **	90	226.3 **
Metals (ng/m^3)				
Al	1548.1	6791.7**	1960.4	10343.9**
Ti	42.3	247.3 **	106.2	488.6 **
Mn	16.5	61.2 **	34.5	132.4 **
Fe	592.6	3516.2 **	1553.9	7019.1 **
Co	0.4	1.7 **	1	4.2 **
Cu	305.2	243.5	76.5	58
Ni	19.8	12.6	24.9	51.5 **
V	6.9	14 **	13.5	27 **
As	0.7	0.5	0.6	1.5 **
Sr	10.4	28.7 **	22	72.7 **
Sn	31.8 **	5.5	120 **	74.9
Sb	4.2	6.2	2.1	3.4
Ba	27.4	35.7	51.2	73.4
Pb	25.9	40.9	37	31.2
WSI ($\mu\text{g}/\text{m}^3$)				
Na ⁺	0.3	0.5 *	0.7	1.2 **
NH ⁺⁴	4.2	2.7	5.1 **	3
K ⁺	0.15	0.2	0.2	0.3 **
Mg ²⁺	0.13	0.4 **	0.4	0.7 **
Ca ²⁺	1	6.2 **	3.6	12 **
Cl ⁻	0.5	0.7	0.7	1.2 **
SO ₄ ²⁻	7.8	7.8	14.3	14.6

NO ₃ ⁻	3.5	4.2	2.5	3.6 **
OC and EC (µg/m ³)				
OC	6.00	7.7 *	7.1	11.1 **
EC	1.89	1.85	1.71	1.17

(Higher values are in **bold**). (* significantly at $p < 0.05$). (** significantly at $p < 0.01$). significance was calculated using paired t.test.

The mean PM_{2.5} mass concentration during dust storm days was approximately 3-fold higher than that during the non-dust storm days in both seasons, as shown in Table 2. Interestingly, the mean PM_{2.5} mass concentration of non-dust storm days in the summer (90 µg/m³) was two times higher than that in the winter (45.4 µg/m³). Also, the mean mass concentration of PM_{2.5} in the summer (226.3 µg/m³) during dust storm days was 1.6 times higher than that in the winter (137 µg/m³). This finding indicates the negative impact of summer on the PM concentration in SA. The crustal metals (Al, Fe, Ti and Mn) concentrations were five times higher during dust period samples than non-dust samples, the contribution of these elements to PM_{2.5} mass was 2-fold higher during dust storms compared to non-dust storms (Fig 4.12). Trace elements measured in this study were not impacted by dust storms, however their contribution to PM_{2.5} mass in Dammam was two times higher in non-dust storm with respect to dust storms samples (Fig 4.13). The crustal element Mg²⁺ and Ca²⁺, also increased by approximately 3-fold during dust storms during the winter and summer. Also, a paired t.test showed that the mean OC concentrations during the dust storms were significantly higher than the mean values in both winter and summer (Table 4.2). Yet, dust storms had a limited impact on the

concentration of EC and the water soluble ions, apart from calcium and magnesium.

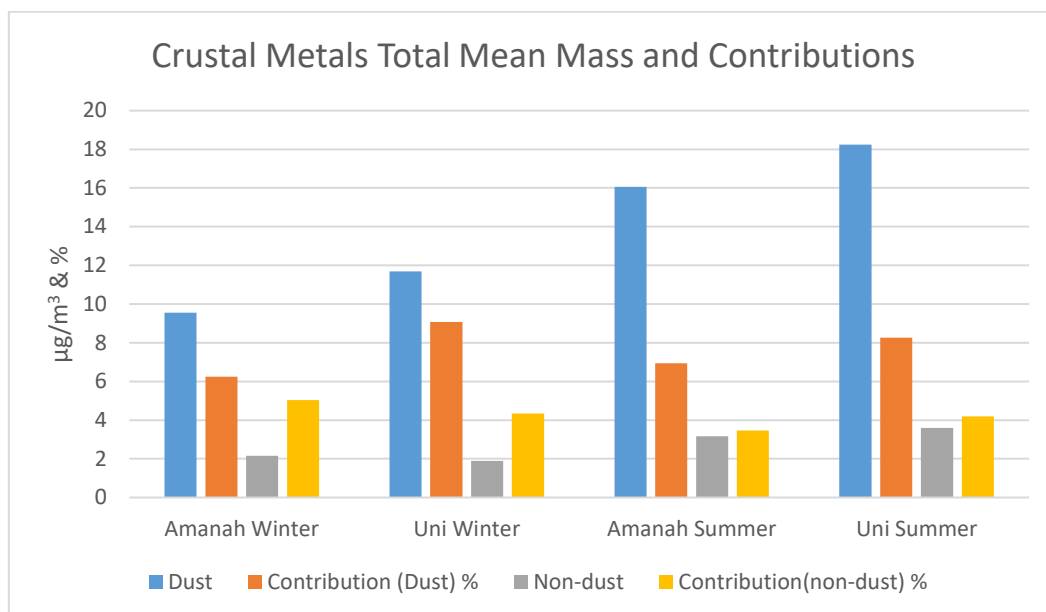


Figure 4.12 Crustal metals' total mass and contribution to PM_{2.5} during dust and non-dust samples.

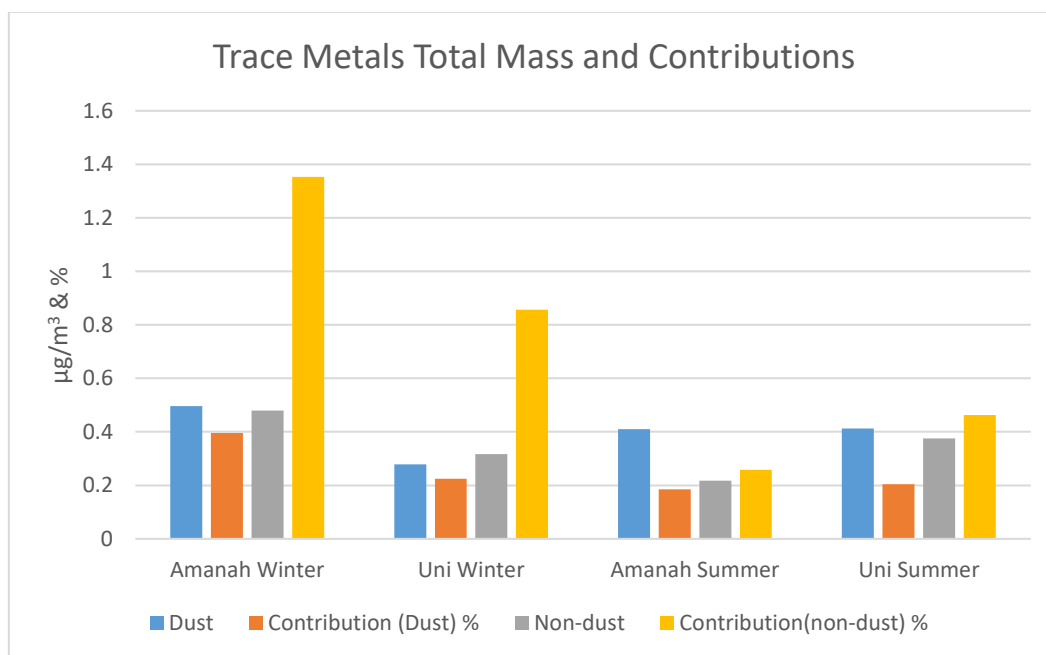


Figure 4.13 Trace metals' total mass and contribution to PM_{2.5} during dust and non-dust samples.

The PMF analysis was rerun using data from non-dust storm-influenced samples only to show the contribution of each PM_{2.5} factor without the impact of

dust storms. The contribution of the crustal factors reduced from 43.2% to 23.7%, the sulfate-rich factor increased from 18.9% to 25.8%, the nitrate-rich factor increased from 12% to 20.2%, the sea salt factor increased from 15.6% to 19%, the biomass burning factor increased from 5.2% to 6% and the traffic factor increased from 5% to 5.3%, as shown in Fig 4.14.

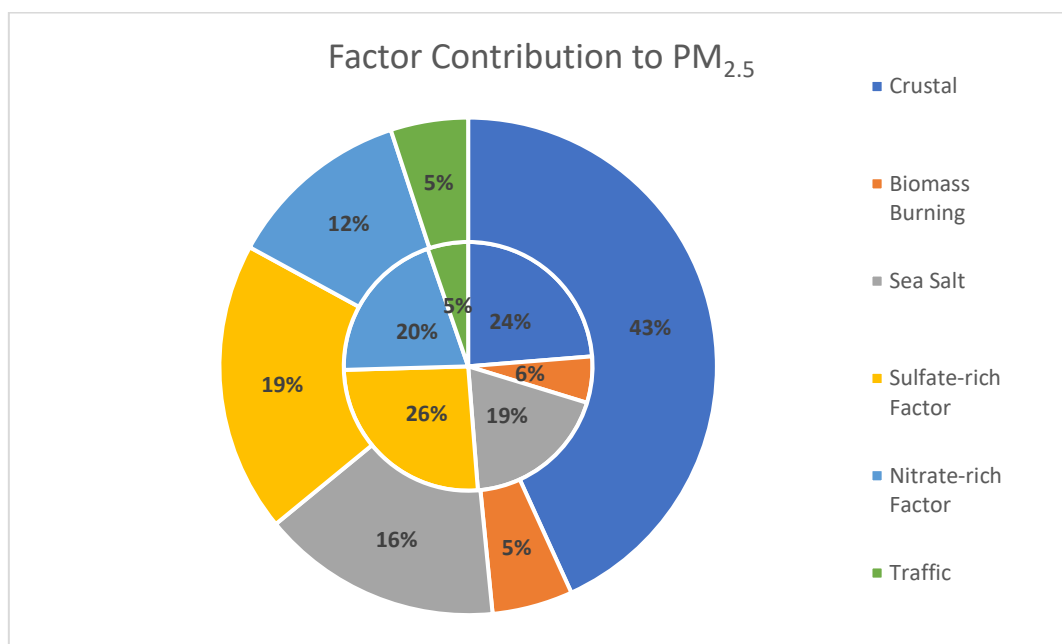


Figure 4.14 Relative contribution of different factors to $PM_{2.5}$ mass during non-dust days (inner circle) compared to all days (outer circle).

Removing dust storm episodes leaves the sulfate-rich factor as the most significant contributor to $PM_{2.5}$ in Dammam (rather than being placed second, after the crustal factor, as was found using all samples, including dust storm period). Additionally, in non-dust samples, crustal elements contributed to less than a quarter of the PM mass compared to about half of PM mass when dust storms were included. Dust storms had little impact on biomass and traffic factors where biomass burning and traffic contribution was 5.2% and 5% for all samples and 6% and 5.2% for non-dust samples, suggesting that the contribution of these factors to $PM_{2.5}$ mass in Dammam is steady.

4.4 Conclusion

We report measurements of PM_{2.5} mass concentration, composition and sources in Dammam, Saudi Arabia. The level of PM_{2.5} was high in Dammam during the winter and summer in the urban/suburban locations explored. Seasonal variations showed a higher PM_{2.5} level during the summer, which was twice that found in the winter. The mean PM_{2.5} concentration in Dammam was 45.4 µg/m³ in samples from non-dust days and 139 µg/m³ in samples from dusty days during the winter. During the summer, the mean PM_{2.5} concentration was 90 µg/m³ for non-dust days and 226.4 µg/m³ in samples from dusty days. Although relative to many anthropogenic sources, potentially less can be done to mitigate the impact of dust storms on arid areas, especially in countries in the Arabian Gulf, planting trees around and inside cities could potentially reduce resuspended dust as well as increase deposition (Nowak *et al.*, 2014). Despite the impact of dust storms and desert soil, the mean concentrations of anthropogenic elements (SO₄²⁻ and OC) were higher than those of all other elements, including crustal elements.

In the PMF analysis, it was possible to identify six factors as primary sources of PM_{2.5} in Dammam, including crustal, sulphate-rich factor, sea salt, nitrate-rich factor, biomass burning and traffic. Among these factors, crustal and sea salt factors are essentially natural sources, representing about 60%, while other anthropogenic sources represent 40% of PM_{2.5} mass concentrations in Dammam. However, removing dust-storm periods reduces the contribution of natural sources to 42% while secondary inorganic sources together were responsible for about 46% of PM_{2.5} in Dammam. As secondary aerosols are formed in the atmosphere from primary pollutants, controlling primary sources

would lead to significant improvements in air quality in Dammam. The contribution of traffic emissions to $PM_{2.5}$ was lower than many results found in other literature studies (Kim et al., 2012; Cheng *et al.*, 2015; Tan *et al.*, 2017), which may be due to the low percentage of diesel vehicles compared to gasoline vehicles in Dammam.

Quantitative assessment of $PM_{2.5}$ sources, explicitly considering the impacts of/allowing for the influence of dust storm data, gives a clearer picture of anthropogenic sources to $PM_{2.5}$ in Dammam, and hence of priorities for clean air policy measures.

Chapter 5. Oxidative potential of PM_{2.5} in Dammam, Saudi Arabia: seasonal variation, chemical composition association and source apportionment

The candidate proxy metric of the toxicity of PM_{2.5} in Dammam was measured using an oxidative potential (OP) acellular assay. OP is a potential metric for measuring the toxicity of PM and the association of specific PM chemical components to health end points. This chapter reports application of the DTT assay to PM samples from Dammam, and the relationship of the OP values obtained to PM_{2.5} mass concentration and chemical components. The relationship of different sources of PM to the measured OP are discussed, with a specific focus on the impact of dust storms and crustal elements on OP activity and sources.

5.1 Introduction

The association of particulate matter (PM) with adverse health impacts is well studied. Still, the toxicity of many of the constituents of PM is unknown; hence the mechanism of the associated health impacts is not clear. One of the suggested mechanisms is the ability of PM to generate reactive oxygen species and induce oxidative stress in the human body, which is known as oxidative potential (OP) (Visentin *et al.*, 2016; Wragg *et al.*, 2016; Paraskevopoulou *et al.*, 2019)

The ability to measure OP in the lab using acellular assays provides more in-depth details of the relationship between PM and adverse health impact. The correlation between OP activity and adverse health impact is more strongly linked than the correlation of PM mass concentration with adverse health impact (Borm *et al.*, 2007b; Bates *et al.*, 2019). In their study, Delfino *et al.*(2013) found

OP activity assessed using dithiothreitol (DTT) and electron spin resonance (ESR) assays to be significantly positively associated with airway inflammation in 45 schoolchildren, but no correlation was found between airway inflammation and PM_{2.5} mass. A significant positive correlation has been found between DTT activity and asthma incidents and the occurrence of asthma symptoms for schoolchildren in Piama, Netherland, while the correlation of asthma in children was not significantly associated with ESR or PM_{2.5} mass (Yang *et al.*, 2016). The results of OP and its correlation to adverse health impact suggesting these assays may provide better health metrics than using PM mass alone.

There are many methods for measuring ROS that are associated with PM, including the dithiothreitol (DTT) and ascorbic acid (AA) assays, electron spin resonance (ESR) and the glutathione assay (GSH) (Bates *et al.*, 2019). These assays usually report OP activity per volume of air (OP activity per min per volume of air (m³)) or per mass of PM sampled (OP activity per min per µg of PM). OP activity unit per unit air volume is useful for epidemiological research, while OP activity unit per unit PM mass is relevant for comparing OP observational studies based on PM sampling, and to identify the component of PM most closely associated with the oxidative effect (Bates *et al.*, 2019).

Within each assay, application of different analyses may affect the results. Many researchers have commonly used deionised water to extract PM for DTT assay (Verma *et al.*, 2012). However, recent studies have found that using methanol as an extraction medium has DTT activity of up to 1.6 times higher than water extraction (Rattanavaraha *et al.*, 2011; Yang *et al.*, 2014; Bates *et al.*, 2019). Water extraction is relevant for measuring the OP activity of water soluble components of PM, while methanol extraction is more relevant for measuring

combined hydrophilic and hydrophobic PM's OP activity. Also, the type of filter used to collect PM has been shown different results. Yang *et al.* (2014) compared the OP activity using Teflon and quartz filters for four different OP assays. They concluded that OP activity per air volume was significantly lower for quartz filters with respect to Teflon filters suggestion the higher efficiency of the extraction of the OP reactive species from Teflon filters compared to quartz filters .

A limited number of studies have integrated sources apportionment analyses with measurement of DTT activity. Moreover, most of these studies reported the impact of PM sources on OP activities used DTT_v activities, but few has used DTT_m activity. For example, in the Bohai sea area, China, the contribution of PM sources defined by positive matrix factorisation (PMF) to DTT_v after removing sea salt spray and suspended soil sources was 26.1% from biomass burning, 24.2% from coal combustion, 23% from secondary sources, 14.3% from industry and 12.3% from traffic source (Liu *et al.*, 2018). The annual contribution of biomass burning to DTT_v in Atlanta, USA, was 35%, followed by secondary aerosols (31%), then vehicle emission (16%) and road dust was responsible for 9% (Verma *et al.*, 2014). Fang *et al.* (2016) reported the contribution of sources to DTT_v from PM_{2.5} collected from seven locations in the southeastern USA. The major drivers of DTT_v were biomass burning (35%), secondary aerosols (31%), traffic emission (16%), road dust (9%) and residual (9%). Biomass burning seems to be the most contributor to DTT_v activity, followed by secondary aerosols and traffic emissions. A common conclusion from these studies is that crustal and natural sources are not significant drivers of measured DTT_v.

This study investigates the OP activity (DTT_m and DTT_v) for PM_{2.5} collected on Teflon filters from Dammam, Saudi Arabia. Methanol was used as an extraction medium, and a DTT assay was used to measure OP. The contribution of different sources in Dammam was performed using the PMF model to investigate sources' impact on DTT activities. To our knowledge, this is the first study to measure OP in Saudi Arabia and surrounding countries. It is the first study in an arid or semi-arid area.

5.2 Methodology

5.2.1 Sampling:

Daily PM_{2.5} samples were collected at two locations in Dammam, SA, over a two-months period in January-February and July-August 2018. The first location was on the roof of the Amanah building, which is in the city centre as an urban area. The second location was on the roof of the Public Health College building inside the campus of Imam Abdulrahman Bin Faisal University as an urban background. PM_{2.5} was collected on pre-baked 100% pure quartz filters and pre-weighed Teflon filters with a diameter of 47mm using MiniVol samplers. Two samplers were running at the urban location, and two samplers were running at the urban background location at the same time.

5.2.2 Organic Carbon and Elemental Carbon analysis (OC and EC):

The total organic carbon loading, separated into organic carbon (OC) and elemental carbon (EC) fractions, was determined by analysing samples collected on the quartz filters by measuring the amount of Carbon evolved from the filter samples as a function of temperature. Organic and elemental Carbon were measured using the DRI Model 2015 Multiwavelength Thermal/Optical Carbon

Analyser using “EUSAAR2 protocol”. All results were corrected using field blank filter results.

5.2.3 Water Soluble Ion (WSI) Concentrations:

5 cm² of quartz filter was extracted in 5 ml of 18.2MΩ-cm deionised water using 15 ml centrifuge tubes. Dionex ICS 1100 was used to measure anions, while Dionex Integrion HPIC was used for cations measurement. All results were corrected using field blank filters results.

5.2.4 Metal Analysis:

PM_{2.5} was extracted from samples collected on quartz filters by adding 10 ml 68% ultrapure Nitric acid using microwave digestion vessels. Vessels were placed in a Mars 6 microwave digestion system (CEM). The digestion acid samples were diluted to the 2% HNO₃ concentration (16.6- fold dilution) required for use with Inductively Coupled Plasma Mass Spectrometry (ICP-MS). Metals were measured using ICP-MS. All results were corrected using field blank filters results.

5.2.5 Filter Extraction for DTT Assay:

Depending on the PM mass loading of each filter, different numbers of 0.5 cm² punches (from 2-12 punches) were taken from the Teflon filter in order to have ~20 μg PM_{2.5} in the reaction. E1 was used to calculate how many punches were needed from each filter:

$$\frac{\frac{\text{Total PM on filter } (\mu\text{g})}{\text{Filter SA } (\text{mm}^2)} \times \sum \text{SA of punches } (\text{mm}^2)}{\text{Final extract } V (\text{mL})} \times V \text{ of sample in reaction } (\text{mL})$$

(E1)

Where SA = surface area

47 mm Teflon filters were used to collect PM_{2.5} from Dammam, so E1 became:

$$\frac{\frac{\text{Total PM on filter } (\mu\text{g})}{855 \text{ mm}^2} \times \sum \text{SA of punches } (\text{mm}^2)}{10 \text{ mL}} \times 0.7 \text{ mL} = \text{PM in reaction } (\mu\text{g}) \text{ (E2)}$$

Punches that were taken from the Teflon filter were placed in a 15 ml centrifuge tube. 5 ml of methanol was added to the tube using a calibrated automatic pipette. PM was extracted through sonication for 15 minutes. The extraction was dried to about 1-2 ml by nitrogen blowdown. DIW was then added to the extraction to make up the final volume of the extraction to 10 ml. Finally, a 0.45 μm syringe filter was used to filter the extraction and move it to a new centrifuge tube. The extract was kept in the fridge until the time of the analysis, which was done within 48 hours.

5.2.6 DTT assay:

0.7 ml of the sample's extraction was mixed with 0.2 ml of K-buffer and heated in a water bath at 37 °C. 100 μl of 1 mM DTT was added to the sample and K-buffer mixture to form the reaction mixture. The reaction mixture was shaken well, then 100 μl of this reaction mixture was taken using a calibrated pipette and added to 0.7 ml of 0.2 mM DTNB in a 1.5 ml amber glass vial to form the coloured mixture. The coloured mixture was immediately measured using dual-beam UV-vis. The reaction mixture was kept in the water bath, and then after various time points (10, 20, 30 and 40 minutes, plus the one taken at 0 minutes), 100 μL was added of 0.2 mM DTNB and measured immediately by UV-vis at 412 and 700 nm. Blank filters received the same treatment as the samples, and all samples were blank corrected. Also, PQN was used as a positive control using the same method, but instead of a sample, a 0.05 μM of PQN was

analysed. To check the validity, repeatability and stability of the result, the coefficient of variation (%CV) was measured every day by repeating one random sample three times where %CV should be below %15 (Cho et al., 2005).

5.3 Results and Discussion

There are two ways to present the results of DTT. The first one is the OP activity per unit PM mass (DTT_m), expressed in units of pmol min⁻¹ μg⁻¹. The second one is OP activity per unit air volume (DTT_v), expressed in units of nmol min⁻¹ m⁻³. In this work, OP will be presented in both ways.

5.3.1 OP Activity overview:

The mean/distribution and range of DTT_m and DTT_v values obtained for the Amanah and University locations in the winter and summer are presented in Fig 5.1 and 5.2.

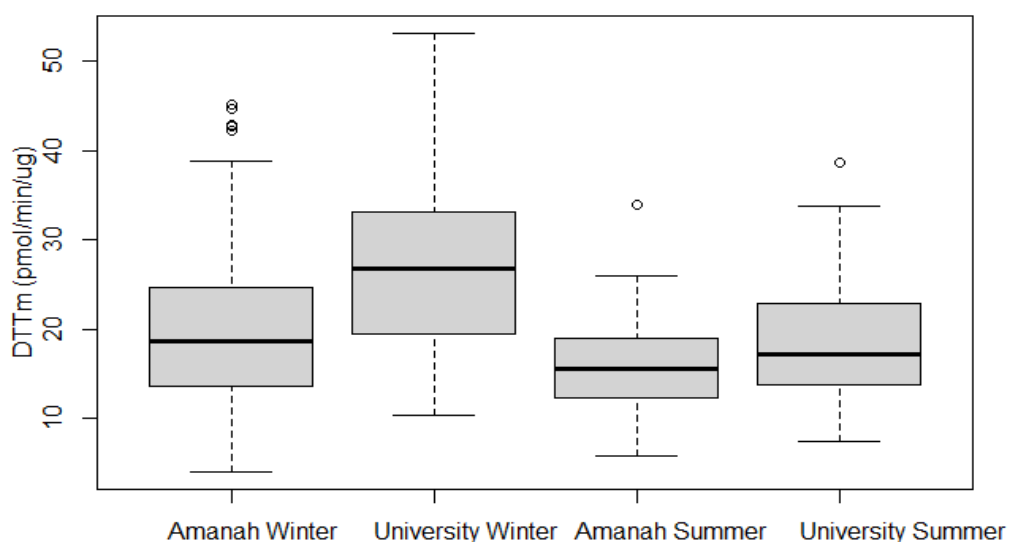


Figure 5.1 Average of DTT_m values at Amanah and University in the winter and summer. shaded range shows the interquartile range, dark black horizontal line in the middle shows the median, black horizontal lines at the top and bottom of the shaded range show the

upper and lower quartile, the two horizontal lines at the top and bottom show the maximum and minimum and the circular points show the outlier data

In the winter, the mean of DTTm at the University location (28.2 pmol min⁻¹ μg⁻¹) was significantly higher ($p = 0.005$, using a paired t.test) than that at the Amanah (20.9 pmol min⁻¹ μg⁻¹) as can be seen in Fig 5.1. In the summer, the mean of DTTm at the University location (18.6 pmol min⁻¹ μg⁻¹) was higher (but not statistically significantly so) ($p = 0.07$, using a paired t.test) than that at the Amanah (15.9 pmol min⁻¹ μg⁻¹) location. Even though PM_{2.5} mean mass concentration was approximately two times higher in the summer than in the winter at both locations, the mean DTTm was higher in the winter than in the summer for the two locations, suggesting that PM components are the key factors driving the ROS generation rather than PM mass (Liu *et al.*, 2018).

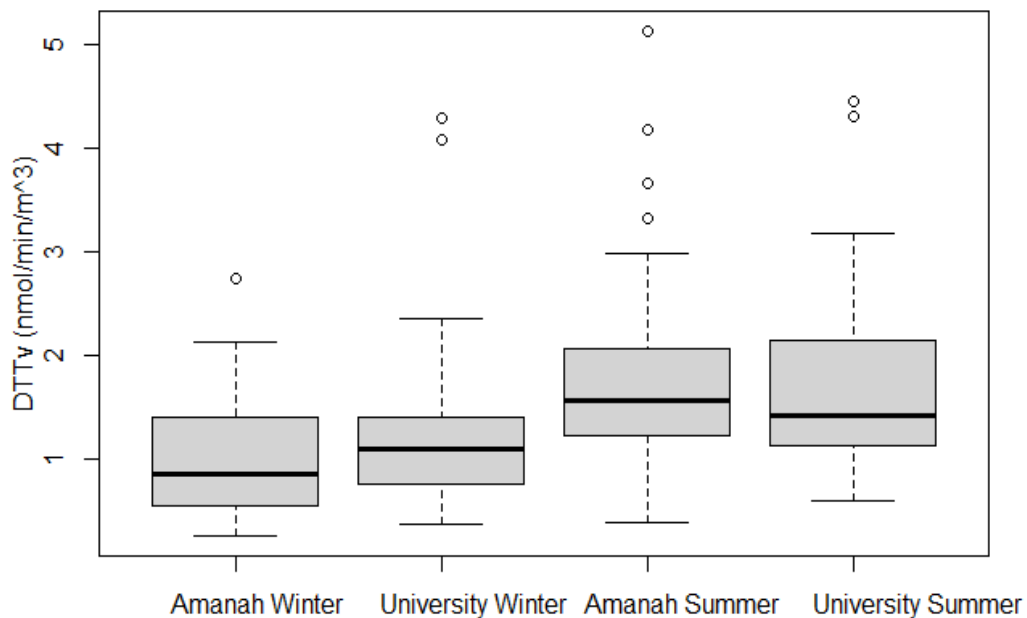


Figure 5.2 Average DTTv values at Amanah and University in the winter and summer. shaded range shows the interquartile range, dark black horizontal line in the middle shows the

median, black horizontal lines at the top and bottom of the shaded range show the upper and lower quartile, the two horizontal lines at the top and bottom show the maximum and minimum and the circular points show the outlier data.

In the winter, the mean DTTv value at the University location (1.2 nmol min⁻¹ m⁻³) was higher (but not statistically significantly different, using a paired t.test) ($p = 0.1$) than that at the Amanah location (1 nmol min⁻¹ m⁻³) as shown in Fig 5.2. In the summer, the mean DTTv value was almost the same at both locations (1.77 nmol min⁻¹ m⁻³ at Amanah and 1.76 nmol min⁻¹ m⁻³ at University). The mean of the DTTv measurements at both locations were significantly higher ($p < 0.05$, using a paired t.test) in the summer than that in the winter.

Compared with previous literature that used the same filter extraction method (methanol), the mean OP values (both DTTm and DTTv) were within the ranges of earlier works, as shown in table 5.1. Even though the DTTv values in Dammam and Netherland are very similar (1.4 nmol m⁻¹ m⁻³), the PM_{2.5} average mass concentration in Dammam (88.5 µg/m³) was much higher than that in the urban area in the Netherlands (17.3 µg/m³) (Janssen *et al.*, 2014). DTTv measures the OP activity per air volume. This comparison suggests that breathing the same amount of air in Netherlands and Dammam possess the same toxicity regardless of the different PM mass concentration, at least as assessed by the DTT assay. Conversely, the average DTTm value found for PM_{2.5} in Dammam (16.4 pmol min⁻¹ µg⁻¹) was lower than that for PM_{2.5} in Atlanta (35 pmol min⁻¹ µg⁻¹) while PM_{2.5} concentrations in Dammam (88.5 µg/m³) were much higher than those in Atlanta (14.6 µg/m³). DTTm in Atlanta was higher than that for Dammam because PM_{2.5} mass in Dammam has high natural sources from dessert and sand storms, which has previously been reported to have minimum role in the DTT

assay (Chirizzi *et al.*, 2017). These findings suggest that the toxicity of PM is driven by PM composition rather than PM mass only.

Table 5.1 comparing mean of DTTm, DTTv and PM_{2.5} mass concentration of this work and earlier studies.

Reference	Location	DTTv (nmol m ⁻¹ m ⁻³)	PM _{2.5} mean mass (µg/m ³)	DTTm (pmol min ⁻¹ µg ⁻¹)
Janssen <i>et al.</i> , 2014	Urban, Netherlands	1.4	17.3	
Verma <i>et al.</i> , 2012	Atlanta, USA		14.6	35
Verma <i>et al.</i> , 2009	Atlanta, USA	0.5	Not reported	9
Yang <i>et al.</i> , 2014	Rotterdam, Netherlands	2.9	16.4	
Gao <i>et al.</i> , 2017	Atlanta, USA	0.4	No reported	
This study	Dammam, SA	1.4	88.5	16.4

5.3.2 Association between OP and PM Chemical Composition:

Pearson correlation coefficients between daily mean PM_{2.5} mass concentrations and each chemical component with the DTTv and DTTm values obtained are presented in table 5.2. For DTTv, the correlations were assessed between DTTv value and the mass concentration of each component (µg/m³ of the component). For the DTTm, the correlations were assessed between the DTTm value and the mass fraction in ng of each component per µg of PM_{2.5}.

Table 5.2 Pearson correlation coefficient (r) and p-values between OP activity and PM_{2.5} mass and composition.

Species (ng/μg PM _{2.5})	DTTm		Species (μg/m ³)	DTTv	
	r	p		r	p
PM _{2.5}	-0.58	0.00	PM _{2.5}	0.72	0.00
Al	-0.15	0.01	Al	0.44	0.00
Ti	-0.28	0.00	Ti	0.56	0.00
Mn	-0.13	0.01	Mn	0.61	0.00
Fe	-0.25	0.00	Fe	0.57	0.00
Co	-0.13	0.12	Co	0.62	0.00
Cu	0.29	0.00	Cu	-0.26	0.00
Ni	0.32	0.00	Ni	0.43	0.00
V	0.46	0.00	V	0.59	0.00
As	0.36	0.00	As	-0.01	0.85
Sr	-0.19	0.03	Sr	0.50	0.00
Sn	0.41	0.00	Sn	0.16	0.12
Sb	0.32	0.00	Sb	0.15	0.08
Ba	0.12	0.14	Ba	0.35	0.00
Pb	0.27	0.00	Pb	0.05	0.55
Na ⁺	0.41	0.00	Na ⁺	0.49	0.00
NH ⁺⁴	0.48	0.00	NH ⁺⁴	0.06	0.43
K ⁺	0.44	0.00	K ⁺	0.45	0.00
Mg ²⁺	-0.03	0.71	Mg ²⁺	0.55	0.00
Ca ²⁺	-0.32	0.00	Ca ²⁺	0.57	0.00
Cl ⁻	0.35	0.00	Cl ⁻	0.35	0.00
SO ₄ ²⁻	0.43	0.00	SO ₄ ²⁻	0.37	0.00
NO ₃ ⁻	0.50	0.00	NO ₃ ⁻	0.30	0.00
OC	0.50	0.00	OC	0.40	0.00
EC	0.55	0.00	EC	0.03	0.76

5.3.2.1 Association between OP and PM_{2.5} mass concentration:

A negative correlation ($r = -0.5$) has been found between DTTm and PM_{2.5} mass. This negative correlation may be impacted by the Saharan dust and crustal elements (Chirizzi *et al.*, 2017). In contrast, a positive correlation ($r = 0.72$) has been found between DTTv and PM_{2.5} mass concentration. These correlations agree with what has been reported in other studies that study the impact of Saharan dust on DTT activity (Chirizzi *et al.*, 2017; Nishita-Hara *et al.*, 2019).

5.3.2.2 Association between OP and OC and EC:

DTTm and DTTv are positively correlated with OC. OC has been reported by many studies to be correlated with DTTv with an r-value range from 0.5 – 0.88 (Verma *et al.*, 2012; Joseph Y. Abrams *et al.*, 2017; Liu *et al.*, 2018). DTTv has a weak positive correlation with EC, and moderate positive correlation was found between DTTm and EC. EC is emitted to the atmosphere as primary emission, while OC is emitted to the atmosphere as primary or may be formed as a secondary component. Primary OC and EC usually share the same sources (Verma *et al.*, 2012; Liu *et al.*, 2018). The similar values for OC and EC correlation with DTTm are consistent with similar sources for both OC and EC.

5.3.2.3 Association between OP and WSI:

DTTm has positive correlation with all WSI except Ca²⁺ and Mg²⁺. Negative correlation saw between DTTm and Ca²⁺ and Mg²⁺. this negative correlation could be from the influence of dust storm as these elements were significantly higher during dust storm periods. Also, a moderate to weak positive correlation was found between DTTv and WSI. In this study, DTTv has smaller correlations with secondary inorganic ions (NO₃⁻, SO₄²⁻ and NH₄⁺) than is shown

for other WSI. The contribution of WSI including secondary inorganic ions to DTT activity is very low; however, the positive correlation is most probably due to their correlation with redox-active organic compound rather than to the actual DTT assay (Cho *et al.*, 2005a; Verma *et al.*, 2009; Liu *et al.*, 2018)

5.3.2.4 Association between OP activity and Metals:

DTTm has weak negative significant correlations with crustal elements (Al, Ti, Mn and Fe). Also, negative (but not significant) correlation observed between DTTm and Co and Sr. Weak to moderately significant ($p < 0.05$) correlations were between DTTm and anthropogenic metals except for Ba where the correlation was not significant, as can be seen in table 5.2. This finding indicates that crustal elements are associated with lower values of DTTm while anthropogenic elements are associated with higher DTTm value. In other words, anthropogenic elements may be more toxic than crustal natural elements. Significant moderate to weak positive correlations were found between DTTv and measured metals except for Cu, As, Sn, Sb, and Pb, as shown in table 5.3. The only significant negative correlation between DTTv and metals was for Cu. DTTv shows a very weak negative non-significant correlation with As. DTTv has weak positive non-significant correlations with Sn, Sb and Pb. The positive correlation between DTT activity and metals generally agrees with those obtained in previous studies, including (Shirmohammadi *et al.*, 2017; Martin *et al.*, 2019; Nishita-Hara *et al.*, 2019; Gao, Mulholland, *et al.*, 2020). Some studies reported that metals don't have a major role in DTT activity compared to organic species (Cho *et al.*, 2005a; Verma *et al.*, 2012). However, Charrier and Anastasio (2012) said transition metals have the ability to oxidize DTT and metals play an important role for DTT loss in the absence of ethylene diamine tetraacetic acid

EDTA (as was the case for this work). EDTA is added to DTT assay by some researchers to minimize the rate of the oxidation of DTT in the blank samples (Charrier and Anastasio, 2012).

5.3.3 Impact of dust storm on DTT:

There was one dust storm during the sampling collection in the winter and three dust storms in the summer. Here, winter dust storm periods were defined as any sample with a PM_{2.5} mass concentration of more than 100 $\mu\text{g}/\text{m}^3$ (4 out of 39 samples), and those from the summer where there was a PM_{2.5} mass concentration of more than 150 $\mu\text{g}/\text{m}^3$ (7 out of 39 samples). The correlation between DTT_m and DTT_v activity were tested separately using data from dust period samples only, and with data from non-dust period samples only. Pearson correlation coefficients (r) between daily PM_{2.5} mass concentrations and each chemical component of all data, dust storm samples, and non-dust storm samples are presented in table 5.3.

The mean DTT_v was significantly higher ($p < 0.01$) for the dust storm samples ($2.5 \text{ nmol m}^{-1} \text{ m}^{-3}$) compared to non-dust samples ($1.2 \text{ nmol m}^{-1} \text{ m}^{-3}$). The higher DTT_v value in the dust storm samples is expected as high PM mass concentration has been reported to have adverse health impacts. On the other hand, the mean DTT_m value for non-dust storm samples ($22.4 \text{ pmol min}^{-1} \mu\text{g}^{-1}$) was significantly ($p < 0.01$) higher than that for the dust storm samples ($13.8 \text{ pmol min}^{-1} \mu\text{g}^{-1}$). DTT_m measures the components of PM most closely associated with the oxidative effect. Lower DTT_m values in the dust storm samples compared to non-dust storm samples period is most probably due to the high concentration of crustal elements in the dust samples that have been reported to have minimum influence on the OP activity. This finding provides further evidence that OP

activity (and hence inferred health impact) is affected by PM components and composition, rather than by PM mass only.

Table 5.3 Pearson correlation coefficient (r) between daily PM_{2.5} and each chemical component of all data, dust storm samples, and non-dust storm samples.

Species (ng/ μ g PM _{2.5})	DTTm			Species (μ g/m ³)	DTTv		
	All	Dust	No Dust		All	Dust	No Dust
PM _{2.5}	-0.58*	-0.18*	-0.48*	PM _{2.5}	0.72*	0.48*	0.65*
Al	-0.15	0.14	-0.03	Al	0.44*	0.57*	0.21*
Ti	-0.28*	0.27	-0.12	Ti	0.56*	0.59*	0.35*
Mn	-0.13	0.26	-0.01	Mn	0.61*	0.61*	0.46*
Fe	-0.25*	0.19	-0.13	Fe	0.57*	0.57*	0.41*
Co	-0.13	0.04	0.01	Co	0.62*	0.55*	0.43*
Cu	0.29*	0.03	0.14	Cu	-0.26*	-0.37	-0.26*
Ni	0.32*	0.07	0.35*	Ni	0.43*	0.44*	0.20*
V	0.46*	0.39	0.37*	V	0.59*	0.63*	0.45*
As	0.36*	0.02	0.35*	As	-0.01	0.41*	-0.16
Sr	-0.19	0.16	-0.13	Sr	0.50*	0.55*	0.26*
Sn	0.41*	0.47	0.10	Sn	0.16	0.30*	0.14*
Sb	0.32*	0.21	0.29*	Sb	0.15	0.09	0.10
Ba	0.12	-0.04	0.11	Ba	0.35*	0.39*	0.19*
Pb	0.27*	0.03	0.18	Pb	0.05	-0.14	0.03*
Na ⁺	0.41*	0.41	0.31*	Na ⁺	0.49*	0.61*	0.39*
NH ⁺⁴	0.48*	0.02	0.40*	NH ⁺⁴	0.06	-0.06	0.28*
K ⁺	0.44*	0.04	0.39*	K ⁺	0.45*	0.25	0.37*
Mg ²⁺	-0.03	0.44*	-0.09	Mg ²⁺	0.55*	0.63*	0.43*
Ca ²⁺	-0.32*	0.30	-0.28*	Ca ²⁺	0.57*	0.63*	0.42*
Cl ⁻	0.35*	0.40	0.26*	Cl ⁻	0.35*	0.51*	0.22*
So ₄ ²⁻	0.43*	0.30	0.29*	So ₄ ²⁻	0.37*	0.44*	0.38*
No ₃ ⁻	0.50*	0.24	0.45*	No ₃ ⁻	0.30*	0.11	0.23*

OC	0.50*	0.11	0.42*	OC	0.40*	0.25	0.308
EC	0.55*	0.32	0.47*	EC	0.03	0.17	0.02*

*= significant (p<0.05)

The correlation between DTTv and PM_{2.5} and chemical components was impacted by dust storms except for As, where r-value for As was -0.01 for all data, -0.16 for non-dust samples and 0.41 for dust samples (table 5.3). However, the impact of dust storms on DTT activity per µg (DTTm) and each chemical component was considerable. DTTm had negative weak correlations with Crustal elements (Al, Ti, Mn, Fe, Ca²⁺ and Mg²⁺) in the non-dust storm samples while DTTm had positive weak correlation with crustal elements for the dust samples (Table 5.3). Thus, these crustal elements have higher concentrations in the dust samples, but their influence on the DTT assay is weak; as a result, DTTm values were higher for non-dust samples compared to dust samples. In contrast, DTTm had stronger correlations with transition metals (except Sr, Cu and Co) for non-dust storm samples compared with dust storm samples. Interestingly, DTTm had almost the same r-value with V for dust and non-dust samples, however, DTTm correlation with V for the dust samples was not statistically significant while its correlation with V for non-dust samples was statistically significant (Table 5.3). Furthermore, DTTm correlations with OC and EC were higher for non-dust storm samples compared to dust storm samples. Also, these correlations were significant for non-dust compared to dust storm samples. In general, this finding suggests that anthropogenic elements drive OP activity more than crustal (natural) elements.

5.3.4 Source Apportionment of OP:

The contribution of different PM sources to DTTm and DTTv activities was assessed to provide more details about the impact of different sources on inferred health impacts. Positive matrix factorisation (EPA-PMF version 5.0.14) model analysis was applied using daily PM composition data and daily DTTm and DTTv activities. First, PMF analysis was conducted to find sources of PM in Dammam (chapter 4). Then the same number of factors and set up was used to find the contribution of these sources to OP activities. Two assessments were performed, one for DTTm and the other one for DTTv. To find source contributions to DTTm, DTTm was set to be “total variable” (default to weak) (Verma *et al.*, 2014), and DTTv and PM_{2.5} mass concentration were set to be bad (excluded from the analyses) within the PMF procedure, so they do not affect the results. For the contribution of sources to DTTv activity, DTTv was chosen as “total variable” (default to weak), and DTTm and PM_{2.5} mass concentration were chosen to be bad (excluded from the analyses). In this way the DTTm and DTTv values were apportioned to different factors (sources) identified in the analysis but provided minimal constraint on the identification of those factors (sources).

Six factors was the best fit for PM_{2.5} sources in Dammam (Crustal, Sea Salt, Nitrate-rich Factor, Sulfate-rich Factor, Biomass Burning and Traffic). The factor contribution pie chart in Fig.5.3 shows how each source contributed to DTTm and PM_{2.5} in Dammam. 39% of DTTm was attributed to traffic factors, even though traffic contributed to only 5% of PM_{2.5} mass concentration. The second highest factor contributing to DTTm is sulfate-rich factor (29%), indicating the important of secondary inorganic aerosols on the OP activity. The nitrate-rich factor contributed to 13% of DTTm activity in Dammam. 8% of

DTTm activity was attributed to sea salt as the highest natural source affecting DTTm in this study while the sea salt factor was responsible for 16% of PM_{2.5} in Dammam. The lowest factor contributed to DTTm in Dammam was biomass burning with 5%. The largest factor that contributed to PM_{2.5} mass in Dammam was crustal elements, yet this factor was attributed to only 6% of DTTm activity in Dammam, suggesting modest impact of crustal elements on DTTm (and hence the health impact of PM), in agreement with previous studies who measured OP for dust and non-dust samples (Chirizzi *et al.*, 2017; Lovett *et al.*, 2018; Nishita-Hara *et al.*, 2019).

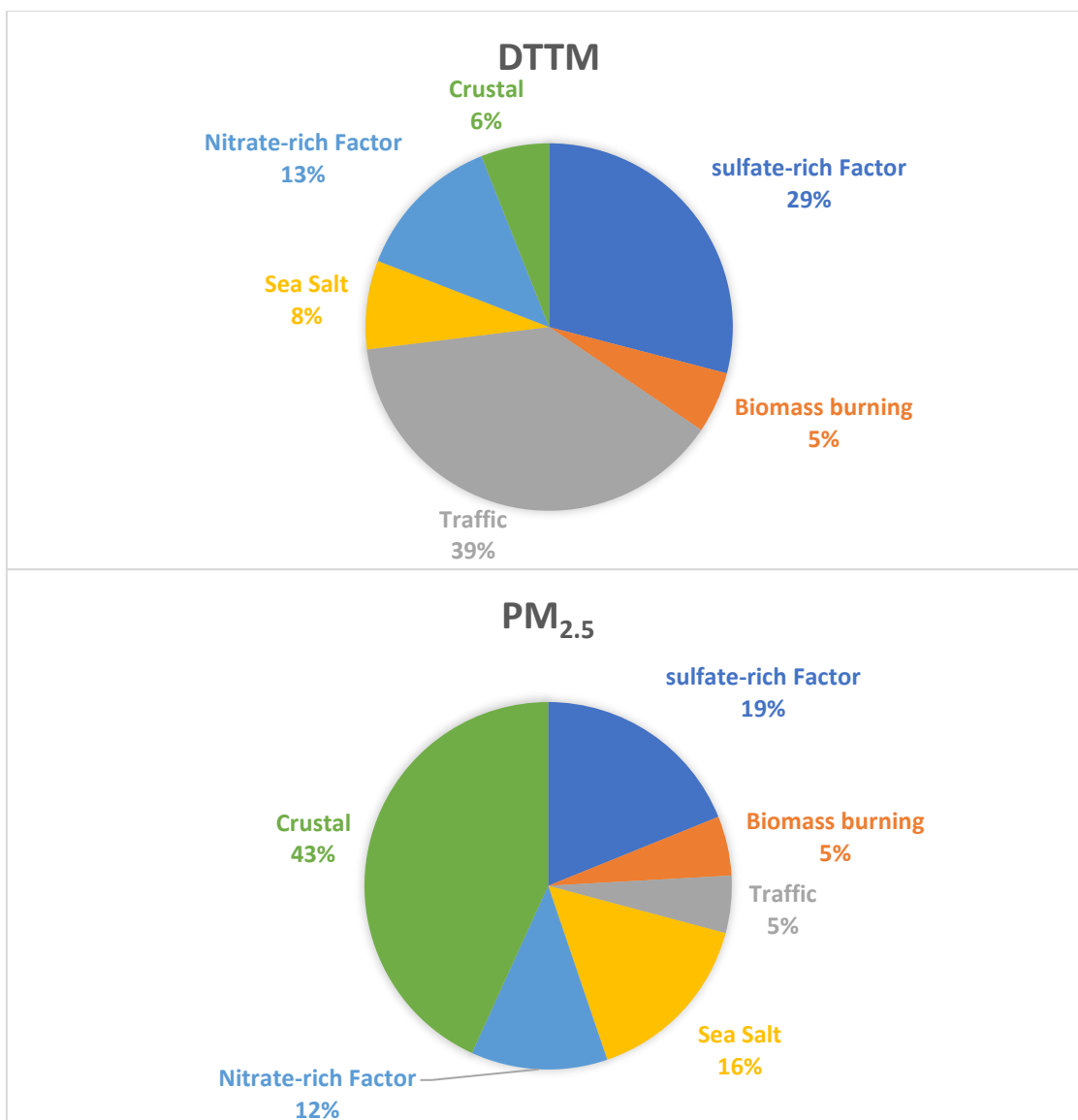


Figure 5.3 Relative factor contributions to oxidative potential (DTTm values) and to PM_{2.5} mass concentrations – obtained from all data.

Fig 5.4 reveals the contribution of different sources in Dammam for DTTv and PM_{2.5}. 36% of DTTv measured in Dammam was attributed to crustal elements. The crustal factor contributed to 40% of PM_{2.5} in Dammam, and its impact on DTTv has almost the same value. Secondary aerosols factors together (Sulfate-rich factor and Nitrate-rich factor) account for 37% of DTTv activity in Dammam. Secondary aerosols factors have been reported to be responsible for 34%, 31%, 31% and 23% of DTTv in Beijing, Atlanta, Southeastern US and

three coastal cities of the Bohai Sea, respectively (Liu, Baumgartner, *et al.*, 2014; Verma *et al.*, 2014; Fang *et al.*, 2016; Liu *et al.*, 2018). The sea salt factor contributed to 14% of DTTv. In the literature, traffic sources have been found to be responsible for 11% to 16% of DTTv activities (Liu, Baumgartner, *et al.*, 2014; Verma *et al.*, 2014; Fang *et al.*, 2016; Liu *et al.*, 2018). In this study, traffic contributed to 8% of DTTv activity in Dammam. The impact of traffic on DTTm was very high (39%). In comparison, its impact on DTTv was much lower (8%), indicating elements emitted from traffic have high OP activity per μg of species and low OP activity per m^{-3} of air. Biomass sources had almost the same impact on DTTv (5%) and DTTm (5%), in agreement with the contribution of Biomass burning sources to PM_{2.5} in Dammam (5.2%).

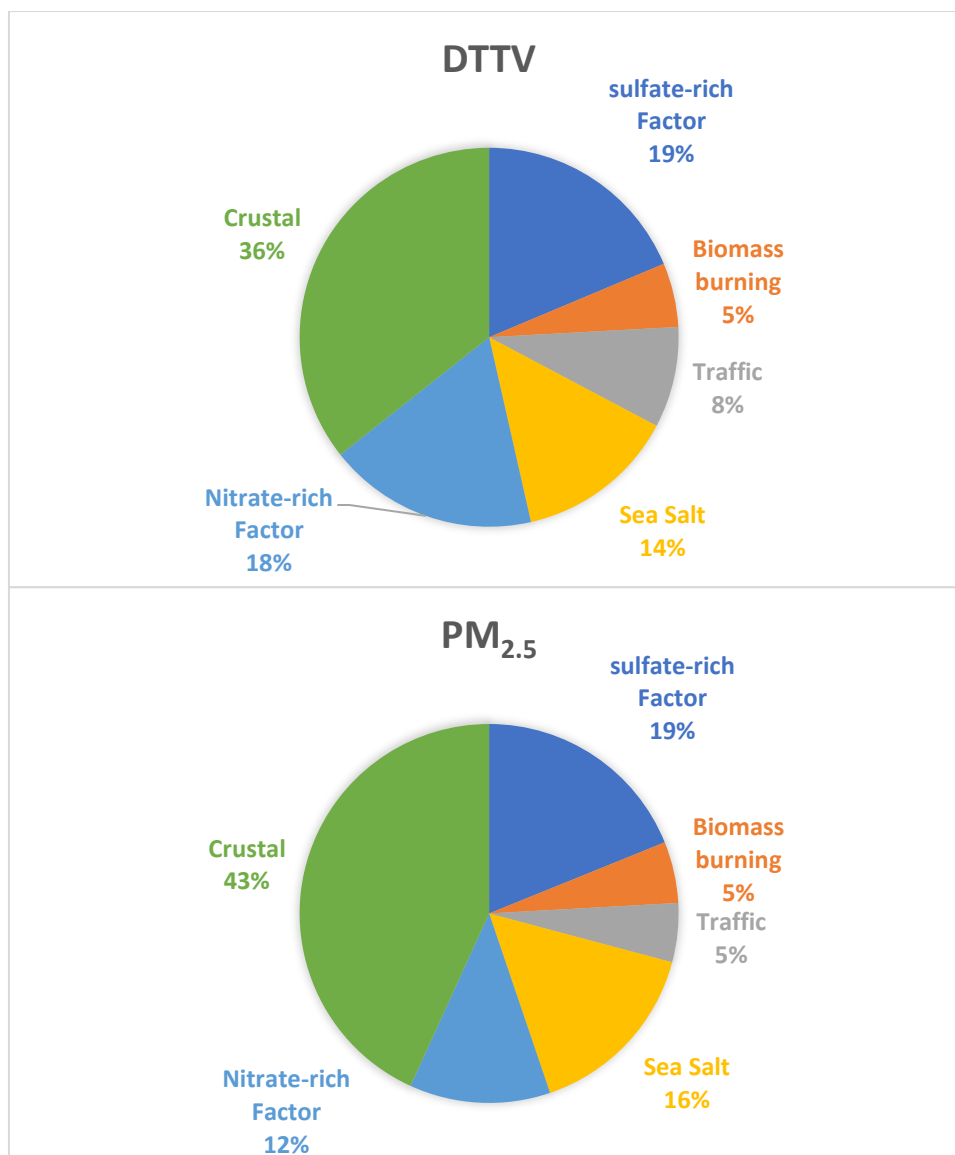


Figure 5.4 Relative factor contributions to oxidative potential (DTTv values) and to PM_{2.5} mass concentrations – obtained from all data.

5.3.4.1 Source Apportionment of OP for Non-dust samples:

The PMF analysis was rerun using data from non-dust storm samples only to study the contribution of each PM_{2.5} factor on DTTm and DTTv using the same methods described above. The crustal factor accounted for 32% of DTTv activity of non-dust samples (Fig 5.5) while this factor is responsible for 36% of DTTv of all data (Fig 5.4). The contribution of the nitrate-rich factor to DTTv increased from 18% for all data to 31% of non-dust samples. 20% of DTTv activities of non-dust periods

was attributed to the sulfate-rich factor compared to 19% for all data. Sea salt factor account for 8%, traffic factor account for 5% and biomass burning sources account for 4% of DTTv of non-dust samples in Dammam, compared to 14%, 8% and 5%, respectively. The contribution of traffic sources to DTTm was 39% for both all data (including dust and non-dust storm results) and non-dust storm samples as the largest contributor for DTTm (Fig 5.3 and Fig5.5). the nitrate-rich factor contribution to DTTm increased from 13% for all data to 18% for non-dust periods. 17% of DTTm of non-dust samples was attributed to the biomass burning sources while this factor was responsible for 5% only of DTTm of all samples. The sulfate-rich factor contributed to 17% of DTTm for non-dust samples. Natural sources together (crustal and sea salt factors) were responsible for 9%. In conclusion, secondary aerosol factors account for 51% of DTTv of non-dust periods. Natural sources (crustal and sea salt sources) contributed to 40% of DTTv of non-dust samples, and traffic and biomass burning factors were responsible for 9% only of DTTv. On the other hand, traffic and biomass burning sources account for 56% of DTTm of non-dust samples, and natural sources contributed to 9% only of DTTm. These results illustrate the influence of anthropogenic sources on the OP activities in the absence of natural occurring of dust storms.

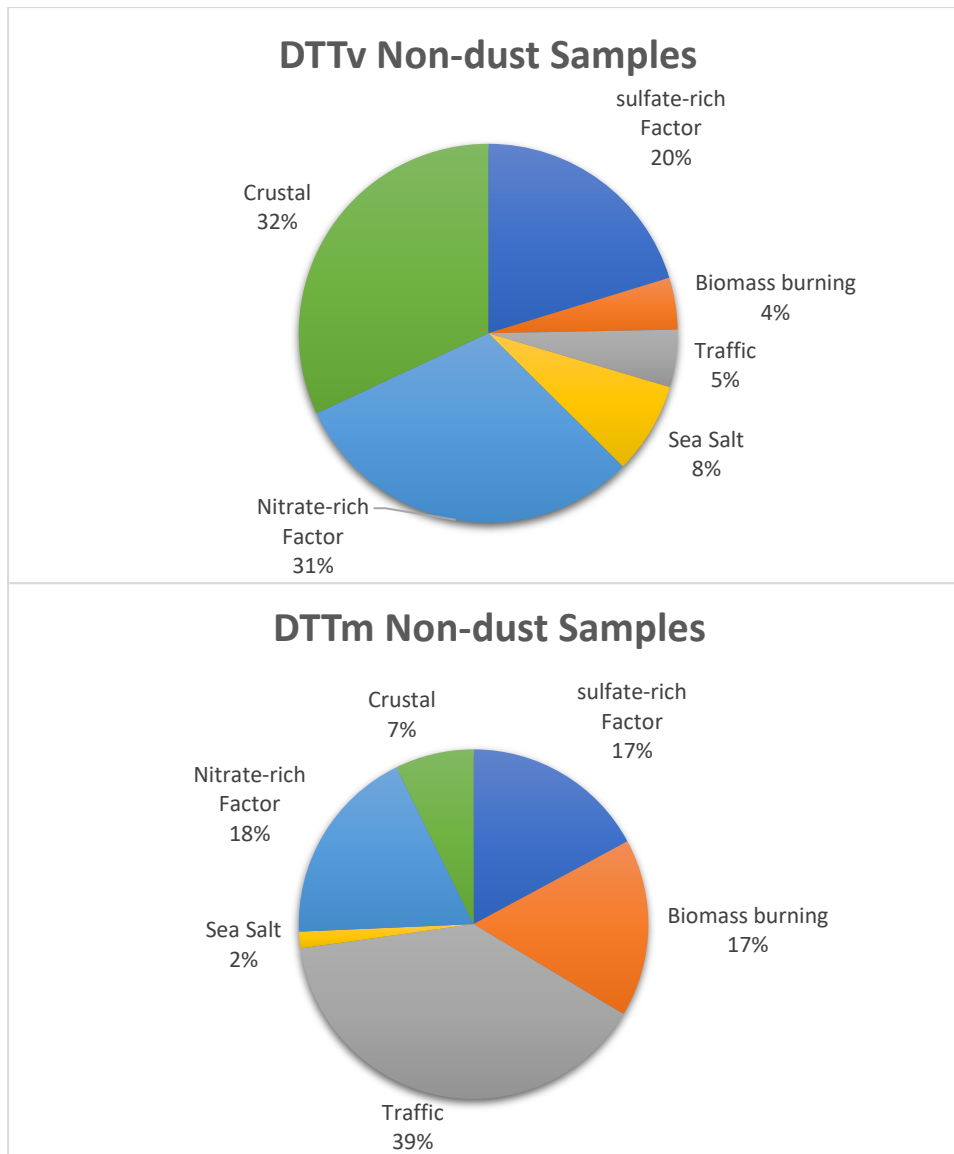


Figure 5.5 Relative factor contributions to oxidative potential DTTv values and to DTTm values— obtained from non-dust storm samples only.

5.4 Conclusions

The oxidative potential (activity) of PM_{2.5} in Dammam was investigated using the DTT assay. OP activity was assessed as both DTTm and DTTv. DTTm showed a negative correlation with PM_{2.5} mass, while DTTv indicated a positive correlation with PM_{2.5} mass concentration for both locations and seasons (as expected). DTTv was positively correlated with PM_{2.5} mass concentration, which

agrees with many epidemiological studies that link exposure to a high concentration of PM_{2.5} and adverse impacts on public health. Traffic was the most important PM source influencing DTTm measured of the OP of PM, while crustal and secondary aerosols sources made the highest contribution to DTTv activity in Dammam, reflecting their high contribution to total PM_{2.5} mass concentration, even during periods deemed “non-dust storm influenced” in this analysis. The high contribution of the traffic factor to DTTm reflects the toxicity of the PM components that are produced from vehicle emission. Efforts need to be done in Dammam to tackle traffic emission to reduce air pollution harm and improve public health. These results show that linking the predicted health impacts of aerosols to OP may be more relevant than considering PM mass concentrations only, as it accounts for differing toxicity of the different constituents of the particles.

Chapter 6 . Conclusions

6.1 Summary

This thesis aimed to investigate the air quality in Dammam, SA. More specifically the PM_{2.5} composition, its toxicity and potential sources. This study provides results which allow policy makers in Saudi Arabia to devise air quality mitigation strategies to improve air quality and most effectively address its associated impacts on human health. Three main research areas were discussed in this thesis:

- Air pollution climatology in Dammam using data obtained between 2016 and 2019 from two air quality stations. Hourly, daily and monthly patterns of NO₂, NO, NO_x, CO, O₃, SO₂ and PM₁₀ were studied to find air pollutant trends and behaviour. The results were compared and contrasted to other Saudi Arabian cities
- PM_{2.5} samples were collected from two locations in Dammam during two seasons and analysed for mass concentrations and chemical composition. Using these data potential pollutants sources were determined using positive matrix factorisation resulting in a six factor solution.
- Oxidative potential as a metric of toxicity was evaluated on the collected PM_{2.5} samples to study the components of PM most closely associated with the oxidative effect, and used as an indicator of their human toxicity.

A range of laboratory methods and data analysis methods were applied/developed in this work. PM_{2.5} components were investigated using ion chromatography (IC) for measuring ions, DRI Model 2015 Multiwavelength Thermal/Optical Carbon Analyser for measuring organic carbon and elemental

carbon (OC and EC) and Inductively Coupled Plasma Mass Spectrometry (ICP-MS) for measuring metals. The sources of PM_{2.5} in Dammam were estimated using positive matrix factorisation (PMF version 5.0.14). The DTT assay as a metric for measuring the toxicity of PM was adapted from Cho *et al.*'s (2005) procedure in the course of this thesis work. This section provides a summary of the main findings and wider implications from each area.

Chapter 3 presented an analysis of hourly air quality data from two stations in Dammam, SA for the period from 2016 to 2019. Hourly, daily and monthly patterns of NO₂, NO, NO_x, O₃, CO, SO₂ and PM₁₀ were studied. The monthly patterns showed an increase in the concentration of traffic-related pollutants (NO₂, NO and NO_x) and SO₂ in the winter, compared to other seasons. CO had its maximum in the winter for Corniche station and in the spring and summer for Rakkah station. O₃ showed its maximum in the spring when the temperature is high, and the sky is clear, from photochemical processes in the presence of NO_x. PM₁₀ was difficult to study due to the impact of dust storms and the movement of dust from the ground, as the stations are situated in arid locations.

The daily pattern of pollutants showed the increase of these elements in the weekdays comparing to weekends in Rakkah as a consequence of the influence of human activities. Further, weekly cycle of traffic-related elements in Corniche had their maximum on Thursday night. This area, as a recreation area, receives more traffic in the weekends compared to other days. In Dammam, people usually like to go outside their homes at night because of the sunlight intensity and high temperatures during the day. Thus, this behaviour is reflected in the level of some pollutants at Corniche station. SO₂ was higher on weekdays than

weekends, indicating the influence of industrial activities on the air quality in Dammam.

The hourly pattern showed the impact of heavy vehicle/trucks on the level of NO_2 , NO , NO_x and CO . These pollutants were higher when heavy trucks were allowed to move inside the city (0800-1200, 1300-1700, 2200-0500). Thus, these pollutants showed their maximum at 0200 and their minimum at 1600. O_3 pattern was almost the inverse of nitrogen dioxide and nitrogen monoxide, suggesting the impact of the $\text{NO} + \text{O}_3$ titration reaction. SO_2 had a steady increase from early morning until about 1700, then decreased for a short time and increased again to reach its maximum at midnight. The diurnal pattern of PM_{10} indicated the influence of rush hours where PM_{10} was high at 0800 and 2200, affected by the traffic.

This analysis shows the impact of traffic on traffic-related pollutants levels in Dammam. In some previous literature, NO_2 and NO were reported to be high in the morning and afternoon during rush hours, while in Dammam, these pollutants were higher in the night when trucks were allowed to be driven inside the city. More works are needed to tackle traffic pollution in Dammam, including improving public transportation to reduce the number of cars, reducing vehicle emission by introducing lower emission cars and educating the public about some behaviours that reduce vehicle emission, such as long time idling. Moreover, National Center for Environmental Compliance in SA (NCEC) needs to maintain and improve the quality of stations to provide high-quality data that gives more and accurate measurements.

Chapter 4 investigated the PM_{2.5} mass concentration, composition and sources for samples collected in the winter and summer from two locations in Dammam. The mean PM_{2.5} mass concentration in the summer was nearly twice that in the winter for all data, non-dust samples and dust samples. PM_{2.5} mass concentrations were above the WHO guidelines for maximum PM_{2.5} concentration in 24 hours during the whole sampling period except for four days in the winter. The mean mass concentration of PM_{2.5} was similar at the two locations for both the winter and summer campaigns, indicating a regional pattern of PM_{2.5} abundance. Local sources, specific to just one of the sampling locations, were concluded to have a minimal impact on PM_{2.5} concentrations.

The mean OC concentrations were significantly (using paired t.test) higher in the summer than in the winter at both locations, while the mean EC concentrations showed no significant seasonal variation. In both locations and seasons, OC/EC ratios were above 3.0. Such a value indicates the impact of gasoline, which is the primary fuel used in Saudi Arabian cars and accounts for 69% of consumed transportation fuel.

Analysis of the concentration of water soluble ions (WSI) showed the significant abundance of secondary inorganic ions (SO₄²⁻, NH₄⁺ and NO₃⁻) among other ions, representing more than 80% of the total measured WSI concentration during the winter and more than 75% during the summer at both locations. The mean total WSI mass analysed during the winter was 17.2 µg/m³ at Amanah and 20 µg/m³ at the university. In comparison, the mean total measured ion concentrations during the summer were 26.8 µg/m³ and 32.2 µg/m³ at Amanah and University, respectively. Even though the mean total measured WSI concentration was higher during the summer than during the winter, the

contribution of the WSI to the total PM_{2.5} mass was higher during the winter compared to the summer at both locations, influenced by the high concentration of PM_{2.5} caused by the greater incidence of dust storms in the summer.

On average, crustal elements, such as Al, Fe and Ti, were more abundant than other elements, as expected in arid areas such as SA. These three elements represented more than 88% and 94% of the total metal mass concentrations found during the winter and summer seasons, respectively, indicating the substantial impact of crustal elements on the PM_{2.5} mass in Dammam. There was no significant difference between the mean metal concentrations at Amanah and University locations in either of the two seasons, indicating the influence of regional sources on PM composition in Dammam.

The impact of dust storms on PM_{2.5} levels and composition was studied in Chapter 4. The results illustrated that PM_{2.5} during dust storms was almost 3 times higher than non-dust storms samples in both seasons. Concentrations of crustal metals (Al, Fe, Ti and Mn) were 5 times higher during dust storms than non-dust storm periods. However, trace element levels were not affected by dust storms for either season. Further, WSI concentrations were not impacted by dust storms except for Ca²⁺ and Mg²⁺, where levels of these two ions were almost three times higher during dust storms than non-dust periods. Also, EC showed no difference for dust and non-dust samples, while OC was significantly higher during dust storms with respect to non-dust storms samples.

Interestingly, the mean PM_{2.5} mass concentration of non-dust storm days in the summer (90 µg/m³) was two times higher than in the winter (45.4 µg/m³). This attributed to dry weather that leads to facilitate lofting of particles from the

ground to the atmosphere. Also, the mean mass concentration of PM_{2.5} in the summer (226.3 µg/m³) during dust storm days was 1.6 times higher than that in the winter (137 µg/m³). This finding indicates the negative impact of summer on the PM concentration in SA. Thus, these results for non-dust samples provide more understanding to the air quality in Dammam. For instance, the mean concentrations of anthropogenic components (SO₄²⁻ and OC) were higher than those of all other elements, including crustal elements. Studying PM level and composition for non-dust periods gives a clear picture of the anthropogenic impact on air quality in Dammam.

Application of a PMF analysis estimated six factors (sources) to be responsible for PM_{2.5} in Dammam. The crustal source was the main contributor to PM_{2.5}, then a sulfate-rich factor, then sea salt, then a nitrate-rich factor, then biomass burning, then traffic.

Chapter 5 described measurements of the Oxidative Potential (OP) of PM_{2.5} in Dammam. The DTT assay was used as a candidate proxy metric of the toxicity of PM. DTT_v and DTT_m values were presented, and their correlation with PM_{2.5}, chemical components and sources of PM_{2.5} were studied. DTT_m showed a negative correlation with PM_{2.5} mass concentrations, and a positive correlation was found between DTT_v and PM_{2.5} mass concentrations. DTT_m had a negative correlation with crustal metals and positive correlation with most trace metals, suggesting the higher toxicity of trace metals than crustal metals. DTT_m showed the highest correlation with carbonaceous elements among other elements in agree with much literature. In general, the OP value per µg was more influenced by anthropogenic species than natural species, suggesting this measurement may provide a better metric of PM toxicity than use

of PM mass concentration alone. DTTv was positively correlated with most of the chemical components in this works.

In addition, DTTm was higher in the winter than in the summer, even though PM_{2.5} mass was higher in the summer. A paired t.test showed that DTTm was significantly higher at the University location comparing to the Amanah location in the winter. At the same time, the difference was not significant in the summer, suggesting the impact of crustal species on the DTTm activity in the summer for both locations. On the other hand, DTTv was significantly higher in the summer than in the winter for both locations. The difference between the two sites was not significant in either season.

Analysing the OP levels for dust and non-dust storm samples showed some interesting changes with regards to DTTm. DTTm was higher for non-dust storm samples than dust storm samples in both seasons. For the dust storm samples, DTTm positively correlated with all crustal elements while these crustal elements negatively impact DTTm for non-dust samples. In contrast, DTTm correlation with transition metals (except Sr, Cu and Co) and OC and EC were stronger for non-dust storm samples than dust storm samples. Interestingly, DTTm almost has the same r-value with V for dust and non-dust samples; however, its correlation with dust samples was not significant, while its correlation with non-dust samples was significant.

In Chapter 5, the contribution of different sources of PM_{2.5} in Dammam were assessed using the PMF model. The traffic factor, which was responsible for 5% of PM_{2.5} in Dammam, had the highest contribution (39%) to DTTm. Crustal sources, which contributed to 40% of PM_{2.5} in Dammam, have the lowest

contribution (6%) to DTTm. Secondary inorganic aerosols were responsible for 42% of DTTm. Thus, these results suggest that traffic emissions pose high toxicity (per unit mass) even if they are present at a small level. DTTv was mainly influenced by natural sources (crustal and sea salt), responsible for about 40% of DTTv. Secondary aerosols participated by about 37%, traffic factor contributed by 8% and biomass burning was responsible by 5% of DTTv in Dammam. Anthropogenic sources account for 86% of DTTm and 60% of DTTv (and hence the health impacts of PM).

In summary of chapter 5, measuring the OP activity of PM provides more in-depth detail about the toxicity of PM, compared to mass or composition data. OP is a potentially new metric for PM toxicity as OP may capture PM components with higher health-relevance than PM mass alone. With more OP studies being reported and understanding of PM chemical components advancing, we can focus policy action to tackle more harmful species and make the air healthier for the public.

6.2 Conclusion

In conclusion, this work presented an investigation of the air pollution in Dammam, SA, focusing upon PM_{2.5}. Different pollutants were analysed, including gases (secondary data) and particulate matter (detailed analysis of primary samples). The significant impact of dust storm events was apparent where PM_{2.5} mean mass concentration was three times higher during dust storm periods compared to non-dust storm periods. However, analysing the data excluding dust storm periods provides more knowledge about the real situation of the air quality in Dammam, and anthropogenic influence. PM in Dammam was

dominated by secondary aerosols and organic carbon compared to other components measured in this thesis. The high level of secondary aerosols is a result of increasing emissions of their primary precursors. As a petroleum producing country, with most human activity occurring in the eastern province of SA, more efforts should be applied to tackle air pollution.

The contribution of natural sources (crustal and sea salt) was estimated by PMF to account for about 60% of PM_{2.5} in Dammam, while anthropogenic sources were responsible for about 40%. However, investigating sources of PM_{2.5} in Dammam after removing dust storms data showed the opposite. The contribution of natural sources for non-dust storm data was 40%, while anthropogenic sources' contribution was about 60%. Furthermore, secondary aerosol factors (Sulfate-rich factor and Nitrate-rich factor) contributed 46% to PM_{2.5}. Tackling anthropogenic secondary aerosols and their precursors needs to be prioritised to improve air quality and enhance public health. Controlling secondary aerosols in Dammam would decrease the mean mass of PM_{2.5} by up to 35%, which means the mean mass concentration of PM_{2.5} for non-dust days would be 30 µg/m³ instead of what was found in this thesis (45 µg/m³). Also, reducing sulfur, ammonium and carbonaceous emissions, would reduce DTTv activity by up to 40%.

Moreover, investigating the sources that contribute to DTTm showed the high influence of harmful traffic emission. Hence, reducing traffic emissions should be a priority for the government to reduce air pollution and improve human health. Efficient public transportation will effectively minimize the number of cars driven in the country alongside better car quality and maintenance. The electrical vehicle will be another solution; however, this

solution will not work properly without the government's desire, which means encouraging and helping people to use electrical vehicles and provide charge point access all over the country.

6.3 Limitations

Any work has its limitations and uncertainty, and this thesis is not immune to this challenge. For the analysis of the air pollution climate in Damman in chapter 3, the data quality was not in very good condition as many measurements were missed. This data might not give the real situation of the air quality in Damman; however, it gave many indications that agreed with a general understanding of activities in Damman. Moreover, the locations of the two monitoring stations from which data were available may not be representative of the city. The locations of these stations are more likely represent urban background area rather than urban area like Damman. Moving one of the stations to be in the city centre or close to one of the main roads would provide more understanding of the air quality in Damman.

The main limitation for chapter 4, was lack of direct data for silicon and sulphur in the PM composition measurements. Silicon (and SiO_2) is one of the main components of desert sands. The ICP-MS cannot measure silicon, and XRF cannot be used because of the limited number and size of filters for this work. Missing silicon measurement could lead to underestimation of the crustal components in the samples. Also, source estimation by PMF could have been influenced without silicon measurement.

Measuring the oxidative potential (OP) of PM is a promising method to quantify PM health impact; however, this may not truly reflect the health impacts.

OP has been shown to be correlated with health end point, including respiratory and cardiovascular diseases. Still, these correlations do not mean an absolute causation. There is no standard method to measure OP, however the established and available method that showed the highest correlation with health end points was used in this thesis.

6.4 Suggestions for Future Research

In general, the number of air quality studies in Saudi Arabia is low compared to the size and population of the country and the diversity of the environment. Many areas in SA need to be investigated to understand the common and local issues in each place. Knowing the air quality in SA will provide scientists and policymakers with an understanding of the major pollutants and sources of pollution. Thus, this knowledge will help to tackle and reduce air pollution and improve public health.

It would be preferable to collect PM samples year-round to study the PM in Dammam or any other area. Collecting samples for a long time, including all seasons, will provide a more in-depth understanding of the PM variation and the impact of natural and anthropogenic sources over different times of the year. Unfortunately, there was no rain during the collection of samples for this work in either campaign, which was unusual in the winter. Collecting samples before, during and after rain will be interesting to measure the impact of rain on air quality as we explored the impact of dust storms in this work. Also, this work can be applied to indoor air quality, including homes, workplaces and health care buildings.

In Dammam, as is the case in much literature, secondary aerosols are the dominant components of $PM_{2.5}$. These species need to be explored more to find the best way to minimize their level in the air. Secondary aerosols are formed in the air in the presence of their precursors. Controlling the precursors would be the best mitigation for these species.

Examining the sources of PM regionally provides a better understanding of the main contributors to PM since each area has its unique sources based on the environment and activities. Knowing the sources of PM will help to tackle these sources and improve air quality. In SA, it would be very helpful to analyse PM sources in urban and rural areas. Rural areas usually reflect the background level of air pollution, and by studying these areas, we will have benchmark data that can be compared to urban and urban background studies.

OP is a potential metric for PM toxicity. More studies are needed to further standardise the method; nonetheless, OP should be used to predict PM health outcomes in parallel with the use PM mass. Also, it would be very helpful to measure OP from different places with high and low level of air pollution and from places contrasting environmental conditions. This work described in this thesis contributed to this effort, by studying OP in an arid area with a high level of crustal elements.

Bibliography

- Abrams, Joseph Y *et al.* (2017) 'Associations between ambient fine particulate oxidative potential and cardiorespiratory emergency department visits', *Environmental Health Perspectives*, 125(10). doi: 10.1289/EHP1545.
- Abrams, Joseph Y. *et al.* (2017) 'Erratum: Associations between Ambient Fine Particulate Oxidative Potential and Cardiorespiratory Emergency Department Visits', *Environmental health perspectives*, 125(12), p. 129001. doi: 10.1289/EHP3048.
- Al-Garni, A.Z., Sahin, A.Z. and Al-Farayedhi, A., 1999. Modelling of weather characteristics and wind power in the eastern part of Saudi Arabia. *International journal of energy research*, 23(9), pp.805-812.
- Alghamdi, M. A. *et al.* (2014) 'Temporal variations of O₃ and NO_x in the urban background atmosphere of the coastal city Jeddah , Saudi Arabia', *Atmospheric Environment*. Elsevier Ltd, 94(x), pp. 205–214. doi: 10.1016/j.atmosenv.2014.03.029.
- Alharbi, B. H., Maghrabi, A. and Tapper, N. (2013) 'The march 2009 dust event in Saudi Arabia: Precursor and supportive environment', *Bulletin of the American Meteorological Society*, 94(4), pp. 515–528. doi: 10.1175/BAMS-D-11-00118.1.
- Alharbi, B., Pasha, M. and N, T. (2014) 'Assessment of ambient air quality in Riyadh City, Saudi Arabia', *Current World Environment*, 9(2), pp. 227–236. doi: 10.12944/cwe.9.2.01.
- Alharbi, B., Shareef, M. M. and Husain, T. (2015) 'Study of chemical characteristics of particulate matter concentrations in Riyadh, Saudi Arabia', *Atmospheric Pollution Research*. Elsevier, 6(1), pp. 88–98. doi: 10.5094/APR.2015.011.
- Allan, J. D. *et al.* (2003) 'Quantitative sampling using an Aerodyne aerosol mass spectrometer 2. Measurements of fine particulate chemical composition in two U.K. cities', *Journal of Geophysical Research: Atmospheres*. Blackwell Publishing Ltd, 108(3). doi: 10.1029/2002JD002359.
- Allan, J. D. *et al.* (2010) 'Contributions from transport, solid fuel burning and cooking to primary organic aerosols in two UK cities', *Atmos. Chem. Phys*, 10, pp. 647–668. Available at: www.atmos-chem-phys.net/10/647/2010/ (Accessed: 11 September 2021).
- Almazroui, M. *et al.* (2012) 'Recent climate change in the Arabian Peninsula: Annual rainfall and temperature analysis of Saudi Arabia for 1978-2009', *International Journal of Climatology*, 32(6), pp. 953–966. doi: 10.1002/joc.3446.
- Atkinson, R. W. *et al.* (2016) 'Short-term associations between particle oxidative potential and daily mortality and hospital admissions in London', *International Journal of Hygiene and Environmental Health*. Urban & Fischer, 219(6), pp. 566–572. doi: 10.1016/J.IJHEH.2016.06.004.
- Barth, H. J. (2001) 'Characteristics of the wind regime north of Jubail, Saudi Arabia, based on high resolution wind data', *Journal of Arid Environments*, 47(3), pp. 387–402. doi: 10.1006/jare.2000.0668.
- Bates, J. T. *et al.* (2015) 'Reactive oxygen species generation linked to sources of atmospheric particulate matter and cardiorespiratory effects', *Environmental Science and Technology*, 49(22), pp. 13605–13612. doi: 10.1021/acs.est.5b02967.
- Bates, J. T. *et al.* (2019) 'Review of acellular assays of ambient particulate matter oxidative

- potential: methods and relationships with composition, sources, and health effects', *Environmental Science and Technology*. American Chemical Society, 53(8), pp. 4003–4019. doi: 10.1021/acs.est.8b03430.
- Bernardoni, V. *et al.* (2011) 'PM10 source apportionment in Milan (Italy) using time-resolved data', *Science of the Total Environment*. Elsevier B.V., 409(22), pp. 4788–4795. doi: 10.1016/j.scitotenv.2011.07.048.
- Bian, Q. *et al.* (2017) 'Sources of PM_{2.5} carbonaceous aerosol in Riyadh, Saudi Arabia', *Atmospheric Chemistry and Physics Discussions*, pp. 1–36. doi: 10.5194/acp-2017-829.
- Bigi, A., Ghermandi, G. and Harrison, R. M. (2012) 'Analysis of the air pollution climate at a background site in the Po valley', *Journal of Environmental Monitoring*, 14(2), pp. 552–563. doi: 10.1039/c1em10728c.
- Bigi, A. and Harrison, R. M. (2010) 'Analysis of the air pollution climate at a central urban background site', *Atmospheric Environment*. Elsevier Ltd, 44(16), pp. 2004–2012. doi: 10.1016/j.atmosenv.2010.02.028.
- Borm, P. J. A. *et al.* (2007a) 'Oxidant generation by particulate matter: From biologically effective dose to a promising, novel metric', *Occupational and Environmental Medicine*, pp. 73–74. doi: 10.1136/oem.2006.029090.
- Borm, P. J. A. *et al.* (2007b) 'Oxidant generation by particulate matter: From biologically effective dose to a promising, novel metric', *Occupational and Environmental Medicine*, 64(2), pp. 73–74. doi: 10.1136/oem.2006.029090.
- Brimblecombe, P. (1987) 'The big smoke : a history of air pollution in London since medieval times'. Methuen, p. 185.
- Calas, A. *et al.* (2019) 'Seasonal variations and chemical predictors of oxidative potential (OP) of particulate matter (PM), for seven urban French sites', *Atmosphere*, 10(11), pp. 1–20. doi: 10.3390/atmos10110698.
- Canova, C. *et al.* (2014) 'PM10 oxidative properties and asthma and COPD', *Epidemiology*. Lippincott Williams and Wilkins, 25(3), pp. 467–468. doi: 10.1097/EDE.0000000000000084.
- Carslaw, D. (2015) 'The openair manual open-source tools for analysing air pollution data', *King's College London*, (January), p. 287.
- Carslaw, D. (2018) 'Package "worldmet"'.
<https://github.com/carslaw/worldmet>
- Cesari, D. *et al.* (2014) 'Source apportionment of PM_{2.5} in the harbour-industrial area of Brindisi (Italy): Identification and estimation of the contribution of in-port ship emissions', *Science of the Total Environment*. Elsevier B.V., 497–498, pp. 392–400. doi: 10.1016/j.scitotenv.2014.08.007.
- Cesari, D. *et al.* (2016) 'Inter-comparison of source apportionment of PM10 using PMF and CMB in three sites nearby an industrial area in central Italy', *Atmospheric Research*. Elsevier B.V., 182, pp. 282–293. doi: 10.1016/j.atmosres.2016.08.003.
- Charrier, J. G. *et al.* (2015) 'Oxidant production from source-oriented particulate matter-Part 1: Oxidative potential using the dithiothreitol (DTT) assay', *Atmos. Chem. Phys*, 15, pp. 2327–2340. doi: 10.5194/acp-15-2327-2015.

- Charrier, J. G. and Anastasio, C. (2012) 'On dithiothreitol (DTT) as a measure of oxidative potential for ambient particles: Evidence for the importance of soluble \newline transition metals', *Atmospheric Chemistry and Physics*. NIH Public Access, 12(19), pp. 9321–9333. doi: 10.5194/acp-12-9321-2012.
- Chen, P. *et al.* (2015) 'Assessment of heavy metal pollution characteristics and human health risk of exposure to ambient PM_{2.5} in Tianjin, China', *Particuology*. Chinese Society of Particuology, 20, pp. 104–109. doi: 10.1016/j.partic.2014.04.020.
- Cheng, Y. *et al.* (2015) 'PM_{2.5} and PM_{10-2.5} chemical composition and source apportionment near a Hong Kong roadway', *Particuology*. Chinese Society of Particuology, 18, pp. 96–104. doi: 10.1016/j.partic.2013.10.003.
- Chester, R. (1999) 'The trace metal chemistry of atmospheric dry deposition samples Mediterranean'.
- Chirizzi, D. *et al.* (2017) 'Influence of Saharan dust outbreaks and carbon content on oxidative potential of water-soluble fractions of PM_{2.5} and PM₁₀', *Atmospheric Environment*. Elsevier Ltd, 163, pp. 1–8. doi: 10.1016/j.atmosenv.2017.05.021.
- Cho, A. K. *et al.* (2005a) 'Redox activity of airborne particulate matter at different sites in the Los Angeles Basin', *Environmental Research*. Academic Press, 99(1), pp. 40–47. doi: 10.1016/j.envres.2005.01.003.
- Cho, A. K. *et al.* (2005b) 'Redox activity of airborne particulate matter at different sites in the Los Angeles Basin', *Environmental Research*, 99(1), pp. 40–47. doi: 10.1016/j.envres.2005.01.003.
- Chow, J. C. *et al.* (2011) PM_{2.5} source profiles for black and organic carbon emission inventories, *Atmospheric Environment*. doi: 10.1016/j.atmosenv.2011.07.011.
- Contini, D. *et al.* (2010) 'Characterisation and source apportionment of PM₁₀ in an urban background site in Lecce', *Atmospheric Research*. Elsevier B.V., 95(1), pp. 40–54. doi: 10.1016/j.atmosres.2009.07.010.
- Crilley, L. R. *et al.* (2015) 'Sources and contributions of wood smoke during winter in London: Assessing local and regional influences', *Atmospheric Chemistry and Physics*, 15(6), pp. 3149–3171. doi: 10.5194/acp-15-3149-2015.
- Crilley, L. R. *et al.* (2017) 'Source apportionment of fine and coarse particles at a roadside and urban background site in London during the 2012 summer ClearfLo campaign', *Environmental Pollution*. Elsevier Ltd, 220, pp. 766–778. doi: 10.1016/j.envpol.2016.06.002.
- Dadashazar, H., Ma, L. and Sorooshian, A. (2019) 'Sources of pollution and interrelationships between aerosol and precipitation chemistry at a central California site', *Science of the Total Environment*. Elsevier B.V., 651, pp. 1776–1787. doi: 10.1016/j.scitotenv.2018.10.086.
- Dai, J. and Wang, T. (2021) 'Impact of international shipping emissions on ozone and PM_{2.5}: the important role of HONO and ClNO₂', (February), pp. 1–29.
- Delfino, R. J. *et al.* (2013) 'Airway inflammation and oxidative potential of air pollutant particles in a pediatric asthma panel', *Journal of Exposure Science and Environmental Epidemiology*. Nature Publishing Group, 23(5), pp. 466–473. doi: 10.1038/jes.2013.25.
- DRI (2015) 'DRI standard operating procedure Title: DRI Model 2015 Multiwavelength

Carbon Analysis Number: 2-231r0 (TOR/TOT) of Aerosol Filter Samples-Method IMPROVE_A for CSN Revision: 1’.

Duan, F. K. *et al.* (2006) ‘Concentration and chemical characteristics of PM_{2.5} in Beijing, China: 2001-2002’, *Science of the Total Environment*, 355(1–3), pp. 264–275. doi: 10.1016/j.scitotenv.2005.03.001.

EEA (2021) *Air pollution — European Environment Agency*. Available at: <https://www.eea.europa.eu/help/glossary/eea-glossary/air-pollution> (Accessed: 4 August 2021).

El-Mubarak, A. H. *et al.* (2014) ‘Identification and source apportionment of polycyclic aromatic hydrocarbons in ambient air particulate matter of Riyadh, Saudi Arabia’, *Environmental Science and Pollution Research*, 21(1), pp. 558–567. doi: 10.1007/s11356-013-1946-9.

El-sharkawy, M. F. and Zaki, G. R. (2015) ‘Effect of meteorological factors on the daily average levels of particulate matter in the Eastern Province of Saudi Arabia : A Cross-Sectional Study’, 5(1), pp. 18–29.

European Commission (2018) *EDGAR: The Emissions Database for Global Atmospheric Research Leaflet, EU Open Data portal*. Available at: <https://edgar.jrc.ec.europa.eu/EDGAR-infographics.pdf> (Accessed: 1 July 2021).

Fang, T. *et al.* (2016) ‘Oxidative potential of ambient water-soluble PM_{2.5} in the southeastern United States: Contrasts in sources and health associations between ascorbic acid (AA) and dithiothreitol (DTT) assays’, *Atmospheric Chemistry and Physics*. Copernicus GmbH, 16(6), pp. 3865–3879. doi: 10.5194/acp-16-3865-2016.

Farahat, A. (2016) ‘Air pollution in the Arabian Peninsula (Saudi Arabia, the United Arab Emirates, Kuwait, Qatar, Bahrain, and Oman): causes, effects, and aerosol categorization’, *Arabian Journal of Geosciences*, 9(3). doi: 10.1007/s12517-015-2203-y.

Francis, D. *et al.* (2021) ‘Summertime dust storms over the Arabian Peninsula and impacts on radiation, circulation, cloud development and rain’, *Atmospheric Research*. Elsevier, 250, p. 105364. doi: 10.1016/J.ATMOSRES.2020.105364.

Gao, D. *et al.* (2017) ‘A method for measuring total aerosol oxidative potential (OP) with the dithiothreitol (DTT) assay and comparisons between an urban and roadside site of water-soluble and total OP’, *Atmospheric Measurement Techniques*, 10(8), pp. 2821–2835. doi: 10.5194/amt-10-2821-2017.

Gao, D., J. Godri Pollitt, K., *et al.* (2020) ‘Characterization and comparison of PM_{2.5} oxidative potential assessed by two acellular assays’, *Atmospheric Chemistry and Physics*, 20(9), pp. 5197–5210. doi: 10.5194/acp-20-5197-2020.

Gao, D., Mulholland, J. A., *et al.* (2020) ‘Characterization of water-insoluble oxidative potential of PM_{2.5} using the dithiothreitol assay’, *Atmospheric Environment*. Elsevier Ltd, 224(February), p. 117327. doi: 10.1016/j.atmosenv.2020.117327.

GAS (2021) *Population Estimates | General Authority for Statistics, General Authority for Statistics Kingdom of Saudi Arabia*. Available at: <https://www.stats.gov.sa/en/43> (Accessed: 27 July 2021).

GASMI, K., ALJALAL, A., AL-BASHEER, W.A.T.H.E.Q. and ABDULAH, M., 2017. Analysis of NO_x, NO and NO₂ ambient levels as a function of meteorological parameters in

- Dhahran, Saudi Arabia. *WIT Transactions on Ecology and the Environment*, 211, pp.77-86.
- Geng, G. *et al.* (2017) 'Chemical composition of ambient PM_{2.5} over China and relationship to precursor emissions during 2005-2012', *Atmospheric Chemistry and Physics*, 17(14), pp. 9187–9203. doi: 10.5194/acp-17-9187-2017.
- González, Lucy T *et al.* (2017) 'Determination of trace metals in TSP and PM_{2.5} materials collected in the Metropolitan Area of Monterrey, Mexico: A characterization study by XPS', *Atmospheric Research*. Elsevier, 196(May), pp. 8–22. doi: 10.1016/j.atmosres.2017.05.009.
- Grivas, G., Cheristanidis, S. and Chaloulakou, A. (2012) 'Elemental and organic carbon in the urban environment of Athens. Seasonal and diurnal variations and estimates of secondary organic carbon', *Science of the Total Environment*. Elsevier B.V., 414, pp. 535–545. doi: 10.1016/j.scitotenv.2011.10.058.
- Guevara, M. (2016a) 'Emissions of primary particulate matter', *Issues in Environmental Science and Technology*. Royal Society of Chemistry, 2016-Janua(42), pp. 1–34. doi: 10.1039/9781782626589-00001.
- Guevara, M. (2016b) 'Emissions of primary particulate matter', *Issues in Environmental Science and Technology*. Royal Society of Chemistry, 2016-January(42), pp. 1–34. doi: 10.1039/9781782626589-00001.
- Hama, S. M. L. *et al.* (2020) 'Four-year assessment of ambient particulate matter and trace gases in the Delhi-NCR region of India', *Sustainable Cities and Society*. Elsevier, 54(December 2019), p. 102003. doi: 10.1016/j.scs.2019.102003.
- Haritash, A. K. and Kaushik, C. P. (2007) 'Assessment of seasonal enrichment of heavy metals in respirable suspended particulate matter of a sub-urban Indian City', *Environmental Monitoring and Assessment*, 128(1–3), pp. 411–420. doi: 10.1007/s10661-006-9335-1.
- Harrison, R.M. ed., 2015. *Pollution: causes, effects and control*. Royal society of chemistry.
- Harrison, R. M. *et al.* (2017) 'Health risk associated with airborne particulate matter and its components in Jeddah, Saudi Arabia', *Science of the Total Environment*. Elsevier B.V., 590–591, pp. 531–539. doi: 10.1016/j.scitotenv.2017.02.216.
- Hewitt, C.N. and Jackson, A.V. eds., 2020. *Atmospheric science for environmental scientists*. John Wiley & Sons.
- Howarth, N., Lanza, A. and Shehri, T. Al (2020) 'Saudi Arabia's 2018 CO₂ Emissions Fall Faster Than Expected', pp. 1–16. Available at: <https://www.kapsarc.org/research/publications/saudi-arabias-2018-co2-emissions-fall-faster-than-expected/> (Accessed: 11 June 2021).
- Jacob, D. J. (1999) 'Introduction to atmospheric chemistry'. Princeton University Press, p. 266.
- Janssen, N. A. H. *et al.* (2014) 'Oxidative potential of particulate matter collected at sites with different source characteristics', *Science of the Total Environment*. 472, pp. 572–581. doi: 10.1016/j.scitotenv.2013.11.099.
- Janssen, N. A. H. *et al.* (2015) 'Associations between three specific a-cellular measures of the oxidative potential of particulate matter and markers of acute airway and nasal inflammation in healthy volunteers', *Occupational and Environmental Medicine*, 72(1), pp. 49–56. doi: 10.1136/oemed-2014-102303.

- Kchih, H., Perrino, C. and Cherif, S. (2015) 'Investigation of desert dust contribution to source apportionment of PM10 and PM2.5 from a southern Mediterranean coast', *Aerosol and Air Quality Research*, 15(2), pp. 454–464. doi: 10.4209/aaqr.2014.10.0255.
- Khalil, M. A. K. *et al.* (2016) 'Air quality in Yanbu, Saudi Arabia', *Journal of the Air & Waste Management Association*, 66(4), pp. 341–355. doi: 10.1080/10962247.2015.1129999.
- Khodeir, M. *et al.* (2012) 'Source apportionment and elemental composition of PM2.5 and PM10 in Jeddah City, Saudi Arabia', *Atmospheric Pollution Research*. Elsevier, 3(3), pp. 331–340. doi: 10.5094/APR.2012.037.
- Kim, E. *et al.* (2004) 'Factor analysis of Seattle fine particles', *Aerosol Science and Technology*, 38(7), pp. 724–738. doi: 10.1080/02786820490490119.
- Kim, E. and Hopke, P. K. (2004) 'Improving source identification of fine particles in a rural northeastern U.S. area utilizing temperature-resolved carbon fractions', *Journal of Geophysical Research D: Atmospheres*, 109(9), pp. 1–13. doi: 10.1029/2003JD004199.
- Kim, E. and Hopke, P. K. (2012) 'Source Apportionment of Fine Particles in Washington, DC, Utilizing Temperature-Resolved Carbon Fractions', <http://dx.doi.org/10.1080/10473289.2004.10470948>. Taylor & Francis Group, 54(7), pp. 773–785. doi: 10.1080/10473289.2004.10470948.
- Kundu, S. and Stone, E. A. (2014) 'Composition and sources of fine particulate matter across urban and rural sites in the Midwestern United States', *Environmental Sciences: Processes and Impacts*. Royal Society of Chemistry, 16(6), pp. 1360–1370. doi: 10.1039/c3em00719g.
- Lee, C. S. L. *et al.* (2007) 'Heavy metals and Pb isotopic composition of aerosols in urban and suburban areas of Hong Kong and Guangzhou, South China-Evidence of the long-range transport of air contaminants', *Atmospheric Environment*, 41(2), pp. 432–447. doi: 10.1016/j.atmosenv.2006.07.035.
- Liang, J. (2013) 'Chemical Modeling for Air Resources', *Chemical Modeling for Air Resources*. Elsevier Inc. doi: 10.1016/C2012-0-07049-4.
- Lihavainen, H. *et al.* (2016) 'Aerosols physical properties at Hada Al Sham, western Saudi Arabia', *Atmospheric Environment*, 135, pp. 109–117. doi: 10.1016/j.atmosenv.2016.04.001.
- Lihavainen, H. *et al.* (2017) 'Aerosol optical properties at rural background area in Western Saudi Arabia', *Atmospheric Research*. Elsevier, 197(June), pp. 370–378. doi: 10.1016/j.atmosres.2017.07.019.
- Lim, C. C. *et al.* (2017) 'Temporal variation of fine and coarse particulate matter sources in Jeddah, Saudi Arabia', *Journal of the Air & Waste Management Association*. Taylor & Francis, 68(2), p. 10962247.2017.1344158. doi: 10.1080/10962247.2017.1344158.
- Liu, C. *et al.* (2019) 'Ambient Particulate Air Pollution and Daily Mortality in 652 Cities', <https://doi.org/10.1056/NEJMoa1817364>. Massachusetts Medical Society, 381(8), pp. 705–715. doi: 10.1056/NEJMoa1817364.
- Liu, Q., Liu, Y., *et al.* (2014) 'Chemical characteristics and source apportionment of PM10 during Asian dust storm and non-dust storm days in Beijing', *Atmospheric Environment*. Elsevier Ltd, 91, pp. 85–94. doi: 10.1016/j.atmosenv.2014.03.057.
- Liu, Q., Baumgartner, J., *et al.* (2014) 'Oxidative Potential and Inflammatory Impacts of Source Apportioned Ambient Air Pollution in Beijing'. doi: 10.1021/es5029876.

- Liu, W. J. *et al.* (2018) 'Oxidative potential of ambient PM_{2.5} in the coastal cities of the Bohai Sea, northern China: Seasonal variation and source apportionment', *Environmental Pollution*. Elsevier Ltd, 236, pp. 514–528. doi: 10.1016/j.envpol.2018.01.116.
- Lomozik, M., Szaja, G. and Nowak, W. (2004) 'Source apportionment of fine particles in Washington, DC, utilizing temperature-resolved carbon fractions', *Journal of the Air and Waste Management Association*, 54(7), pp. 773–785. doi: 10.1080/10473289.2004.10470948.
- Lovett, C. *et al.* (2018) 'Oxidative potential of ambient particulate matter in Beirut during Saharan and Arabian dust events', *Atmospheric Environment*. Elsevier Ltd, 188, pp. 34–42. doi: 10.1016/j.atmosenv.2018.06.016.
- Loyola, J. *et al.* (2009) 'Concentration of airborne trace metals in a bus station with a high heavy-duty diesel fraction', *Journal of the Brazilian Chemical Society*. Sociedade Brasileira de Química, 20(7), pp. 1343–1350. doi: 10.1590/S0103-50532009000700020.
- Martin, N. R. *et al.* (2019) 'Characterization and comparison of oxidative potential of real-world biodiesel and petroleum diesel particulate matter emitted from a nonroad heavy duty diesel engine', *Science of the Total Environment*. Elsevier B.V., 655, pp. 908–914. doi: 10.1016/j.scitotenv.2018.11.292.
- Masiol, M. *et al.* (2015) 'Spatial, seasonal trends and transboundary transport of PM_{2.5} inorganic ions in the Veneto region (Northeastern Italy)', *Atmospheric Environment*. Elsevier Ltd, 117, pp. 19–31. doi: 10.1016/j.atmosenv.2015.06.044.
- Masiol, M. *et al.* (2020) 'Hybrid multiple-site mass closure and source apportionment of PM_{2.5} and aerosol acidity at major cities in the Po Valley', *Science of The Total Environment*. Elsevier, 704, p. 135287. doi: 10.1016/J.SCITOTENV.2019.135287.
- Megido, L. *et al.* (2017) 'Enrichment factors to assess the anthropogenic influence on PM₁₀ in Gijón (Spain)', *Environmental Science and Pollution Research*. Environmental Science and Pollution Research, 24(1), pp. 711–724. doi: 10.1007/s11356-016-7858-8.
- MEWA (2017) 'the General Authority for Meteorology and Environmental Protection'. Available at: <https://mewa.gov.sa/en/Partners/Pages/الهيئة-العامة-للأرصاد-وحماية-البيئة.aspx> (Accessed: 28 July 2021).
- Miller, R. L., Tegen, I. and Perlwitz, J. (2004) 'Surface radiative forcing by soil dust aerosols and the hydrologic cycle', *Journal of Geophysical Research: Atmospheres*. John Wiley & Sons, Ltd, 109(D4), p. 4203. doi: 10.1029/2003JD004085.
- Munir, S. *et al.* (2016) 'Spatiotemporal analysis of fine particulate matter (PM_{2.5}) in Saudi Arabia using remote sensing data', *Egyptian Journal of Remote Sensing and Space Science*. National Authority for Remote Sensing and Space Sciences, 19(2), pp. 195–205. doi: 10.1016/j.ejrs.2016.06.001.
- Munir, S. *et al.* (2017) 'Analysing PM_{2.5} and its Association with PM₁₀ and Meteorology in the Arid Climate of Makkah, Saudi Arabia', *Aerosol and Air Quality Research*, 17(2), pp. 453–464. doi: 10.4209/aaqr.2016.03.0117.
- Murillo-tovar, M. (2011) 'Enrichment Factor and Profiles of Elemental Composition of PM_{2.5} in the City of Guadalajara, Mexico', pp. 545–549. doi: 10.1007/s00128-011-0369-x.
- Nayebare, S. R. *et al.* (2016) 'Chemical characterization and source apportionment of PM_{2.5} in Rabigh, Saudi Arabia', *Aerosol and Air Quality Research*, 16(12), pp. 3114–3129. doi: 10.4209/aaqr.2015.11.0658.

- Nayebare, S. R. *et al.* (2018) ‘Ambient air quality in the holy city of Makkah: A source apportionment with elemental enrichment factors (EFs) and factor analysis (PMF)’, *Environmental Pollution*. Elsevier Ltd, 243, pp. 1791–1801. doi: 10.1016/j.envpol.2018.09.086.
- Nishita-Hara, C. *et al.* (2019) ‘Dithiothreitol-Measured Oxidative Potential of Size-Segregated Particulate Matter in Fukuoka, Japan: Effects of Asian Dust Events’, *GeoHealth*, 3(6), pp. 160–173. doi: 10.1029/2019gh000189.
- Nowak, D. J. *et al.* (2014) ‘Tree and forest effects on air quality and human health in the United States’, *Environmental Pollution*, 193, pp. 119–129. doi: 10.1016/j.envpol.2014.05.028.
- Ntziachristos, L. *et al.* (2007) ‘Relationship between redox activity and chemical speciation of size-fractionated particulate matter’, *Particle and Fibre Toxicology*, 4, pp. 1–12. doi: 10.1186/1743-8977-4-5.
- Pant, P. and Harrison, R. M. (2012) ‘Critical review of receptor modelling for particulate matter : A case study of India’, *Atmospheric Environment*. Elsevier Ltd, 49, pp. 1–12. doi: 10.1016/j.atmosenv.2011.11.060.
- Paraskevopoulou, D. *et al.* (2019) ‘Yearlong variability of oxidative potential of particulate matter in an urban Mediterranean environment’, *Atmospheric Environment*. Elsevier, 206(August 2018), pp. 183–196. doi: 10.1016/j.atmosenv.2019.02.027.
- Park, K. and Dam, H. D. (2010) ‘Characterization of metal aerosols in PM10 from urban, industrial, and Asian Dust sources Kihong Park · Hung Duy Dam’, *Environ Monit Assess*, 160, pp. 289–300. doi: 10.1007/s10661-008-0695-6.
- Perrone, M. G. *et al.* (2016) ‘PM chemical composition and oxidative potential of the soluble fraction of particles at two sites in the urban area of Milan, Northern Italy’, *Atmospheric Environment*. Elsevier Ltd, 128, pp. 104–113. doi: 10.1016/j.atmosenv.2015.12.040.
- Perrone, M. R. *et al.* (2009) ‘Ionic and elemental composition of TSP, PM10, and PM2.5 samples collected over South-East Italy’, *Nuovo Cimento della Societa Italiana di Fisica B*, 124(3), pp. 341–356. doi: 10.1393/ncb/i2009-10770-2.
- Perrone, M. R. *et al.* (2016) ‘Saharan dust impact on the chemical composition of PM10 and PM1 samples over south-eastern Italy’, *Arabian Journal of Geosciences*, 9(2), pp. 1–11. doi: 10.1007/s12517-015-2227-3.
- Pio, C. *et al.* (2011) ‘OC / EC ratio observations in Europe : Re-thinking the approach for apportionment between primary and secondary organic carbon’, *Atmospheric Environment*. Elsevier Ltd, 45(34), pp. 6121–6132. doi: 10.1016/j.atmosenv.2011.08.045.
- Polissar, A. V. *et al.* (1998) ‘Atmospheric aerosol over Alaska 2. Elemental composition and sources’, *Journal of Geophysical Research Atmospheres*, 103(D15), pp. 19045–19057. doi: 10.1029/98JD01212.
- Prakash, P. J. *et al.* (2015) ‘The impact of dust storms on the Arabian Peninsula and the Red Sea’, *Atmos. Chem. Phys*, 15, pp. 199–222. doi: 10.5194/acp-15-199-2015.
- Prendes, P. *et al.* (1999) ‘Source apportionment of inorganic ions in airborne urban particles from Coruña a city (N.W. of Spain) using positive matrix factorization’, *Talanta*, 49, pp. 165–178.

- Rai, P. *et al.* (2016) ‘Composition and source apportionment of PM₁ at urban site Kanpur in India using PMF coupled with CBPF’, *Atmospheric Research*. Elsevier B.V., 178–179, pp. 506–520. doi: 10.1016/j.atmosres.2016.04.015.
- Rao, L. *et al.* (2020) ‘Oxidative potential induced by ambient particulate matters with acellular assays: A review’, *Processes*, 8(11), pp. 1–21. doi: 10.3390/pr8111410.
- Rattanavaraha, W. *et al.* (2011) ‘The reactive oxidant potential of different types of aged atmospheric particles: An outdoor chamber study’, *Atmospheric Environment*. Elsevier Ltd, 45(23), pp. 3848–3855. doi: 10.1016/j.atmosenv.2011.04.002.
- Reff, A., Eberly, S. I. and Bhave, P. V. (2007) ‘Receptor modeling of ambient particulate matter data using positive matrix factorization: Review of existing methods’, *Journal of the Air and Waste Management Association*, 57(2), pp. 146–154. doi: 10.1080/10473289.2007.10465319.
- Rushdi, A. I. *et al.* (2013) ‘Air quality and elemental enrichment factors of aerosol particulate matter in Riyadh City, Saudi Arabia’, *Arabian Journal of Geosciences*, 6(2), pp. 585–599. doi: 10.1007/s12517-011-0357-9.
- Saffari, A. *et al.* (2014) ‘Seasonal and spatial variation in dithiothreitol (DTT) activity of quasi-ultrafine particles in the Los Angeles Basin and its association with chemical species’, *Journal of Environmental Science and Health - Part A Toxic/Hazardous Substances and Environmental Engineering*, 49(4), pp. 441–451. doi: 10.1080/10934529.2014.854677.
- Von Schneidemesser, E. *et al.* (2015) ‘Chemistry and the Linkages between Air Quality and Climate Change’, *Chemical Reviews*, pp. 3856–3897. doi: 10.1021/acs.chemrev.5b00089.
- Seinfeld, J. H. (2016) *Atmospheric chemistry and physics : from air pollution to climate change / John H. Seinfeld, Spyros N. Pandis.*
- Shaltout, A. A. *et al.* (2015) ‘Spectroscopic investigation of PM_{2.5} collected at industrial, residential and traffic sites in Taif, Saudi Arabia’, *Journal of Aerosol Science*. Elsevier, 79, pp. 97–108. doi: 10.1016/j.jaerosci.2014.09.004.
- Sharma, S. K. and Mandal, T. K. (2017) ‘Chemical composition of fine mode particulate matter (PM_{2.5}) in an urban area of Delhi, India and its source apportionment’, *Urban Climate*. Elsevier B.V., 21, pp. 106–122. doi: 10.1016/j.uclim.2017.05.009.
- Shi, Z. *et al.* (2019) ‘Introduction to the special issue “in-depth study of air pollution sources and processes within Beijing and its surrounding region (APHH-Beijing)”’, *Atmospheric Chemistry and Physics*, 19(11), pp. 7519–7546. doi: 10.5194/acp-19-7519-2019.
- Shirmohammadi, F. *et al.* (2017) ‘Oxidative potential of on-road fine particulate matter (PM_{2.5}) measured on major freeways of Los Angeles, CA, and a 10-year comparison with earlier roadside studies’, *Atmospheric Environment*. Elsevier Ltd, 148, pp. 102–114. doi: 10.1016/j.atmosenv.2016.10.042.
- Sofia, D. *et al.* (2020) ‘Novel air pollution measurement system based on ethereum blockchain’, *Journal of Sensor and Actuator Networks*, 9(4). doi: 10.3390/jsan9040049.
- Sørensen, M. *et al.* (2003) ‘Linking exposure to environmental pollutants with biological effects’, in *Mutation Research - Reviews in Mutation Research*. Elsevier, pp. 255–271. doi: 10.1016/j.mrrev.2003.06.010.
- Squizzato, S. *et al.* (2016) ‘Factors, origin and sources affecting PM₁ concentrations and

composition at an urban background site', *Atmospheric Research*. Elsevier, 180, pp. 262–273. doi: 10.1016/J.ATMOSRES.2016.06.002.

Srivastava, D. *et al.* (2018) 'Speciation of organic fraction does matter for source apportionment. Part 1: A one-year campaign in Grenoble (France)', *Science of the Total Environment*. Elsevier B.V., 624, pp. 1598–1611. doi: 10.1016/j.scitotenv.2017.12.135.

Strak, M. *et al.* (2012) 'Respiratory health effects of airborne particulate matter: The role of particle size, composition, and oxidative potential-the RAPTES project', *Environmental Health Perspectives*, 120(8), pp. 1183–1189. doi: 10.1289/ehp.1104389.

Su, J. *et al.* (2021) 'Insights into measurements of water-soluble ions in PM_{2.5} and their gaseous precursors in Beijing', *Journal of Environmental Sciences (China)*. Elsevier B.V., 102, pp. 123–137. doi: 10.1016/j.jes.2020.08.031.

Tan, J. *et al.* (2017) 'Chemical characteristics and source apportionment of PM_{2.5} in Lanzhou, China', *Science of the Total Environment*. Elsevier B.V., 601–602, pp. 1743–1752. doi: 10.1016/j.scitotenv.2017.06.050.

Taylor S.R (1964) 'Abundance of chemical elements in the continental crust: a new table', *Geochimica et Cosmochimica Acta*, 28, pp. 1273–1285.

Theodore, L. (2008) *Air Pollution Control Equipment Calculations*, *Air Pollution Control Equipment Calculations*. doi: 10.1002/9780470255773.

Thorpe, A. and Harrison, R. M. (2008) 'Sources and properties of non-exhaust particulate matter from road traffic : A review', *Science of the Total Environment*, *The*. Elsevier B.V., 400(1–3), pp. 270–282. doi: 10.1016/j.scitotenv.2008.06.007.

Tiwary, A. and Williams, I. (2010) 'Air pollution: measurement, modelling and mitigation', *Choice Reviews Online*, 47(08), pp. 47-4447-47-4447. doi: 10.5860/choice.47-4447.

Tiwary, A. and Williams, I. (2018) 'Air pollution control and mitigation', in *Air Pollution*, pp. 361–413. doi: 10.1201/9780429469985-9.

Tsai, Y. I. *et al.* (2013) 'Source indicators of biomass burning associated with inorganic salts and carboxylates in dry season ambient aerosol in Chiang Mai Basin, Thailand', *Atmospheric Environment*. Elsevier Ltd, 78, pp. 93–104. doi: 10.1016/j.atmosenv.2012.09.040.

Tuet, W. Y. *et al.* (2017) 'Chemical oxidative potential of secondary organic aerosol (SOA) generated from the photooxidation of biogenic and anthropogenic volatile organic compounds', *Atmospheric Chemistry and Physics*. Copernicus GmbH, 17(2), pp. 839–853. doi: 10.5194/ACP-17-839-2017.

US-EPA (2014) 'EPA Positive Matrix Factorization (PMF) 5.0 Fundamentals and', *Environmental Protection Agency Office of Research and Development*, *Publusing House Whashington, DC 20460*, p. 136.

Velali, E. *et al.* (2016) 'Redox activity and in vitro bioactivity of the water-soluble fraction of urban particulate matter in relation to particle size and chemical composition', *Environmental Pollution*. Elsevier, 208, pp. 774–786. doi: 10.1016/J.ENVPOL.2015.10.058.

Verma, V. *et al.* (2007) 'Physicochemical and Toxicological Profiles of Particulate Matter in Los Angeles during the October 2007 Southern California Wildfires Physicochemical and Toxicological Profiles of Particulate Matter in Los Angeles during the October 2007 Southern Californ', *Environmental Science & Technology*, 43(October), pp. 954–960. doi:

10.1021/es8021667.

Verma, V. *et al.* (2009) ‘Redox activity of urban quasi-ultrafine particles from primary and secondary sources’, *Atmospheric Environment*, 43(40), pp. 6360–6368. doi: 10.1016/j.atmosenv.2009.09.019.

Verma, V. *et al.* (2012) ‘Contribution of water-soluble and insoluble components and their hydrophobic/hydrophilic subfractions to the reactive oxygen species-generating potential of fine ambient aerosols’, *Environmental Science and Technology*, 46(20), pp. 11384–11392. doi: 10.1021/es302484r.

Verma, V. *et al.* (2014) ‘Reactive oxygen species associated with water-soluble PM_{2.5} in the southeastern United States: Spatiotemporal trends and source apportionment’, *Atmospheric Chemistry and Physics*. Copernicus GmbH, 14(23), pp. 12915–12930. doi: 10.5194/acp-14-12915-2014.

Verma, V. *et al.* (2015) ‘Organic Aerosols Associated with the Generation of Reactive Oxygen Species (ROS) by Water-Soluble PM_{2.5}’, *Environmental Science and Technology*. American Chemical Society, 49(7), pp. 4646–4656. doi: 10.1021/ES505577W.

Vincent, P. (2008a) *Saudi Arabia: An environmental overview, Saudi Arabia: An Environmental Overview*. doi: 10.1201/9780203030882.

Vincent, P. (2008b) ‘Saudi Arabia: An environmental overview’, *Saudi Arabia: An Environmental Overview*. CRC Press, pp. 1–311.

Visentin, M. *et al.* (2016) ‘Urban PM_{2.5} oxidative potential: Importance of chemical species and comparison of two spectrophotometric cell-free assays’, *Environmental Pollution*. Elsevier Ltd, 219, pp. 72–79. doi: 10.1016/j.envpol.2016.09.047.

Vodička, P. *et al.* (2015) ‘Detailed comparison of OC/EC aerosol at an urban and a rural Czech background site during summer and winter’, *Science of the Total Environment*, 518–519, pp. 424–433. doi: 10.1016/j.scitotenv.2015.03.029.

Watson, J. G., Chow, J. C. and Chen, L. A. (2005) *Summary of Organic and Elemental Carbon / Black Carbon Analysis Methods and Intercomparisons*.

Weber, E. (1982) ‘Air pollution. Assessment methodology and modeling’. Available at: <https://www.osti.gov/biblio/5911483> (Accessed: 4 August 2021).

Weichenthal, S. *et al.* (2016) ‘Oxidative burden of fine particulate air pollution and risk of cause-specific mortality in the Canadian Census Health and Environment Cohort (CanCHEC)’, *Environmental Research*. Elsevier, 146, pp. 92–99. doi: 10.1016/j.envres.2015.12.013.

WHO (2018a) ‘Air quality and health’, *International Journal of Environmental Research and Public Health*. doi: 10.3390/ijerph15112399.

WHO (2018b) *Ambient (outdoor) air pollution*, [https://www.who.int/en/news-room/fact-sheets/detail/ambient-\(outdoor\)-air-quality-and-health](https://www.who.int/en/news-room/fact-sheets/detail/ambient-(outdoor)-air-quality-and-health). Available at: [https://www.who.int/news-room/fact-sheets/detail/ambient-\(outdoor\)-air-quality-and-health](https://www.who.int/news-room/fact-sheets/detail/ambient-(outdoor)-air-quality-and-health) (Accessed: 21 July 2021).

WHO (no date) *Air Pollution - Ambient Air Pollution, 2021*. Available at: [https://www.who.int/news-room/fact-sheets/detail/ambient-\(outdoor\)-air-quality-and-health](https://www.who.int/news-room/fact-sheets/detail/ambient-(outdoor)-air-quality-and-health) (Accessed: 2 July 2021).

- Wragg, F. P. H. *et al.* (2016) ‘An automated online instrument to quantify aerosol-bound reactive oxygen species (ROS) for ambient measurement and health-relevant aerosol studies’, *Atmospheric Measurement Techniques*. Copernicus GmbH, 9(10), pp. 4891–4900. doi: 10.5194/amt-9-4891-2016.
- Wragg, F. P. H. *et al.* (2017) ‘A semi-automated system for quantifying the oxidative potential of ambient particles in aqueous extracts using the dithiothreitol (DTT) assay: Results from the Southeastern Center for Air Pollution and Epidemiology (SCAPE)’, *Atmospheric Environment*. Elsevier Ltd, 43(1), pp. 471–482. doi: 10.5194/amt-8-471-2015.
- Xiao, H. *et al.* (2020) ‘Chemical characteristics of major inorganic ions in PM_{2.5} based on year-long observations in Guiyang, southwest China-Implications for formation pathways and the influences of regional transport’, *Atmosphere*, 11(8). doi: 10.3390/ATMOS11080847.
- Xiong, Q. *et al.* (2017) ‘Rethinking Dithiothreitol-Based Particulate Matter Oxidative Potential: Measuring Dithiothreitol Consumption versus Reactive Oxygen Species Generation’, *Environmental Science and Technology*. American Chemical Society, 51(11), pp. 6507–6514. doi: 10.1021/ACS.EST.7B01272.
- Xu, J., Song, S., *et al.* (2020) ‘An interlaboratory comparison of aerosol inorganic ion measurements by ion chromatography: Implications for aerosol pH estimate’, *Atmospheric Measurement Techniques*, 13(11), pp. 6325–6341. doi: 10.5194/amt-13-6325-2020.
- Xu, J., Liu, D., *et al.* (2020) ‘Source Apportionment of Fine Aerosol at an Urban Site of Beijing using a Chemical Mass Balance Model’, *Atmospheric Chemistry and Physics Discussions*, 2(December), pp. 1–28. doi: 10.5194/acp-2020-1020.
- Yang, A. *et al.* (2014) ‘Measurement of the oxidative potential of PM_{2.5} and its constituents: The effect of extraction solvent and filter type’, *Atmospheric Environment*, 83, pp. 35–42. doi: 10.1016/j.atmosenv.2013.10.049.
- Yang, A. *et al.* (2016) ‘Children’s respiratory health and oxidative potential of PM_{2.5}: The PIAMA birth cohort study’, *Occupational and Environmental Medicine*. BMJ Publishing Group, 73(3), pp. 154–160. doi: 10.1136/oemed-2015-103175.
- Yang, L. *et al.* (2020) ‘Characteristics and formation mechanisms of secondary inorganic ions in PM_{2.5} during winter in a central city of China: Based on a high time resolution data’, *Atmospheric Research*. Elsevier, 233(October 2018), p. 104696. doi: 10.1016/j.atmosres.2019.104696.
- Zereini, F. and Wiseman, C. (2010) *Urban Airborne Particulate Matter*, Springer. doi: 10.1007/978-3-642-12278-1.
- Zhao, P. *et al.* (2013) ‘Characteristics of carbonaceous aerosol in the region of Beijing, Tianjin, and Hebei, China’, *Atmospheric Environment*, 71, pp. 389–398. doi: 10.1016/j.atmosenv.2013.02.010.